

การทำสารลูทีนจากดอกดาวเรืองให้บริสุทธิ์ด้วยกระบวนการของเหลวโครมาโทกราฟีขนาดกึ่ง
อุตสาหกรรม และการขึ้นรูปสารลูทีนอิสระด้วยวิธีการคาร์บอนไดออกไซด์วิกฤติ

นายปณัฐพงศ์ บุญนวล

วิทยานิพนธ์นี้เป็นส่วนหนึ่งของการศึกษาตามหลักสูตรปริญญาวิทยาศาสตรดุษฎีบัณฑิต

สาขาวิชาวิศวกรรมเคมี ภาควิชาวิศวกรรมเคมี

คณะวิศวกรรมศาสตร์ จุฬาลงกรณ์มหาวิทยาลัย

ปีการศึกษา 2555

ลิขสิทธิ์ของจุฬาลงกรณ์มหาวิทยาลัย

บทคัดย่อและแฟ้มข้อมูลฉบับเต็มของวิทยานิพนธ์ตั้งแต่ปีการศึกษา 2554 ที่ให้บริการในคลังปัญญาจุฬาฯ (CUIR)

เป็นแฟ้มข้อมูลของนิสิตเจ้าของวิทยานิพนธ์ที่ส่งผ่านทางบัณฑิตวิทยาลัย

The abstract and full text of theses from the academic year 2011 in Chulalongkorn University Intellectual Repository (CUIR)

are the thesis authors' files submitted through the Graduate School.

PURIFICATION OF FREE LUTEIN FROM MARIGOLD FLOWER BY
PREPARATIVE CHROMATOGRAPHY AND PARTICLE FORMATION
OF FREE LUTEIN BY SUPERCRITICAL CARBON DIOXIDE

Mr. Panatpong Boonnoun

A Dissertation Submitted in Partial Fulfillment of the Requirements
for the Degree of Doctor of Engineering Program in Chemical Engineering

Department of Chemical Engineering

Faculty of Engineering


Chulalongkorn University


Academic Year 2012


Copyright of Chulalongkorn University

ปณัฐพงศ์ บุญนวล: การทำสารลูทีนจากดอกดาวเรืองให้บริสุทธิ์ด้วยกระบวนการของเหลวโครมาโทกราฟีขนาดกึ่งอุตสาหกรรมและการขึ้นรูปสารลูทีนอิสระด้วยวิธีการคาร์บอนไดออกไซด์วิกฤติ. (PURIFICATION OF FREE LUTEIN FROM MARIGOLD FLOWER BY PREPARATIVE CHROMATOGRAPHY AND PARTICLE FORMATION OF FREE LUTEIN BY SUPERCRITICAL CARBON DIOXIDE) อ.ที่ปรึกษาวิทยานิพนธ์หลัก: รศ.ดร. อาทิวรรณ โชติพฤษย์, อ.ที่ปรึกษาวิทยานิพนธ์ร่วม: Prof. Motonobu Goto, 102 หน้า.

ดอกดาวเรืองอุดมไปด้วยสารลูทีน ซึ่งเป็นสารในกลุ่มแซนโทฟิล และมีความสัมพันธ์ในการลดความเสี่ยงของโรคเกี่ยวกับตาและป้องกันการโรคหลอดเลือดหัวใจและโรคหลอดเลือดสมอง ฯลฯ แต่การใช้คุณสมบัติทางยาเหล่านี้ต้องการสารลูทีนที่มีความบริสุทธิ์สูง โดยของเหลวโครมาโทกราฟีได้รับการใช้กันอย่างแพร่หลายเพื่อแยกสารลูทีนออกจากสิ่งสกปรกอื่น ๆ เพื่อใช้ในการวิเคราะห์ แต่ในของเหลวโครมาโทกราฟีขนาดใหญ่นั้นมีการศึกษาเพียงไม่มากนัก ดังนั้นในส่วนแรกของงานนี้จึงมีวัตถุประสงค์เพื่อพัฒนาการทำให้บริสุทธิ์ของสารลูทีนจากดอกดาวเรืองด้วยขนาดของเหลวโครมาโทกราฟีขนาดกึ่งอุตสาหกรรม ซึ่งจากการทดลองพบว่าได้สารลูทีนที่มีความบริสุทธิ์สูงถึง 97.1 % เมื่อใช้ซิลิกาเจล เป็นเฟสอยู่หนึ่ง และ ส่วนผสมของเฮกเซน: เอทิลอะซิเตต 70:30 อัตราส่วน โดยปริมาตร (อัตราภาวไหล 10 มิลลิลิตรต่อนาที) เป็นเฟสเคลื่อนที่ อย่างไรก็ตาม นอกเหนือจากปัญหาความบริสุทธิ์แล้วอีกข้อจำกัดหนึ่งของสารลูทีนคือ ความสามารถในการละลายน้ำได้น้อย ซึ่งทำให้เกิดการดูดซึมโดยร่างกายมนุษย์ต่ำ ดังนั้นเพื่อลดปัญหานี้ จึงได้ศึกษาการขึ้นรูปสารลูทีนให้มีขนาดเล็กด้วยวิธีการคาร์บอนไดออกไซด์วิกฤติ โดยในส่วนที่สองของงานนี้ จะศึกษาความเป็นไปได้ที่จะใช้ไดคลอโรมีเทนและเอทานอลเป็นตัวทำละลายลูทีนก่อนการทดลองการขึ้นรูปสารลูทีนให้มีขนาดเล็กด้วยวิธีการคาร์บอนไดออกไซด์วิกฤติ โดยจากผลการทดลองพบว่าขนาดของอนุภาคลูทีนลดลง จาก 202.3 ไมครอน เป็น 1.58 ไมครอน และ 902 นาโนเมตร เมื่อใช้ไดคลอโรมีเทนและเอทานอลตามลำดับ นอกจากนี้ในส่วนสุดท้ายของงาน ได้ศึกษาความเป็นไปได้ของกระบวนการขึ้นรูปสารลูทีนให้มีขนาดเล็กด้วยวิธีการคาร์บอนไดออกไซด์วิกฤติโดยใช้สารละลายเป็นสารผสมของเฮกเซนและเอทิลอะซิเตต (70:30 อัตราส่วน โดยปริมาตร) ซึ่งเป็นสารชนิดเดียวกันกับเฟสเคลื่อนที่ในกระบวนการทำให้บริสุทธิ์ด้วยของเหลวโครมาโทกราฟีข้างต้น โดยพบว่า การละลายน้ำของอนุภาคลูทีนหลังขึ้นรูปด้วยวิธีการนี้เพิ่มขึ้นอย่างมีนัยสำคัญ จากแทบจะไม่ละลายเลยไปเป็นละลายได้ประมาณ 20% โดยการประสบความสำเร็จในการขึ้นรูปสารลูทีนให้มีขนาดเล็กด้วยวิธีการคาร์บอนไดออกไซด์วิกฤตินั้นสามารถลดขั้นตอนของการระเหยตัวทำละลายจากสารตัวอย่าง รวมไปถึงการละลายตัวอย่างแห้งกลับเข้าไปในตัวทำละลายอีกชนิด โดยวิธีการนี้ไม่เพียงจะลดค่าใช้จ่ายในกระบวนการยังสามารถลดความเสี่ยงในการเสื่อมสภาพของลูทีนซึ่งอาจเกิดขึ้นระหว่างกระบวนการที่ซับซ้อน

ภาควิชา.....วิศวกรรมเคมี..... ลายมือชื่อนิลิต.....  บุญนวล

สาขาวิชา.....วิศวกรรมเคมี..... ลายมือชื่อ อ. ที่ปรึกษาวิทยานิพนธ์หลัก 

ปีการศึกษา.....2555..... ลายมือชื่อ อ. ที่ปรึกษาวิทยานิพนธ์ร่วม 

5271863521: MAJOR CHEMICAL ENGINEERING

KEYWORDS : MARIGOLD / LUTEIN / SUPERCRITICAL ANTISOLVENT / SUPERCRITICAL FLUIDS / PREPARATIVE CHROMATOGRAPHY

PANATPONG BOONNOUN: PURIFICATION OF FREE LUTEIN FROM MARIGOLD FLOWER BY PREPARATIVE CHROMATOGRAPHY AND PARTICLE FORMATION OF FREE LUTEIN BY SUPERCRITICAL CARBON DIOXIDE. ADVISOR: ASSOC. PROF. ARTIWAN SHOTIPRUK, Ph.D., CO-ADVISOR: PROF. MOTONOBU GOTO, Ph.D., 102 pp.

Marigold flowers is a rich source of lutein, a type of xanthophylls that has been demonstrate to reduce the risk of ocular diseases and provide protective effect against cardiovascular diseases and stroke, etc. However, to exhibit some of these pharmaceutical properties, the compound should be of high purity. Liquid chromatography has widely been used to effectively separate lutein from other impurities for analytical purposes. However, only few reports were found on larger preparative scale. The first part of this work therefore aims to develop a protocol for preparative scale liquid chromatography purification of free lutein derived from marigold flowers. With silica gel as a stationary and mixture of hexane:ethyl acetate at 70:30 volume ratio (10 ml/min flow rate) as a mobile phase, as high as 97.1 % purity lutein could be obtained. Unfortunately, other than the purity issue, one other limitation to the applicability of the compound is its poor water solubility. This causes low oral and dermal bioavailability. To reduce this problem, supercritical anti-solvent (SAS) micronization of lutein particles were investigated using carbon dioxide (CO₂) as anti-solvent. In the second part of this work, because their binary phase equilibrium data with CO₂ are available in literature, the possibility to use dichloromethane (DCM) and ethanol as solvents in which lutein was dissolved prior to the SAS experiments was investigated. The reduction in size of lutein from 202.3 μm of unprocessed lutein to 1.58 μm and 902 nm could be achieved by SAS technique using DCM and ethanol, respectively. In addition, the last part of this work aims to demonstrate the feasibility of SAS micronization of lutein dissolved in mixture of hexane and ethyl acetate (70:30 v/v). The solubility of the SAS micronized lutein particles in aqueous solution was found to increase significantly from being almost insoluble to having approximately 20% solubility. Success in SAS micronization in hexane:ethyl acetate solvent mixture, which was used as a mobile phase for the chromatographic purification, implies that a step of solvent evaporation from the eluted samples and re-dissolving the dried sample into another organic solvent can be omitted. By this, not only the process cost can be reduced, the degradation of lutein during complicated processing steps can also be minimized.

Department :.....Chemical Engineering... Student's SignaturePanatpong Boonnoun
 Field of Study :..Chemical Engineering.. Advisor's SignatureAssoc. Prof. Artawan Shotipruk
 Academic Year :2012..... Co-advisor's SignatureProf. Motonobu Goto.....

ACKNOWLEDGEMENTS

I would like to express my deeply gratitude to all who gave me the possibility to complete this thesis. First, I am particularly grateful for my advisor, Associate professor Dr. Artiwan Shotipruk for her warm encouragement throughout my graduate studies. I am most grateful for her invaluable support, guidance and discussions. I am also appreciated Professor Dr. Motonobu Goto, my co-advisor for his invaluable support and suggestions. Moreover, I also grateful for the members of thesis examination committee, Associate Professor Dr. Muenduen Phisalaphong, Professor Dr. Suttichai Assabumrungrat, Assistant Professor Dr. Apinan Soottitantawat, and Dr. Phatthanon Prasitchoke, who gave helpful suggestions and information for this thesis. I would like to thank the Thailand Research Fund (TRF) through the Royal Golden Jubilee Ph.D. Program (RGJ-TRF) for financial support. Finally, I would like to dedicate this thesis to my parents and my families for their always support and encouragement as well as my friends in the Department of Chemical Engineering, Chulalongkorn University and Department of Applied Chemistry and Biochemistry, Kumamoto University.

CONTENTS

	PAGE
ABSTRACT (THAI).....	iv
ABSTRACT (ENGLISH).....	v
ACKNOWLEDGEMENTS	vi
CONTENTS	vii
LIST OF TABLES	xii
LIST OF FIGURES	xiii
 CHAPTER	
I INTRODUCTION	1
1.1 Motivation	1
1.2 Objectives	4
1.3 Working scopes.....	4
1.4 Expected benefits.....	5
II LITERATURE REVIEWS	6
2.1 Marigolds.....	6
2.2 Lutein & lutein fatty acid ester.....	6
2.3 Lutein & lutein fatty acid ester	9
2.3.1 Solvent extraction.....	9
2.3.2 Supercritical fluid extraction.....	9
2.4 Saponification of lutein fatty acid ester.....	11
2.5 Purification of free lutein.....	12
2.6 Previous studies of liquid chromatography purification of lutein.....	13
2.7 Particle micronization.....	16
2.7.1 Particle micronization by supercritical fluids.....	16

CHAPTER	PAGE
2.8 Mechanisms of supercritical anti solvent (SAS) micronization.....	19
2.8.1 Phase equilibrium of CO ₂ and organic solvent.....	20
2.8.2 Jet characteristic of solution flow.....	25
2.8.3 Mass transfer between organic solvent droplet and surrounding CO ₂	28
2.8.4 Nucleation and growth mechanisms.....	32
III PURIFICATION OF FREE LUTEIN FROM MARIGOLD FLOWERS BY LIQUID CHROMATOGRAPHY	34
3.1 Introduction	34
3.2 Materials and methods	35
3.2.1 Materials and chemicals.....	35
3.2.2 Solvent extraction	35
3.2.3 Saponification	36
3.2.4 Purification by Chromatography.....	36
3.2.4.1 Screening suitable mobile phase by thin layer chromatography (TLC).....	36
3.2.4.2 Column packing procedures.....	36
3.2.4.3 Semi-preparative open column chromatography.....	37
3.2.4.4 Preparative column chromatography.....	37
3.2.5 Analysis of free lutein by high pressure liquid chromatography (HPLC).....	37
3.2.6 Analysis of saponified sample by liquid chromatography mass spectrometry (LC-MS).....	37
3.2.7 Analysis of purified sample by Hydrogen Nuclear Magnetic Resonance Spectrometry (H-NMR).....	38

CHAPTER	PAGE
3.3 Results & discussion	38
3.3.1 Liquid chromatography purification.....	38
3.2.4.1 Screening suitable mobile phase by thin layer chromatography (TLC).....	39
3.2.4.2 Chromatographic purification on semi-preparative column.....	40
3.2.4.3 Chromatographic purification on preparative column.....	41
3.4 Conclusions.....	45
 IV SUPERCRITICAL ANTI-SOLVENT MICRONIZATION OF MARIGOLD-DERIVED LUTEIN DISSOLVED IN DICHLOROMETHANE AND ETHANOL.....	46
4.1 Introduction	46
4.2 Materials and methods	48
4.2.1 Materials and chemicals.....	48
4.2.2 Preparation of lutein sample	48
4.2.3 SAS Micronization of lutein	49
4.2.4 Evaluation of particle morphology, MPS and PSD.....	54
4.3 Results & discussion	54
4.3.1 SAS Micronization of lutein dissolved in DCM.....	54
4.3.2 SAS Micronization of lutein dissolved in ethanol.....	58
4.4 Conclusions.....	61
 V SUPERCRITICAL ANTI-SOLVENT MICRONIZATION OF CHROMATOGRAPHY PURIFIED MARIGOLD LUTEIN USING HEXANE AND ETHYL ACETATE SOLVENT MIXTURE.....	63

CHAPTER	PAGE
5.1 Introduction	63
5.2 Materials and methods	65
5.2.1 Materials and chemicals	65
5.2.2 Preparation of lutein sample	66
5.2.3 SAS Micronization of lutein	67
5.2.4 Evaluation of particle morphology, MPS, and PSD of micronized lutein samples	70
5.2.5 Particle characterization	70
5.2.5.1 X-ray powder diffraction (XRD)	70
5.2.5.2 Fourier Transform Infrared Spectrometer (FT-IR)	70
5.2.5.3 Dissolution test	70
5.3 Results & discussion	71
5.3.1 Micronization of lutein by supercritical anti solvent (SAS)	71
5.3.1.1 Effect of pressure	71
5.3.1.2 Effect of lutein initial concentration	73
5.3.1.3 Effect of SC-CO ₂ flow rate	75
5.3.2 Characterization of micronized lutein	77
5.3.3 Dissolution of micronized lutein particles	79
5.4 Conclusions	80
 VI CONCLUSIONS & RECOMMENDATIONS	 82
6.1 Conclusions	82
6.2 Research contributions	83
6.3 Recommendations	84

	PAGE
REFERENCES.....	86
APPENDIX.....	95
VITA.....	102

LIST OF TABLES

TABLE	PAGE
2.1	Composition of lutein fatty acid esters in marigold flower.....7
2.2	T_c and P_c , of fluids used for SFE.....11
2.3	Reviews of studies on preparative scale chromatography for purification of free lutein.....14
2.4	Equations of State.....24
3.1	Purity, yield and amount of free lutein in each fractionation solutions.....42
4.1	Operating conditions for SAS micronization of lutein using DCM as solvent.....52
4.2	Operating conditions for SAS micronization of lutein using ethanol as solvent.....53
5.1	Operating conditions for SAS micronization of free lutein and resulting mean particle size (MPS) and yield.....69

LIST OF FIGURES

FIGURE	PAGE
2.1 Lutein and its commonly found diesters in marigold flowers.....	6
2.2 Structure of isomers lutein of marigold flower Sowbhagya et al., 2004.....	8
2.3 Phase diagram.....	10
2.4 Saponification of lutein fatty acid esters.....	12
2.5 Schematics of particle formation using supercritical CO ₂ . (a) RESS process, (b) SAS-EM process, (c) PGSS process, and (d) DELOS process.....	19
2.6 Part of VLEs of binary system DMSO and CO ₂ at 328.95 K ; Region A : supercritical mixture, Region B : subcritical gas, Region C : two-phases region, Region D : expanded liquid.....	22
2.7 P-x,y of CO ₂ and acetone calculated with Soave- Redlich-Kwong Equation of State (SRK-EoS).....	22
2.8 Different particle morphology obtained by SAS micronization at different state ; (a) particle morphology obtained at supercritical state, (b) particle morphology obtained at subcritical gas, (c) particle morphology obtained at two-phases region, (d) particle morphology obtained at expanded liquid state.....	23
2.9 Dripping flow of liquid from nozzle.....	26
2.10 Jet flow of liquid from nozzle as laminar regime.....	27
2.11 Jet flow of liquid from nozzle as turbulent regime.....	27
2.12 gas-mixing flow patterns.....	27
2.13 Ohnesorge chart (Shimasaki et al., 2009).....	28
2.14 The simulation of toluene droplet size changing with time at various Pressures (318 K) Werling et al, 1999.....	30
3.1 HPLC chromatogram of saponified lutein sample.....	39

FIGURE	PAGE
3.2 LC-MS chromatogram of saponified lutein sample.....	39
3.3 Separations on TLC by hexane: ethyl acetate mobile phases at various compositions: (a) hexane: ethyl acetate = 100:0 v/v, (b) hexane: ethyl acetate = 90:10 v/v, (c) hexane: ethyl acetate = 80:20 v/v, (d) hexane: ethyl acetate = 70:30 v/v, (e) hexane: ethyl acetate = 60:40 v/v.....	40
3.4 HPLC chromatograms of lutein sample after liquid chromatography purification ; (a) fraction 2-4, (b) fraction 8-9, (c) fraction 10-17, (d) washed solution.....	44
3.5 H-NMR chromatograms of lutein sample after chromatographic purification.....	44
4.1 Chemical structure of lutein	46
4.2 SEM image of un-processed lutein sample.....	49
4.3 Schematic of supercritical anti solvent apparatus.....	51
4.4 SEM images of SAS micronized lutein samples using DCM as solvent at 55 °C, 0.25 ml/min solution flow rate, and at pressure (a) 10 MPa (b) 12 MPa for 20 ml/min CO ₂ flow rate, and (c) 10 MPa (d) 12 MPa for 25 ml/min CO ₂ flow rate.....	57
4.5 PSD of SAS micronized lutein samples using DCM as solvent at 55 °C, 0.25 ml/min solution flow rate, and at pressure (a) 10 MPa (b) 12 MPa for 20 ml/min CO ₂ flow rate, and (c) 10 MPa (d) 12 MPa for 25 ml/min CO ₂ flow rate.....	58
4.6 SEM images of SAS micronized lutein samples using ethanol as solvent at 55 °C, 0.25 ml/min solution flow rate and pressure (a) 10 MPa (b) 12 MPa for 20 ml/min CO ₂ flow rate and (c) 10 MPa (d) 12 MPa for 25 ml/min CO ₂ flow rate.....	60

FIGURE	PAGE
4.7 PSD of SAS micronized lutein samples using ethanol as solvent at 55 °C, 0.25 ml/min solution flow rate, and (a) 10 MPa (b) 12 MPa for 20 ml/min CO ₂ flow rate, and (c) 10 MPa (d) 12 MPa for 25 ml/min CO ₂ flow rate.....	61
5.1 Chemical structure of lutein (C ₄₀ H ₅₆ O ₂ , M.W. = 568.87).....	63
5.2 Schematic diagram of SAS micronization apparatus.....	68
5.3 SAS micronized lutein samples: (a) fine powder obtained at 8 MPa, (b) agglomerated particles obtained at 10 and 12 MPa.....	72
5.4 SEM images of SAS micronized lutein samples obtained at 50 °C, 0.5 ml/min solution flow rate, 20 ml/min CO ₂ flow rate, 2.5 mg/ml lutein concentration, and at various pressures (a) 8 MPa, (b) 10 MPa, (c) 12 MPa (sample number 2, 5, and 3).....	73
5.5 SEM images of SAS micronized lutein samples obtained at 50 °C, 10 MPa, 0.5 ml/min solution flow rate, 20 ml/min CO ₂ flow rate, and various lutein concentrations (a) 1.5 mg/ml, (b) 2.5 mg/ml, (c) 3.2 mg/ml (sample number 4, 5, and 6).....	74
5.6 SEM images of SAS micronized lutein samples obtained at 50 °C, 8 MPa, 0.25 ml/min solution flow rate, 2.5 mg/ml lutein concentration, and various CO ₂ flow rates (a) 15 ml/min, (b) 20 ml/min, (c) 25 ml/min (sample number 7, 8, and 9).....	76
5.7 PSD of SAS micronized lutein samples obtained at 50 °C, 8 MPa, 0.25 ml/min solution flow rate, 2.5 mg/ml lutein concentration, and various CO ₂ flow rates (a) 15 ml/min, (b) 20 ml/min, (c) 25 ml/min (sample number 7, 8, and 9).....	77

FIGURE	PAGE
5.8 XRD pattern of SAS micronized lutein samples; (a) un-processed lutein (b) SAS micronized lutein sample obtained at 50 °C, 8 MPa, 0.25 ml/min solution flow rate, 2.5 mg/ml lutein concentration, and 15 ml/min CO ₂ flow rates	78
5.9 FTIR Transmission of lutein samples; (a) un-processed lutein (b) SAS micronized lutein sample obtained at 50 °C, 8 MPa, 0.25 ml/min solution flow rate, 2.5 mg/ml lutein concentration, and 15 ml/min CO ₂ flow rates	79
5.10 Dissolution profile of (a) un-processed lutein and (b) SAS micronized lutein sample obtained at 50 °C, 8 MPa, 0.25 ml/min solution flow rate, 2.5 mg/ml lutein concentration, 15 ml/min CO ₂ flow rates (dissolution conditions at 37 °C, rotating speed of 100 rpm, 15 mg of samples in 500 ml of medium solution (pH=1.2)).....	80

CHAPTER I

INTRODUCTION

1.1 Motivation

Marigold flower is becoming known as of the most important sources of lutein, a type of xanthophylls that possesses many health beneficial effects such as reducing the failure of the eyesight due to age-related macular degeneration (AMD) and preventing coronary heart disease and cancers (Mingchen et al., 2006, Sowbhagya et al., 2004).

Lutein found in their natural sources including fruits, vegetables and marigold flowers generally exists in the form of lutein fatty acid esters that must first be converted to the free form by saponification with alkali solution before it can be taken up by human (Olmedilla et al., 2003, Khachik et al., 1995, Khachik et al., 2001). The recovery of free lutein from marigold flowers therefore involves extraction of lutein esters with an organic solvent, generally hexane, followed by drying off the hexane to obtain marigold oleoresin, which was then saponified with KOH or NaOH in alcohol to free lutein. Alternatively, the environmentally friendly and non-toxic extraction solvent such as supercritical carbon dioxide (SC-CO₂) can also be used so as to provide milder extraction conditions (Palumpitag et al., 2011). In addition, with this process, product isolation can readily be carried out by depressurization of the system (Facundo et al., 2009). The resulting oleoresin can further be saponified in the same described above.

The resulting saponified product yet contains other impurities such as soap, oil and un-reacted lutein fatty acid esters, and therefore further purification process is required. Crystallization is a common and easy process to purify free lutein from the saponified solution, however the process results in rather low purity (Vechpanich et al., 2011). Although high purity lutein could be achieved by re-crystallization, the process requires several steps, making it rather complicated, and could thus lower the overall yield. Alternatively, liquid chromatography is extensively used to purify high value compounds from natural product due to high purity and yield given. The

isolation procedure on such analytical scale high performance liquid chromatography (HPLC) used to identify and quantize the compounds has been reported in existing literatures for free lutein derived from different raw materials, including fruits, vegetables and marigold flowers (Jiang et al., 2005, Alisa et al., 2009, Dias et al., 2009). However, very few reports were found on chromatographic purification of lutein in a larger scale aiming to isolate a certain amount of a purified. The first of the three parts of the proposed study therefore aims to study the purification of lutein derived from marigold flowers by using larger scale of semi-preparative and preparative liquid chromatography. Silica gel coated thin layer chromatography (TLC) was firstly employed for screening suitable composition of hexane:ethyl acetate mixture that was used as mobile phase. The possibility of lutein purification in semi-preparative and preparative column chromatography was then investigated using the suitable mobile phase from the previous TLC test and silica gel as stationary phase.

Lutein has various applications such as being a natural colorant and an antioxidant. Moreover, it is able to reduce the risk of ocular diseases, provide protective effect against cardiovascular diseases and stroke, and increase the elasticity and hydration of the skin by reducing the peroxidation process of skin lipids. (Bartlett et al., 2004, Landrum et al., 2001, Moeller et al., 2008, Asplund, 2002, Hak et al., 2004, Lee et al., 2004, Palombo et al., 2007). Unfortunately, lutein has poor water solubility causing low oral and dermal bioavailability. One approach to improve water solubility of lutein is by micronization technique which leads to increased particle surface area, thus the dissolution rate increases and subsequently bioavailability. However, due to its antioxidant activity, lutein becomes easily oxidized in the presence of oxygen (degradation), with light or at moderate temperatures, problems arise when employing conventional micronization processes such as in milling and grinding due to the frictional heat generated.

In the past decades, there has been increasing number of studies that involve various means of particle micronization using supercritical carbon dioxide (SC-CO₂) as a processing medium (Miguel et al., 2008, Franceschi et al., 2008, Wu et al., 2005). Since CO₂ is non-toxic, the processes are safe and environment friendly, and since they are operated at milder conditions, making the processes particularly suitable for

heat-sensitive compounds. Of these techniques, supercritical anti-solvent (SAS) micronization is one of the simplest processes and is suitable for compounds that have rather low solubility in SC-CO₂. In a typical SAS process, a solution in an organic solvent is flown through a nozzle into a chamber simultaneously with SC-CO₂, which acts as an anti-solvent. Mass transfer between the solution and the fluid thus occurs, leading to the supersaturation state, which then results in the formation of the solute particles. Moreover, by the continuously flowing of CO₂ during this process, the organic solvent residues can be removed from interested solute, providing the solvent-free product without a complex process (Can et al., 2009). The achievement of the SAS process can be predicted by phase equilibrium of the system (solute, organic solvent and carbon dioxide). SAS micronization must be conducted at the supercritical state, since at this conditions, CO₂ would behave as an anti-solvent.

Therefore, in the second part of this research, the SAS technique using CO₂ as an anti-solvent was employed for micronization of marigold derived lutein particles, due to its near zero solubility in CO₂ at our operating conditions (Gomez-Prieto et al., 2007). Because their binary phase equilibrium data with CO₂ are available in literature (Tsvintzelis et al., 2004), dichloromethane (DCM) and ethanol were chosen as solvents in which lutein was dissolved prior to the SAS experiments. The effects of micronization operating conditions including pressure and SC-CO₂ flow rate on the morphology, MPS and PSD of the resulting particles were investigated.

In addition, in the last part of this study, the feasibility of employing SAS technique was investigated for micronization of marigold derived purified lutein dissolved in mixture of hexane:ethyl acetate which used as mobile phase in previous liquid chromatography purification. This solvent system was hardly used in previous SAS micronization study, and to our knowledge, the phase equilibrium data with CO₂ are not available. Nevertheless, the success of SAS micronization using such solvent system will imply that a step of solvent evaporation from the eluted samples and re-dissolving the dried sample into another organic solvent can be omitted. By this, not only the process cost can be reduced, the degradation of lutein during complicated processing steps can also be minimized. Here, the effects of SAS conditions for lutein micronization such as pressure, initial concentration of lutein and SC-CO₂ flow rate on mean particle size (MPS), particle size distribution (PSD), particle morphology

were determined in this study. Moreover, the crystallinity of the micronized particles was examined from the X-ray diffraction (XRD) patterns and any chemical structural changes of the micronized lutein particles compared to un-processed lutein were examined by the analysis of Fourier transform infrared (FTIR) spectrum. Furthermore, the solubility in aqueous solution of micronized lutein and un-processed lutein were also investigated.

1.2 Objectives

1.2.1 To find the suitable mobile phase for purification of saponified lutein by normal phase chromatography system.

1.2.2 To investigate effects of pressure and SC-CO₂ flow rate on the particle micronization of lutein by SAS technique using dichloromethane (DCM) and ethanol as solvent.

1.2.3 To investigate effects of pressure, SC-CO₂ flow rate, initial concentration of lutein on the particle micronization of lutein by SAS technique using the suitable mobile phase from liquid chromatography purification as solvent.

1.3 Working scopes

1.3.1 For the normal phase chromatography, silica gel was used as a stationary phase and the mobile phase employed was the mixture of hexane and ethyl acetate at various compositions (100:0, 90:10, 80:20, 70:30, and 60:40).

1.3.2 Investigate the chromatographic separations in a normal phase semi-preparative (8×240 mm) and preparative column (35×240 mm) based on the suitable mobile phase.

1.3.3 Investigate effect of lutein micronization by SAS using DCM and ethanol as solvent such as pressure (8, 10, 12 MPa) and SC-CO₂ flow rate (20 and 25 ml/min) on the characteristics (particle size distribution, morphology) of the resulting particles.

1.3.4 Investigate effect of lutein micronization by SAS using the suitable mobile phase from liquid chromatography purification as solvent such as pressure (6.5, 8, 10, 12 MPa), SC-CO₂ flow rate (20 and 25 ml/min) and initial concentration of free lutein

(1.5, 2.5, 3.2 mg/ml) on the characteristics (particle size distribution, morphology, crystal configuration, dissolution rate) of the resulting particles.

1.4 Expected benefits

1.4.1 To obtain necessary process protocols for purification of free lutein by preparative column chromatography useful for the future process development in a pilot and industrial scale system.

1.4.2 To obtain suitable SAS micronization conditions of free lutein that provides high product quality.

CHAPTER II

LITERATURE REVIEWS

2.1 Marigolds

Marigold is a popular plant grown widely in South Asia and Southeast Asia including Thailand, and is normally used for making garland, used for religious or other Buddhism ceremonies. There are various species of marigold flower including *Tagetes erecta* (American Marigold), *Tagetes patula* (French marigold) and *Tagetes tenuifolia* (Marigold signet). Despite the traditional use of, marigold flowers, the pigments in marigold petals have now been popularly used as natural colorants in food and feed. In addition, it is well perceived as the most important natural source of lutein; an active pharmaceutical ingredient (API).

2.2 Lutein & lutein fatty acid ester

Lutein ($C_{40}H_{56}O_2$) whose molecular structure is shown in Figure 2.1 is major xanthophylls that present in marigold flowers. It is also found in various sources such as fruits, vegetables, and egg yolk. However the best source is marigold. Generally, the lutein in natural source usually was found in form of lutein fatty acid esters. In marigold flowers, lutein fatty acid esters content range between 3.8 and 791 mg/g. The major lutein fatty acid ester in marigold is lutein palmitate and the other lutein fatty acid esters are dimyristate, myristate palmitate, palmitate stearate, and distearate (Table 2.2) (Sowbhagya et al., 2004).

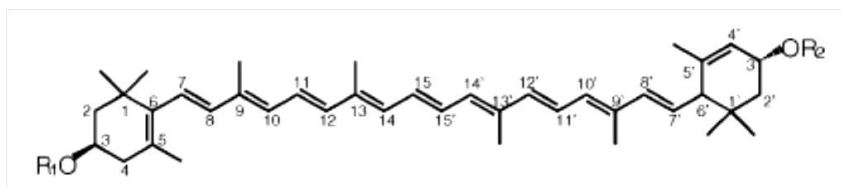


Figure 2.1 Lutein and its commonly found diesters in marigold flowers.

Table 2.1 Composition of lutein fatty acid esters in marigold flower⁵

Lutein fatty acid esters	Structure of lutein fatty acid esters	
	R1	R2
Free lutein	OH	OH
Monomyristate	OH	OCO(CH ₂) ₁₂ CH ₃
Monopalmitate	OH	OCO(CH ₂) ₁₄ CH ₃
Monostearate	OH	OCO(CH ₂) ₁₆ CH ₃
Dimyristate	OCO(CH ₂) ₁₂ CH ₃	OCO(CH ₂) ₁₂ CH ₃
Myristate palmitate	OCO(CH ₂) ₁₂ CH ₃	OCO(CH ₂) ₁₄ CH ₃
Dipalmitate	OCO(CH ₂) ₁₄ CH ₃	OCO(CH ₂) ₁₄ CH ₃
Palmitate stearate	OCO(CH ₂) ₁₄ CH ₃	OCO(CH ₂) ₁₆ CH ₃
Distearate	OCO(CH ₂) ₁₆ CH ₃	OCO(CH ₂) ₁₆ CH ₃

⁵Rong Tsao et al., 2004

The lutein fatty acid esters must be converted to free lutein before it can be absorbed and metabolized by human body. Although lutein fatty acid esters can be hydrolyzed in the body, the process for conversion of lutein fatty acid esters into free lutein usually involves a saponification process. Generally, free lutein is present in two forms which are trans-forms (60% – 90%) and cis-forms (10% – 40%). Some examples of different isomers of lutein in marigold such as 9-cis lutein, 13-cis lutein, 15-cis lutein, and all-trans lutein are shown in Figure 2.2 (Sowbhagya et al., 2004).

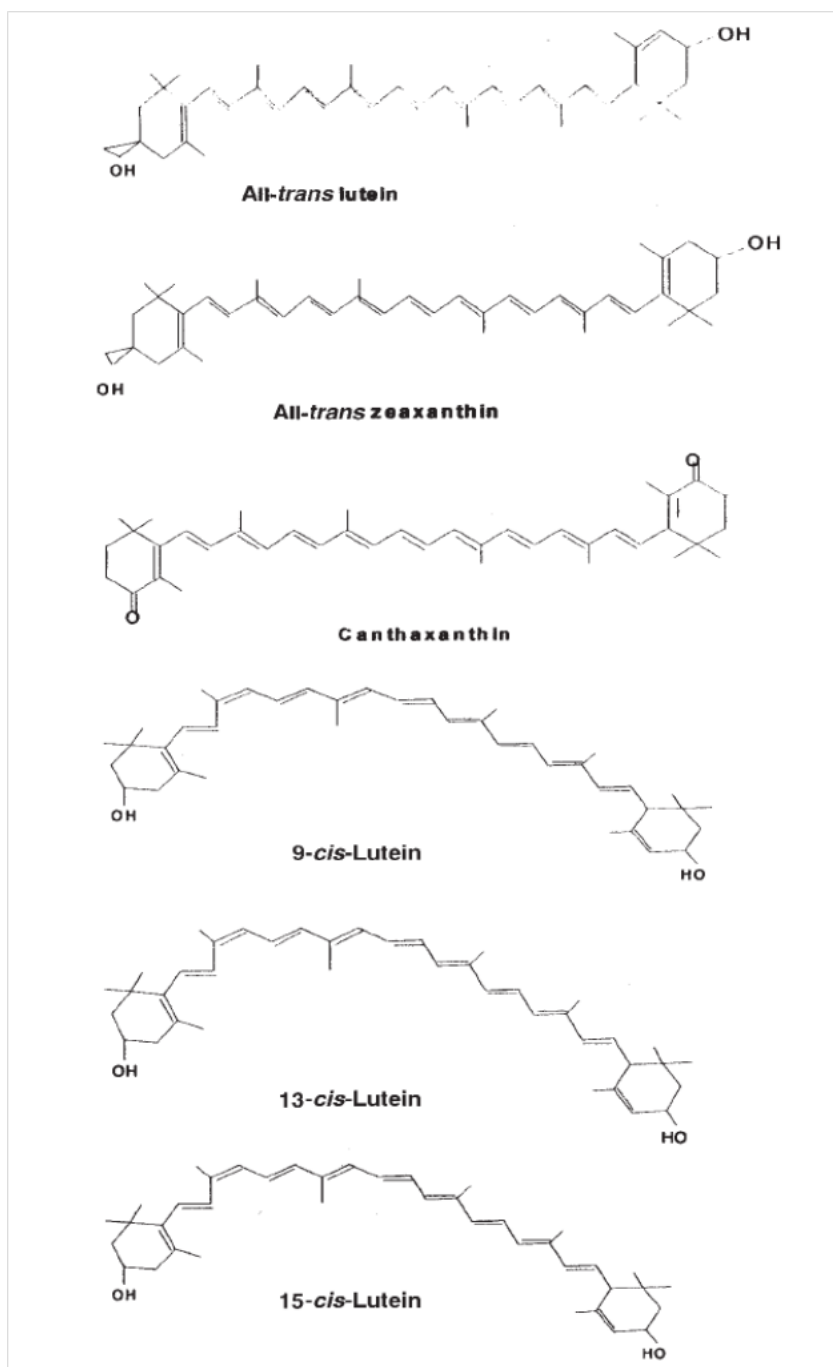


Figure 2.2 Structure of isomers lutein of marigold flower⁴

Sowbhagya et al., 2004

Lutein is used as a food coloring agent and nutrient supplement (food additive) in a wide range of industries. It has been found to have many health beneficial effects

such as supporting the eye and skin health, by reducing the failure of the eyesight due to age-related macular degeneration (AMD), coronary heart disease and cancer (Mingchen et al., 2006). Since lutein cannot be synthesized by the body, thus intake of lutein becomes essential. A 6-10 mg intake of lutein per day is necessary to realize lutein's health benefits, and extraction of lutein from marigold has nowadays gained wide interest.

2.3 Extraction of lutein fatty acid esters from Marigold Flowers

Lutein fatty acid esters can be extracted from marigold flowers by several extraction methods, such as solvent extraction and supercritical fluid extraction.

2.3.1 Solvent extraction

Solvent extraction is a technique to separate a compound from either a solid or liquid based on their relative solubility of solute compound in solvent. The sample is contacted with a solvent that will dissolve the solutes of interest. Solvent extraction is the first commercial method to choose for chemical and biochemical industries because of its simplicity and costs. Several solvents have been tested such as hexane, acetonitrile and ethanol; however hexane was found to be the most efficient solvent for extraction of lutein (Verghese et al., 1998). Due to the non-polar activity of lutein esters, more efficient solvents for its extractions are non-polar solvents. The polar solvents such as ethanol or acetonitrile have lower chemical potentials against lutein esters and consequently have lower solubility properties. Despite the simplicity of this technique, solvent extraction methods use time-consuming since it requires multiple extraction steps, uses large quantities of organic solvents that are not suitable for the production of food products.

2.3.2 Supercritical fluid extraction

A supercritical fluid (SF) is any substance at a temperature and pressure above its critical point (T_c and P_c , respectively), as indicated by the shaded region in figure 2.3. These fluids can neither be classified as a liquid or a gas and the variation of their properties is monotonous. SF can diffuse through solids like a gas, and dissolve materials like a liquid. Supercritical fluid extraction (SFE) is suitable for extraction of compounds that are easily degraded by light, oxygen and high temperatures such as natural products from vegetable and essential oil (Brunner et al., 2004). The ease of controlling the fluid property by change the temperature or pressure in order to increase the solvent power makes this technology a good option for the recovery of natural substances. SFE is an important process in the food, pharmaceutical, and cosmetic industries because it is possible to obtain products without toxic residues, without degradation of active compound, and with high purity.

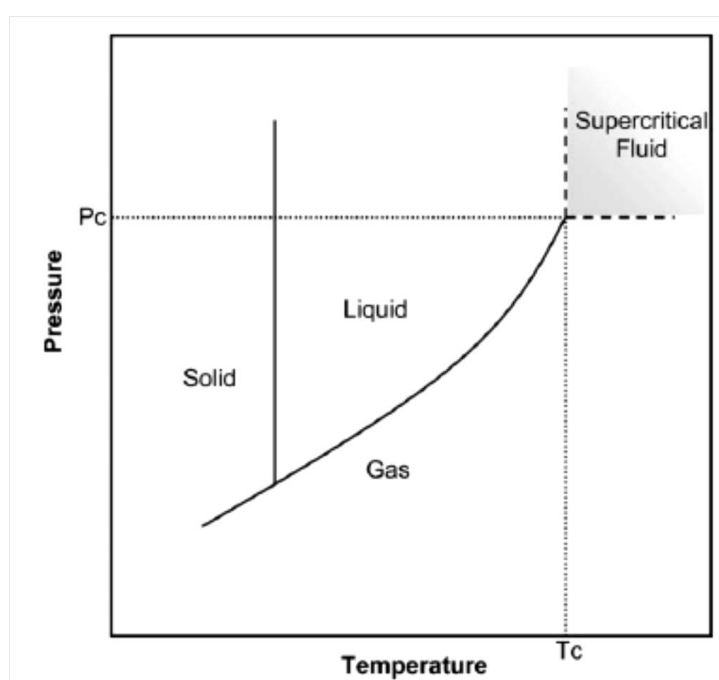


Figure 2.3 Phase diagram

Some examples of fluids that have been employed for various process applications are given in table 2.2. Carbon dioxide is the most suitable of the gases listed for natural product extraction purposes since it is not only cheap and readily available at high purity, but it is also safe due to low toxicity and environmental impact. Also, it has low critical temperature (304.1K) and therefore, supercritical

carbon dioxide (SC-CO₂) is becoming an important commercial and industrial solvent.

Table 2.2 T_c and P_c, of fluids used for SFE⁵

Solvent	T_c (K)	P_c (MPa)
Ammonia	405.4	11.35
Carbon dioxide	304.1	7.37
Dimethyl ether	400.1	5.27
Ethane	305.3	4.87
Ethylene	282.3	5.04
Methanol	512.6	8.09
n-Hexane	507.5	3.02
Propane	369.8	4.25
Water	647.1	22.06
Xenon	290.1	5.80

⁵ Facundo et al., 2009

2.4 Saponification of lutein fatty acid ester

Due to the inability to uptake lutein fatty acid esters by human (Piccaglia et al., 1998), the extract should be converted to the free form by saponification, the hydrolysis reaction of esters with metallic alkali to form an alcohol and the salt of a carboxylic acid. Sodium hydroxide (NaOH) and potassium hydroxide (KOH) were often used in metallic alkali. Generally, saponification is performed during the manufacture of commercial preparations to enhance the pigmentation value of the extract. The saponification process is shown in Figure 2.4. In this process, the lutein fatty acid esters (consist of R1 and R2 function) are converted to free lutein and obtained fatty acid salt or soap as by-product.

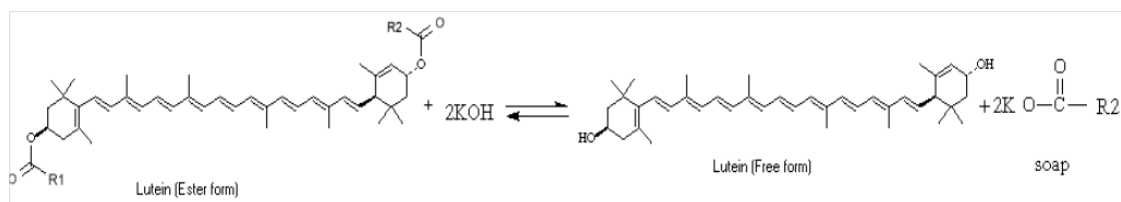


Figure 2.4 Saponification of lutein fatty acid esters

2.5 Purification of free lutein

Nowadays, the application of free lutein such as pharmaceutical and drugs is extensive. Therefore, the purification processes that give high purity free lutein must be required. Generally, crystallization is conventionally used for purifying free lutein after saponification (Khachik et al., 1995, Khachik et al., 2001), however it results in rather low purity (85.53%) (Vachpanich et al., 2011). Although high purity could be achieved by re-crystallization, the process requires several steps, making it rather complicated, and thus lowering the overall yield further.

Alternatively, the liquid chromatography technique is a more interesting process. This process employs the principle that compounds have different affinities for a stationary phase and a mobile phase. Therefore, the interested compound could be separated from the others by suitable stationary phase and mobile phase used. For stationary phase, silica gel is the commonly used. Although, the modified surface of silica gel as C18 and C30 (Curt et al., 1995, Jiang et al., 2005, Alisa et al., 2009, Dias et al., 2009) are developed to replace silica gel but the high cost of these materials is the disadvantage for the large scale liquid chromatography. To determine an appropriate mobile phase, the classical thin layer chromatography is a basic method to test the mobile phase system for liquid chromatography. Several of computer software such as DryLab and ChromSword (Snyder et al., 1997, Wolcott et al., 2000) is available for mobile phase prediction, however the prediction by these software have are still subjected to some errors, especially when applied to chromatographic purification of natural samples containing wide arrays of impurities.

To develop the liquid chromatography, the thin layer chromatography may be used to screen the suitable mobile phase and then semi-preparative liquid

chromatography column is employed to study the possibility of this purification process. The scale up factor as shown in the below equation is often used to roughly estimate the operating condition such as mobile phase flow rate, maximum sample loading and mass of silica used. Therefore, the conditions for the larger scale preparative liquid chromatography can be briefly estimated from the suitable conditions of semi-preparative scale by multiply this scale up factor with those conditions.

$$\text{scale up factor} = \frac{\left(\frac{D_2}{2}\right)^2}{\left(\frac{D_1}{2}\right)^2}$$

Where, D_1 is inner diameter of smaller column and D_2 is inner diameter of bigger column

2.6 Previous studies of liquid chromatography purification of lutein

Liquid chromatography has been developed to analyze and purify lutein in various natural sources. The summary of related studies is given in Table 2.3. Most of the previous studies employing semi-preparative and preparative liquid chromatography for the purification of lutein dealt with lutein from other sources such as *chlorella* and corn. For lutein derived from marigold flowers however, information was available only on the analytical scale HPLC. Although the larger scale semi-preparative or preparative liquid chromatography were seldom studied, relevant suitable materials for mobile and stationary phases as well as the process conditions can still be drawn from those used for the analytical scale. It is generally known that the types of mobile phase and stationary phase are important factors among many others that determine the success of the purification process. For chromatographic purification of lutein, several stationary phases have been employed, such as silica gel, C18 and C30. Compared with C18 and C30, silica gel is a lower cost packing material. However, C18 and C30 can be used for widely range of compound's polarity due to its moderate polarity. Therefore, the selection of the suitable materials should be a compromise between these several factors.

Table 2.3: Reviews of studies on preparative scale chromatography for purification of free lutein.

	Raw material	Stationary phase	Mobile phase	Results
Curt et al.,1995	six common carotenoids (lutein, zeaxanthin, β -cryptoxanthin, α -carotene, β -carotene, and lycopene)	polymeric synthesis of a C30 alkyl-bonded phase onto silica supports	A binary mobile phase of MTBE in methanol,	For all of the carotenoid isomer sets included in this work, cis-isomers were separated on the C30 phase
Shibata et al.,2004	Chlorella Powder	Flash column chromatography (30 mm i.d. \times 260 mm) on silica gel	hexane-acetone-chloroform (7:2:1 v/v)	Purity was 99% as determined by HPLC analysis. The final yield of lutein was approximately 50%
Jiang et al., 2005	marigold flowers	Eurospher-100 C 18 column (inside diameter of 4.6 mm, length of 300 mm, diameter of packing material of 5 μ m)	Acetonitrile: Methanol: Ethyl acetate with volume ratio of 55 : 1 : 44 at the flow rate of 1.0 mL/min	With acetonitrile: Methanol: Ethyl acetate solution with volume ratio of 55: 1: 44, the baseline separation of the lutein and lutein esters can be achieved.

	Raw material	Stationary phase	Mobile phase	Results
Alisa et al., 2009	Food product	C30 column (3 mL, 150 mm × 4.6 mm, YMC, Wilmington, NC)	mobile phase was methanol:MTBE: water (95:3:2, v/v, with 1.5% ammonium acetate in water, solvent A) and methanol:MTBE:water (8:90:2, v/v, with 1.0% ammonium acetate in water, solvent B (gradient))	The data from this study will provide added information to the current database for lutein and zeaxanthin content of commonly consumed foods.
Dias et al.,2009	Fruits and vegetables	reverse phase C18 (Vydac, cat. no. 201TP54), 5 µm, 250 ×4.6 mm	acetonitrile:methanol (containing 0.05 M ammonium acetate):dichloromethane, 75:20:5, v/v/v	Portuguese leafy vegetables are very good sources of lutein (0.52–7.2 mg/100 g) and B-carotene (0.46–6.4 mg/100 g).

2.7 Particle micronization

Natural compounds, drugs and Active Pharmaceutical Ingredients (APIs) including lutein have poor water solubility causing low oral and dermal bioavailability. However, they must be dissolved in water in order to exert their effects. Particle micronization is a technique whose purpose is to improve their water solubility of compounds by means of increasing particle surface areas as a result of the particle size reduction. By this, the dissolution rate increases, thus the bioavailability subsequently increases. However, there are some concerns over the conventional particle micronization such as grinding, milling, chemical precipitation and spray drying. APIs undergoing mechanical processes could be degraded by friction heat; and those undergoing chemical processes may contain toxic organic solvent residues.

2.7.1 Particle micronization by supercritical fluids

Supercritical fluids especially carbon dioxide (CO₂) has recently played an important role in separation process of natural products and APIs due to their low toxicity and environmental friendliness. As in another application, supercritical CO₂ (SC-CO₂) is employed for particle micronization, the process which has gained much interest in recent years. SC-CO₂ particle micronization can be operated at low temperature and allows easy solvent separation, recovery and recycle, since SC-CO₂ returns to gas phase at ambient temperature and pressure, while very fine and uniform particles of solvent-free product are collected. Therefore, various techniques of particle formation by SC-CO₂ have been widely studied in recent years. In this section, four main processes of particle formation by SC-CO₂ including of Rapid Expansion of Supercritical Solutions (RESS), Particle formation from Gas Saturated Solutions (PGSS), Depressurization of an Expanded Liquid Organic Solution (DELOS) and Supercritical Anti-Solvent (SAS) are reviewed. In addition, some modifications of each of these processes may be reported and given different names, nevertheless they have the same basic idea.

Rapid expansion of supercritical solutions (RESS)

In RESS system, SC-CO₂ is employed as the solute carrier. The interested solute is first dissolved in SC-CO₂ at required pressure and temperature. The solution (SC-CO₂ and solute) is then sprayed rapidly through a nozzle to a vessel at

atmospheric condition as shown in Figure 2.5 (a). The solute in SC-CO₂ is in high super-saturation state and the formation of micron-sized liquid droplets or particles occur in the vessel.

RESS was reported to be a successful system for micronization of various pharmaceuticals such as carbamazepine (Gosselin et al., 2003), griseofulvin (Hu et al., 2003), phytosterol (Jiang et al., 2003), ibuprofen (Kayrak et al., 2003) and b-sitosterol (Turk et al., 2003). In another technique such as the RESOLV (rapid expansion of a supercritical solution into a liquid solvent) process, the supercritical solution is fed into an aqueous solution containing surfactants or reducing agents. The interested solute inside the nano-droplet reacts with the surfactant or reducing agent to form nano-sized particles. However, this system has some disadvantages such as low solubility of many materials (e.g. polymers) in SC-CO₂ and a high cost technique compared with other techniques such as DELOS and SAA, which are described below.

Particle formation from gas saturated solutions (PGSS)

The PGSS system is often used for polymer formation because compressed CO₂ can dissolve into molten polymers. For this process, polymers are first melted at required temperature, and then compressed CO₂ is fed into the system. The saturated polymer solution is accordingly sprayed into a precipitation vessel as show in Figure 2.5(c). Afterwards, the solution is expanded and cooled via the Joule–Thomson effect. The fine polymer particles are produced by the very high rate of expansion of the solution and a high degree of super-cooling. The advantages of the PGSS process are low solvent gas usage, low-pressure operation, solvent-free product and a wide range of application.

Depressurization of an expanded liquid organic solution (DELOS)

SC-CO₂ is used as a co-solvent in addition to an organic solvent for the DELOS process as show in Figure 2.5(d). In the PGSS process as discussed previously, the interested substrate must be heated to liquid state and there is a problem due to thermal degradation of substrate. This DELOS technique can be useful to achieve fine particle formation with reduced substrate degradation. For

DELOS method, SC-CO₂ is mixed with the substances solution (dissolved in an organic solvent) at required temperature and pressure in a high-pressure vessel. The fine particle formation is formed in atmospheric pressure vessel. For this case, SC-CO₂ plays the role as co-solvent during the mixing and anti-solvent and viscosity reducing agent during the spraying. Another SAA (supercritical assisted atomization) process is also similar to the DELOS process except that SAA uses water as solvent.

Supercritical anti-solvent (SAS)

SC-CO₂ in SAS technique is used as an anti-solvent that reduces the solubility of a solute dissolved into a solvent. A double-tube nozzle is employed for delivery of SC-CO₂ and interested solution. The interested solute is firstly dissolved in an organic solvent and then is flowed through inner tube of the concentric nozzle. The SC-CO₂ is fed simultaneously with the solution (organic solvent and solute) through the annular cross-sectional surface of the concentric nozzle into the precipitation vessel at controlled pressure and temperature. The solution containing SC-CO₂, organic solvent and interested solute is reduced in its viscosity due to the phase behavior of CO₂ and the solubility of that solute in the liquid phase also decreases. This solution becomes supersaturated, thus forcing the interested solute to precipitate as micro-sized particles. The supercritical anti-solvent systems were further improved by adding some special equipments or adding some solvent into the systems, resulting in varieties of supercritical anti-solvent systems such as those described below.

PCA (precipitation with compressed anti-solvent) and ASES (aerosol solvent extraction system) are the same idea with SAS process in which the organic solution containing the interested solute is sprayed through a nozzle into a precipitation vessel which is filled with SC-CO₂. The solution flowed into the vessel then becomes supersaturated and the interested solute can be precipitated. The difference between ASES and PCA is the aerosol which is made from suspension of interested solute and polymer in organic solvent is used for ASES, however the dissolved solute in organic solvent is used for PCA. Mass transfer between the solvent and SC-CO₂ is enhanced and fine particles are obtained. In SEDS (solution enhanced dispersion by supercritical fluids) system, SC-CO₂ is mixed with solvent involving the interested substrate by a co-axial double nozzle, the mixed solution is sprayed into a vessel that is maintained at ambient temperature and pressure. The SEDS allows both effective

mixing and expansion of the SC-CO₂ and enables finer particles to form. The SAS-EM (supercritical anti-solvent with enhanced mass transfer) process is an improved SAS technique in which a special device, a sonicator, is added to the system and is used for forming nano-sized droplets as show in Figure 2.5(b). The sonicated vibration is effective for preventing particle agglomeration in nozzle and the smaller droplets are contained.

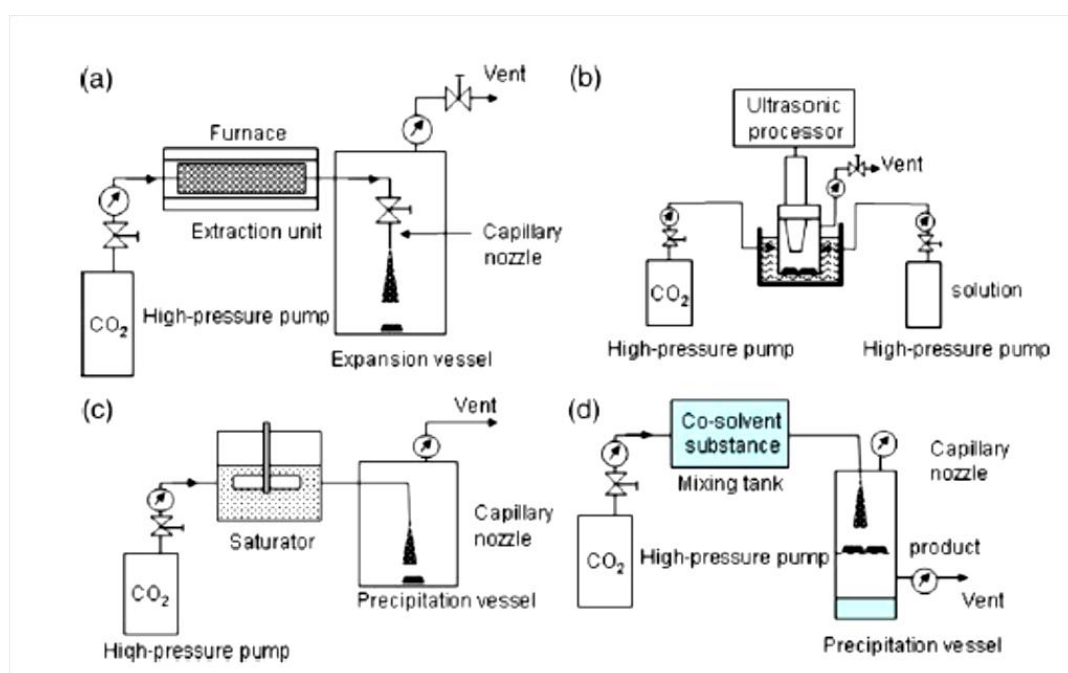


Figure 2.5 Schematics of particle formation using supercritical CO₂. (a) RESS process, (b) SAS-EM process, (c) PGSS process, and (d) DELOS process.

2.8 Mechanisms of supercritical anti solvent (SAS) micronization

Generally, the aims of particle micronization are to achieve small mean particle size (MPS), narrow particle size distribution (PSD) and good particle shape. However, a good control of size, size distribution and morphology of micronized particle by SAS technique requires understanding of the fluid phase equilibrium of the system, jet characteristic (droplet formation), the mass transfer kinetics between the jet (solute solution) and the continuous phase (anti solvent), and the nucleation and growth mechanisms. Phase equilibrium data (normally P_{x,y}-diagram) of the system is used for prediction of suitable operating points which should be carried out at

supercritical state because CO₂ acts as anti-solvent and results in formation of fine particle. The three mechanisms of hydrodynamic relaxation, mass transfer relaxation, and supersaturation and nucleation occurred in SAS process (Dukhin et al. 2005). In the initial hydrodynamic relaxation process, there is no mass transfer between the organic solvent and anti-solvent, the solvent stream is flown into the surrounding fluid (CO₂). Therefore, the flow pattern of organic solvent could be classified by the principal regimes of liquid phase dispersion or jet characteristic observed for liquid–liquid and liquid–gas systems (Badens et al., 2005). The different organic solvent droplet formations can be induced by different flow regimes;(i) the dripping regime, in which the droplets are formed at the outlet of the nozzle; (ii) the laminar regime, in which the solvent was flowed smoothly and continuously before a break-up zone where uniform size droplets are formed; (iii) the turbulent regime, in which the jet surface becomes irregular and the resulting non-uniform droplets are formed as stretched and small broken droplets. For mass transfer relaxation, beyond the hydrodynamic relaxation and during which there is mutual mass-transfer between the solvent droplet and surrounding fluid. At the single supercritical condition, the surrounding fluid can largely diffuse into organic solvent droplet. As a result, the solute solution immediately reached the supersaturation state and then fine particles are formed (supersaturation and nucleation). Therefore, for better understanding at these mechanisms of fluid phase equilibrium, jet characteristic, mass transfer, and nucleation and growth which affect the SAS process, each mechanism is reviewed below.

2.8.1 Phase equilibrium of CO₂ and organic solvent

As previously described in SAS system, SC-CO₂ is utilized as an anti-solvent which reduces the solubility of solute in organic solvent. With the introduction of SC-CO₂ into the system, the solute becomes supersaturated, and then precipitated as fine particles. Generally, phase equilibrium of CO₂ and organic solvent mixture is investigated prior to the SAS operation, in order to predict suitable range of operating conditions of system.

To explain phase equilibrium of CO₂ and organic solvent mixtures, p-x,y isothermal diagram is often used. An example of phase equilibrium data for CO₂ in

DMSO obtained and presented by Reverchon et al. (2011) at 328.95 K is shown in Figure 2.6. From this Figure, the critical points of the system were determined as the highest points on the p-x, y diagram. The different areas in Figure 2.6 represent the different state of the mixture. Area A, B, C, and D are the supercritical state, subcritical gas state, two-phases region and expanded liquid state, respectively. SAS experiments must be operated at area A within the supercritical state, at the operating conditions ranging from near to far above the mixture critical point (as show in Figure 2.7), since at this conditions, CO₂ would behaves as an anti-solvent. However, the SAS operating conditions carried out at supercritical state, subcritical gas, two-phases region and expanded liquid have been studied by several research groups and the different results were observed at different states of the mixture. For supercritical state, the spherical particle as shown in Figure 2.8(a) should be obtained theoretically because solute is completely precipitated from spherical organic solvent droplet. However, the various particle morphologies could be observed due to the effect of the other mechanisms (jet characteristic, mass transfer or nucleation and growth). For subcritical gas, the non-uniform morphology and wide range particle size distribution as shown in Figure 2.8(b) were obtained since the SAS conducted at this condition prefers evaporation. For two-phase region, dense cake particle as shown in Figure 2.8(c) might be obtained and no observable particle can be observed in some case because carbon dioxide at this state did not act as anti-solvent, thus making the solute remain dissolved in organic solvent, which was then carried over out of system by the flowing stream of carbon dioxide, before any particle formation could occur. For expanded liquid, expanded micro-particle as shown in Figure 2.8(d) can be obtained due to the expansion of liquid mixture occurred in this state (Chang et al., 2008 and 2012).

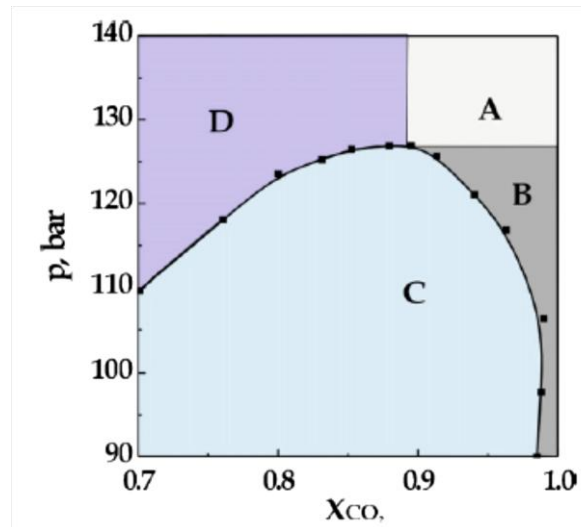


Figure 2.6 Part of VLEs of binary system DMSO and CO₂ at 328.95 K ; Region A :
supercritical mixture, Region B : subcritical gas, Region C : two-phases region,
Region D : expanded liquid

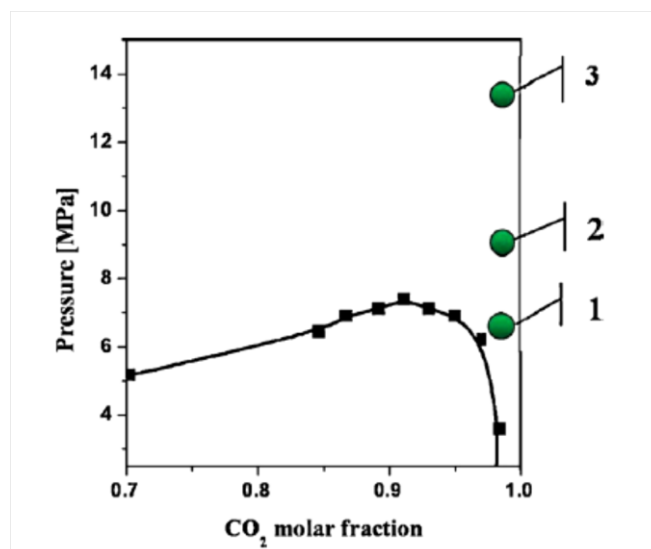


Figure 2.7 P-x,y of CO₂ and acetone calculated with Soave- Redlich-Kwong
Equation of State (SRK-EoS)

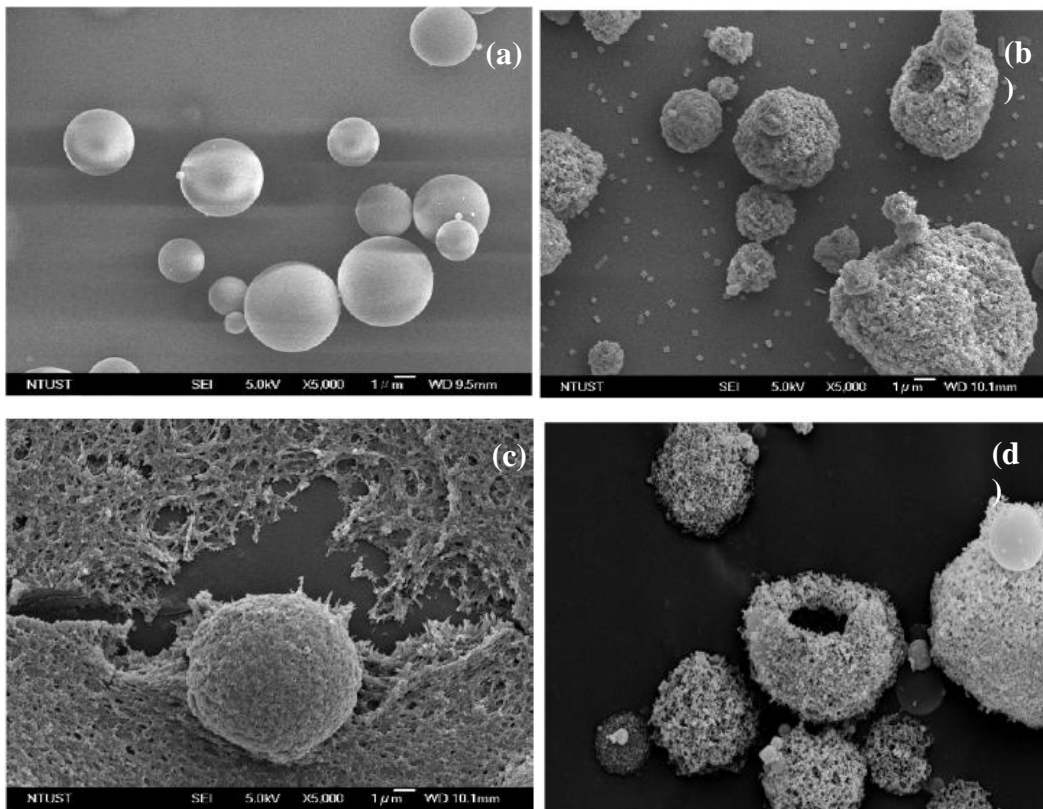


Figure 2.8 Different particle morphology obtained by SAS micronization at different state ; (a) particle morphology obtained at supercritical state, (b) particle morphology obtained at subcritical gas, (c) particle morphology obtained at two-phases region, (d) particle morphology obtained at expanded liquid state

Thermodynamic model for high pressure fluid phase equilibrium calculation

Since obtaining accurate experimental measurements of equilibrium data at high pressure are often expensive and difficult, for convenience, in some special design problem, thermodynamic models are often used to help reduce the number of experimental data points. Thermodynamic models with various Equations of State (EOS) as show in Table 2.4, and appropriate mixing rules are often used for phase equilibrium calculation of mixtures. The simplest EoS is ideal gas law (Equation 1), which applies only at low pressures or high temperatures because it neglects the volume occupied by the molecules and intermolecular forces. The ideal gas EOS can hardly be used to describe a high pressure system. Consequently, the equation which is referred to as a law of corresponding states is used in which a compressibility factor (Z) is added into the equation (Equation 2) as the generalized equation. Nevertheless, Redlich-Kwong (R-K), Soave- Redlich-Kwong (S-R-K) and Peng-Robinson (P-R)

Equation of State are used extensively in phase equilibrium calculation because they are not too complicate and give rather accurate prediction of experimental results (Franceschi et al, 2004 and 2008, Reverchon et al, 2010, Imsanguan et al, 2010).The details on thermodynamic models describing mixture phase equilibrium at high pressure can be found in previously published literatures (Dohrn et al., 1995, Fonseca et al., 2011, Martin et al., 2011).

Table 2.5 Equations of State

Name	Equations	Equation constants and Functions
(1) Ideal gas law	$P = \frac{RT}{v}$	None
(2) Generalize	$P = \frac{ZRT}{v}$	$Z = \{P_r, T_r, Z_c \text{ or } \omega\}$ or derived form data
(3) Redlich-Kwong (R-K)	$P = \frac{RT}{v-b} - \frac{a}{v^2 + bv}$	$b = 0.08664RT_c/P_c$ $a = 0.42748R^2T_c^{2.5}/P_cT^{0.5}$
(4) Soave-Redlich-Kwong (S-R-K)	$P = \frac{RT}{v-b} - \frac{a}{v^2 + bv}$	$b = 0.08664RT_c/P_c$ $a = 0.42748R^2T_c^2[1 + f_\omega(1 - T_r^{0.5})]^2/P_c$ $f_\omega = 0.48 + 1.574\omega - 0.176\omega^2$
(5) Peng-Robinson (P-R)	$P = \frac{RT}{v-b} - \frac{a}{v^2 + 2bv - b^2}$	$b = 0.07780RT_c/P_c$ $a = 0.45724R^2T_c^2[1 + f_\omega(1 - T_r^{0.5})]^2/P_c$ $f_\omega = 0.37464 + 1.54226\omega - 0.26992\omega^2$

When dealing with gas and liquids mixtures, it is necessary to define combining rules for a_{mix} and b_{mix} as shown in following equations to use the equation of state to calculate mixture properties. In this development, the Van der Waals-1 mixing rules that assume random mixing of the components is used.

$$a_{mix} = \sum_i \sum_j x_i x_j a_{ij}$$

$$a_{ij} = (a_{ii} a_{jj})^{0.5} (1 - k_{ij})$$

$$b_{mix} = \sum_i \sum_j x_i x_j b_{ij}$$

$$b_{ij} = \frac{(b_{ii} + b_{jj})}{2}(1 - \eta_{ij})$$

Where k_{ij} and η_{ij} are mixture parameters, usually determined by fitting pressure-composition data, and x denotes either liquid or gas phase mole fraction.

2.8.2 Jet characteristic of solution flow

For SAS micronization process, the organic solvent containing interested solute is simultaneously flown with SC-CO₂ into the precipitation vessel through double pipe nozzle. SC-CO₂ is flown through the annular cross-sectional surface of the concentric nozzle whereas; organic solvent is flown through the inner tube of the concentric nozzle. The hydrodynamic relaxation occurs at the early in the process as organic solvent flows out of the nozzle with the assumption that there is no mass transfer between organic solvent and anti-solvent (SC-CO₂). Therefore, it could be classified by principal regime of liquid phase dispersion or jet characteristic observed for liquid-liquid and liquid-gas systems. Although phase behavior, on the other hand, comes in to play at later stage, it determines the success of the SAS process, and the micronization conditions must lie above the mixture critical point as described in the previous section. The jet characteristic depends on many factors such as operating condition (pressure and temperature), experimental set up (nozzle type and nozzle inner diameter), nature of the organic solvent, and solution flow rate. For this section, the three principal regimes of the dripping regime, the laminar regime, and the turbulent regime are reviewed. The other gas-mixing flow pattern is also reviewed. In this case, droplets are not formed at the exit of the injector, since the liquid solution mixes with the gas phase, from which solids can nucleate and eventually grow.

For dripping regime, the solution droplets are formed at the outlet of the nozzle (as show in Figure 2.9), droplet size is therefore approximately the diameter of the inner nozzle. This droplet formation occurs at very low solution flow rate. The expected particle morphology of dripping is micro sphere due to the uniform droplet formation. However, the flow pattern can be changed from dripping regime to laminar jet or turbulent jet by the increasing of solution flow rate. For laminar regime, the liquid jet is formed smoothly and continuously before a break-up zone (as show in Figure 2.10). For the lower Reynolds numbers, the mode of laminar jet is

characterized by axially symmetrical disturbances, producing the jet break-up. The axisymmetrical jet theory has been firstly proposed by Rayleigh and the surface tension is assumed as the controlling force for the break-up of an axisymmetrical jet. Weber extended Rayleigh's theory to the break-up of a viscous jet, when both viscous and inertial forces offer significant resistance. For higher Reynolds numbers, the inertial forces compete with the capillary forces so the formation of an asymmetrical jet (a sinuous wave) can be formed. For the turbulent regime (as show in Figure 2.11), in which the jet surface presents irregularities and the resulting droplets have different sizes. This flow pattern is formed at high solution flow rate or at low value surface tension of solution flow. The various particle size, non-uniform morphology and wide particle size distribution of micronized particle are observed at this flow pattern due to the non-uniform droplet formation. For gas-mixing flow pattern (as show in Fig. 2.12), no droplet are formed, thus the SAS mechanisms are the nucleation and growth. This flow pattern can be occurred by the surface tension disappearance in jets of miscible fluids (solvent and anti-solvent) due to the increasing of pressure and resulting in nano-size particles produced.

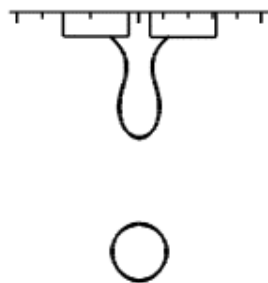


Figure 2.9 Dripping flow of liquid from nozzle



Figure 2.10 Jet flow of liquid from nozzle as laminar regime

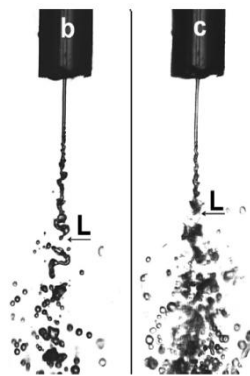


Figure 2.11 Jet flow of liquid from nozzle as turbulent regime



Figure 2.12 gas-mixing flow patterns

The jet characteristic of dispersed liquid can be predicted using dimensionless numbers: the Reynolds' number ($Re = \rho DU/\mu$; where ρ is density, D is nozzle diameter, U is liquid velocity and μ is liquid viscosity) and the Ohnesorge number ($Oh = (\mu/(D\rho\sigma))^{1/2}$; where σ is interfacial tension). The Ohnesorge chart (Shimasaki et

al., 2009) as shown in Figure 2.13 describes the dispersion modes as a function of the Reynolds number and the liquid properties. Four different zones are distinguished: the Rayleigh break-up zone or laminar flow regime, a sinuous wave, turbulent flow regime and finally the gas-mixing zone.

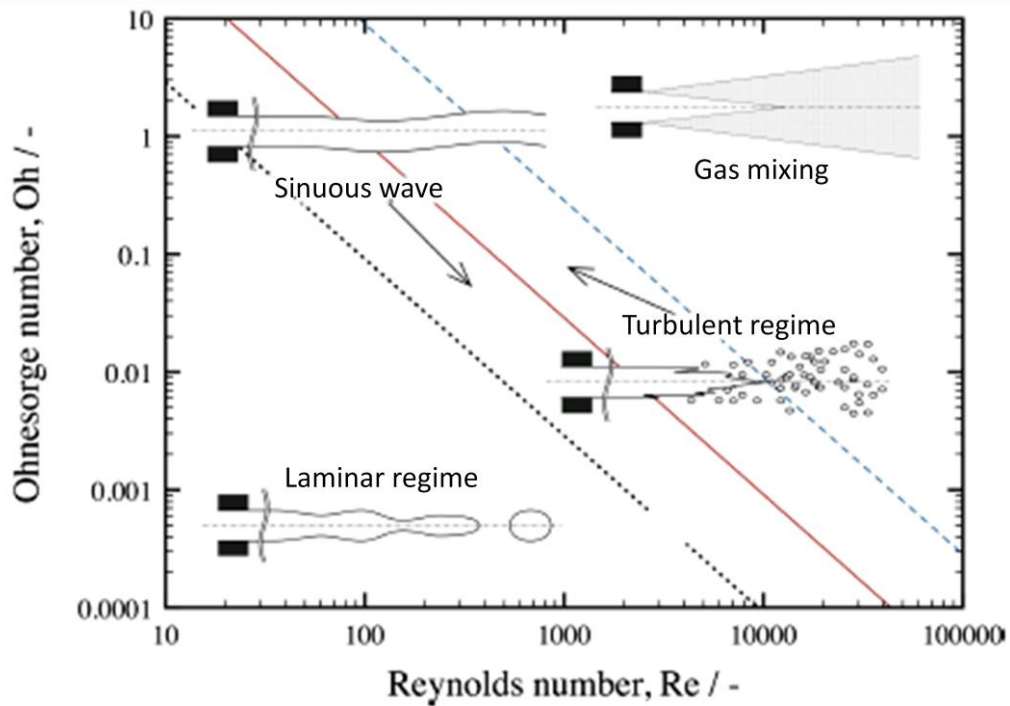


Figure 2.13 Ohnesorge chart (Shimasaki et al., 2009)

2.8.3 Mass transfer between organic solvent droplet and surrounding CO₂

Mass transfer in SAS process occurs in both directions, from the droplet to the SC-CO₂ and vice versa. The flux at interface of droplet and SC-CO₂ (\tilde{N}) as shown in following equation is used to explain mass transfer mechanism. The first term refers to mass transfer of organic solvent to the surrounding SC-CO₂ (evaporation) and second term refers to mass transfer of surrounding SC-CO₂ into organic solvent droplet (droplet swelling).

$$\tilde{N} = \left(\frac{\rho_g^* D_g^*}{x_A^* + y_B^* - 1} \right) \frac{\partial y_B}{\partial r} \Big|_{r=R} + \left(\frac{\rho_l^* D_l^*}{x_A^* + y_B^* - 1} \right) \frac{\partial x_A}{\partial r} \Big|_{r=R}$$

Where \tilde{N} is flux at interface [mol/(length² time)], ρ_g^* is density in gas phase at saturation state (mol/length³), D_g^* is modified diffusion coefficient in gas phase containing thermodynamic correction at saturation state (length²/time), ρ_l^* is density

in liquid phase at saturation state (mol/length³), \mathcal{D}_i^* is modified diffusion coefficient in liquid phase containing thermodynamic correction at saturation state (length²/time), x_A is mole fraction of CO₂ in the liquid phase, y_B is mole fraction of organic solvent in the gas phase, x_A^* is mole fraction of CO₂ in the liquid phase at saturation state, y_B^* is mole fraction of organic solvent in the gas phase at saturation state, r is radius, \mathcal{R} is instantaneous droplet radius (length).

For most organic solvent–CO₂ mixtures, the solubility of the CO₂ in the organic liquid (x_A^*) is much greater than the solubility of the organic in CO₂ (y_B^*). Therefore, the term ($x_A^* + y_B^* - 1$) is always negative. This causes the first term in the above equation to be positive, favoring evaporation, whereas the second term will be negative, favoring swelling.

This net molar flux at the interface (\tilde{N}) is a useful measure of system behavior. It is also important to know how the size of the droplet is changing with time. The following equation is used to explain droplet size changing with time.

$$\frac{d\mathcal{R}}{dt} = -\frac{1}{\mathcal{R}^2 \rho_l^*} \int_0^{\mathcal{R}} r^2 \frac{\partial \rho_l}{\partial t} dr - \frac{\tilde{N}}{\rho_l^*}$$

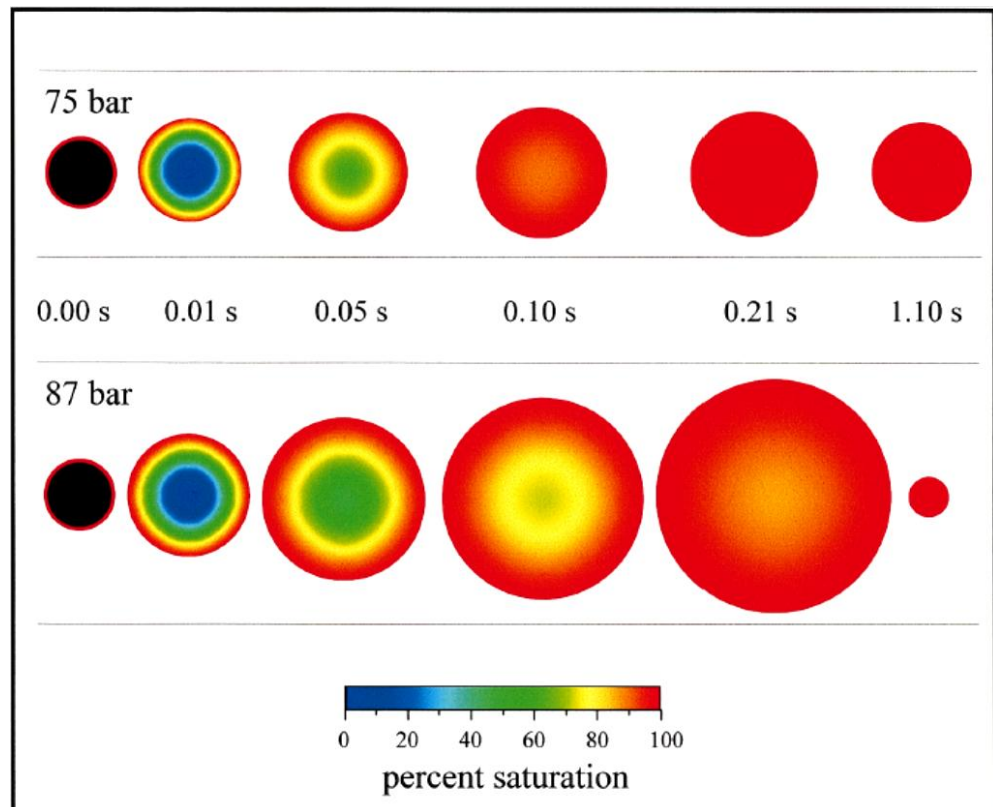


Figure 2.14 The simulation of toluene droplet size changing with time at various pressures (318 K) Werling et al, 1999.

From the equation, solvent density and net molar flux at interface are the important factors of the droplet size changing mechanism. The droplet size is become bigger when the solvent density is decreased and net molar flux is more negative value (more favoring swelling). However, the competition of solvent density and net molar flux effects may be occurred due to the pressure increase. Because the increasing of pressure leads to the solvent density increase and net molar flux is more negative value but mass transfer entering the droplet is large that the increase in density is overwhelmed, thus the droplet size increases nevertheless. As show in Figure 2.14, the droplet size of toluene reported by Werling et al, 1999 is slightly increased and then slightly decreased at 75 bar of pressure however; it is sharply increased and then suddenly shrunk at 87 bar. These increasing and decreasing of droplet size or shrinking can be explained by the net molar flux equation. For lower pressure, the mass transfer favors evaporation mechanism and CO_2 can little diffuse into the droplet then at almost saturated state the solvent is evaporated from the droplet thus, the droplet size is slightly decreased. For higher pressure, the mass

transfer favors swelling mechanism and CO₂ can largely diffuse into the droplet thus, there is large driving force difference and leads to the sudden diffusion of solvent out from the droplet resulting in the smaller final droplet size.

In addition, the characteristic time for mass transfer is normally longer than the characteristic time for droplet formation. Under these conditions, it is reasonable to assume that, by the time the jet breaks up into droplets, little CO₂ has diffused into the organic solvent. Correspondingly, the nucleation occurs later inside droplets. The driving force for the solute precipitation is supersaturation. The supersaturation inside droplet occurs due to the CO₂ diffusion in it from the CO₂. Correspondingly the kinetics of the supersaturation onset is characterized by so-called diffusion time τ_D , which is developed in

$$\tau_D \sim \frac{R^2}{D}$$

Where R is the droplet radius and D is the diffusivity in solvent to CO₂. As soon as the supersaturation becomes sufficiently large, the intradroplet nucleation starts, whose rate increases tremendously with the increasing supersaturation. The key characteristic time for the nucleation rate is the time τ_N it takes to nucleate one nucleus in one droplet. On the basis of the relative magnitudes of the characteristic times of the diffusion and of the nucleation, two different regimes are identified.

$$\frac{\tau_D}{\tau_N} \ll 1$$

When the diffusion process is rapid, i.e. when the diffusion will almost finish first, i.e. the equilibrium between the droplet and the CO₂ will establish before the first nucleus is formed. In this case, the mixture composition and correspondingly supersaturation are uniform within each droplet volume. The first nucleus will arise in the condition of the uniform supersaturation within droplets. This means that the nucleation rate is the same at any point inside droplet. This case simplifies the nucleation quantification. The diffusion-limited nucleation is expected to occur when

$$\frac{\tau_D}{\tau_N} \gg 1$$

As the diffusion is slow in comparison with nucleation, the nucleation may start not far from droplet surface as soon as the diffusion front forms here, while the anti

solvent concentration and supersaturation are negligible within the main portion of the droplet volume.

2.8.4 Nucleation and growth mechanisms

For SAS technique, the interested solute is precipitated from liquid organic solvent due to the solubility decrease by anti-solvent (SC-CO₂) thus, the nucleation and growth of interested solute become the one of the important mechanisms used to describe SAS micronization. The classical nucleation theory of homogeneous nucleation and diffusion controlled growth rate of spherical precipitates are reviewed in this section.

Nucleation

The nucleation of solute precipitated from solution can be described by the classical theory of homogeneous nucleation (Lindenberg and Mazzotti, 2009), nucleation rate (J) is given as:

$$J = A_{hom} S \exp\left(\frac{B_{hom}}{(\ln S)^2}\right)$$

Where A_{hom} is a kinetic parameter and B_{hom} is a thermodynamic parameter. A_{hom} depends on the mechanisms of attachment (Lindenberg and Mazzotti, 2009), namely interface-transfer control and volume diffusion control. According to Lindenberg and Mazzotti (2009), volume diffusion control never applies to the new nuclei formed in the solution in the early phase of growth as diffusion is infinitely fast for such particles. Therefore, it is assumed that for nucleation step, the main mechanism of attachment is the interface-transfer controlled. A_{hom} for interface-transfer control is given as (Lindenberg and Mazzotti, 2009),

$$A_{hom} = \left(\frac{4\pi}{3\omega}\right)^{1/3} \left(\frac{\gamma}{kT}\right)^{1/2} D_{AB} C^* N_A$$

and B_{hom} is defined as follows:

$$B_{hom} = \frac{16\pi\omega^2\gamma^3}{3(kT)^3}$$

D_{AB} , the diffusion coefficient is given by Stokes–Einstein equation:

$$D_{AB} = \frac{kT}{6\pi r_0 \eta}$$

where r_0 is the radius of the molecule, ω is the molecular volume, C^* is the equilibrium solid solubility in the solution, S is the degree of supersaturation, γ is the surface tension at the solid–liquid interface, k is the Boltzmann constant, N_A is the Avogadro’s number, and T is the solution temperature.

Growth

The diffusion controlled growth rate of spherical precipitates (molar composition X^p , radius R) embedded in a supersaturated solid solution (mean solute mole fraction in the matrix X , equilibrium solute mole fraction X^i at the precipitate/matrix interface) has been proposed by Zener under the assumption of small supersaturation ($X^0 - X^i \ll \alpha X^p - X^i$) and local equilibrium

$$\frac{dR}{dt} = \frac{D}{R} \frac{X - X^i}{\alpha X^p - X^i}$$

Where $\alpha = v_{at}^M/v_{at}^P$ is the ratio of matrix to precipitates atomic volumes (mean volume per atom).

Interface curvature plays an important role on equilibrium mole fraction X^i , this is the so-called Gibbs–Thomson effect. Hence, in a stoichiometric binary precipitate of composition A_xB_y , radius R and matrix/precipitate surface energy γ , precipitate/matrix interface equilibrium mole fractions X_A^i and X_B^i are modified

$$X_A^i(R)^x X_B^i(R)^y = X_A^i(\infty)^x X_B^i(\infty)^y \exp\left(\frac{2\gamma(x+y)v_{at}^P}{Rk_B T}\right)$$

Leading to the growth rate equation

$$\frac{dR}{dt_{growth}} = \frac{D}{R} \frac{X - X^i(R)}{\alpha X^p - X^i(R)}$$

CHAPTER III

PURIFICATION OF FREE LUTEIN FROM MARIGOLD FLOWERS BY LIQUID CHROMATOGRAPHY

3.1 Introduction

Marigold flower is one of the richest sources of natural carotenoids. The major carotenoid in marigold is lutein, which has been reported to be beneficial in several aspects to human health such as supporting eyes and skin, and reducing the failure of the eyesight due to age-related macular degeneration (AMD), coronary heart disease and cancer (Wang et al., 2006). Therefore, lutein has gained much interest due to its potential in nutraceutical and pharmaceutical applications.

In marigold flowers, lutein generally exists in the form of lutein fatty acid esters. Conventional method for marigold lutein fatty acid esters extraction is achieved by solvent extraction (generally using hexane). Alternatively, the environment friendly and non-toxic extraction solvent such as supercritical carbon dioxide (SC-CO₂) can also be used so as to provide milder extraction conditions (Palumpitag et al., 2011). Since only in its free form that lutein can be taken up by human body (Khachik et al., 1995, 2001), marigold extract or marigold oleoresin must therefore be saponified with an alkali solution, i.e. KOH solution, to obtain free lutein (Olmedilla et al., 2003). Unfortunately, the saponified lutein mixture contains many impurities such as soap, oil, unreacted lutein fatty acid esters. Thus, a purification process is generally required to obtain purified lutein for human applications. Crystallization is a common process for purifying free lutein, however it results in rather low yield and purity. Although high purity could be achieved by re-crystallization, the process requires several steps, making it rather complicated, and thus lowering the overall yield (Vechpanich et al., 2011).

Alternatively, liquid chromatography is extensively used to purify high value compounds from natural product. The development of an appropriate protocol (i.e.,

the optimization of mobile phase system) for chromatographic purification of a specific compound is generally performed via trial-and-error on an analytical High Performance Liquid Chromatography (HPLC). The isolation procedure on such analytical scales has been reported in existing literatures for free lutein derived from different raw materials, including fruits, vegetables and marigold flowers (Alisa et al., 2009, Dias et al., 2009). However, very few reports on chromatographic purification of lutein in larger semi-preparative and preparative scale were found.

In this work, normal phase chromatography with silica gel as a stationary phase was used for purifying free lutein from the saponified marigold oleoresin. Firstly, the suitable mobile phase system was investigated by using a thin layer chromatography (TLC), and with this suitable mobile phase, a preliminary study on an open column semi-preparative chromatography for lutein purification was conducted. Finally, a chromatographic separation was carried out on a preparative column to obtain the high purity free lutein.

3.2 Materials and methods

3.2.1 Materials and chemicals

Dried marigold flowers were obtained from PTT Global Chemical Public Company limited (Rayong, Thailand). All the samples were finely powdered prior to use. Hexane (purity>99.5%) used for solvent extraction, recovery of total xanthophylls and mobile phase of semi-preparative, preparative liquid chromatography was supplied by Sigma-Aldrich. Chemicals used for saponification such as ethanol, potassium hydroxide and hydrochloric acid were purchased from Merck, USA. Diethyl ether was supplied by Merck, Thailand. Silica gel supplied by Merck, Thailand, was used as a chromatography column packing material. Ethyl acetate supplied by Merck, Thailand, was used as one of the components in the mobile phase of semi-preparative and preparative liquid chromatography. Lutein standards (analytical grade) were purchased from Sigma-Aldrich, Germany.

3.2.2 Solvent extraction

100 grams of dried marigold powder was extracted with 500 ml of hexane in a 1 L beaker. The extraction was carried out for 4 h in a water bath whose temperature

was controlled at 40°C. After extraction, the mixture was left to stand for 20 min at room temperature to allow the residue to settle. The supernatant was isolated and the carotenoids containing hexane solution was concentrated by a rotary evaporator at 40 °C. The extract was then dried by a vacuum oven at 30 °C for 8 h. The remaining solid (marigold oleoresin) was collected and stored in a refrigerator at -20 °C for use in the next saponification step (Vechpanich et al., 2011).

3.2.3 Saponification

0.6 of gram KOH was dissolved in 10 ml of ethanol in a 125 ml flask, into which one gram of marigold oleoresin was then added. The flask was shaken at 150 rpm and 50°C for 4 h. After the reaction was completed, 50 ml of ethanol was added into the saponified mixture, and this mixture was then transferred to a separation funnel, into which 100 ml of 5% Na₂SO₄ solution (in distilled water) and 80 ml of diethyl ether were added. All components were allowed to mix, and then separated into two phases. The upper phase (ether fraction) was collected as free lutein stock solution, while the lower phase was discarded water-soluble impurities still remained in the free lutein stock solution were extracted repeatedly with water until the water phase became colorless (Shibata et al., 2004). The resulting free lutein stock solution was then stored in a -20°C refrigerator for use in a column chromatography.

3.2.4 Purification by Chromatography

3.2.4.1 Screening suitable mobile phase by thin layer chromatography (TLC)

Silica gel coated thin layer chromatography plates (TLC silica gel 60, 25 Aluminium sheets 20 x 20 cm, Merck, USA) were used for screening for a proper mobile phase. Lutein stock solution was spotted onto TLC plates, each of which was then placed in a chamber containing the mobile phase of different composition. Mobile phases tested were mixtures at various compositions of hexane and ethyl acetate (at the ratios of 100:0, 90:10, 80:20, 70:30 and 60:40 hexane:ethyl acetate).

3.2.4.2 Column packing procedures

Silica gel was suspended in hexane to the slurry at a concentration of 5% (w/v). The suspension was then degassed overnight using a sonicator. The slurry was

packed into a 8 mm × 240 mm semi-preparative open column or a 35 mm × 240 mm preparative chromatography column.

3.2.4.3 Semi-preparative open column chromatography

5 grams of silica gel slurry prepared as described above were packed into a glass column (8×240 mm) and 0.5 ml of lutein stock solution was then loaded into the semi-preparative glass column. Then mobile phase mixture of hexane: ethyl acetate (70:30 v/v) was allowed to flow by means of gravity. Fractions were collected on a one minute intervals for the HPLC analysis of free lutein content.

3.2.4.4 Preparative column chromatography

100 grams of silica gel slurry was packed into a glass column (35×240 mm). 10 ml of lutein stock solution was loaded to the column and eluted with the mixture of hexane: ethyl acetate (70:30 v/v). The sample was eluted from the bottom of the column by means of a peristaltic pump (Masterflex, model number 7523-60, Cole Parmer Thailand) at a flow rate of 10 ml/min. The fractions were collected at 10 minute intervals and were analyzed by HPLC.

3.2.5 Analysis of free lutein by high pressure liquid chromatography (HPLC)

The extracted, saponified and chromatography purified samples were analyzed by HPLC to identify luteins components in the samples. The reversed phase HPLC analysis was carried out using Agilent 1100, Lichrocart C-18 column (30 cm length), a Diode Array Detector Module 335 and an automatic injector. The mobile phase was a gradient solvent system composed of acetonitrile:methanol (9:1,v:v) (A) and ethyl acetate (B). The gradient system was run by linearly increasing solvent B from 0% to 100% over 30 min, at a flow rate of 1 ml/min. The sample injection volume was 20 µl and the detection wavelength was set at 450 nm (Piccaglia et al., 1998).

3.2.6 Analysis of saponified sample by liquid chromatography mass spectrometry (LC-MS)

The saponified sample was analyzed by HPLC to identify the lutein components. The reversed phase HPLC analysis was carried out using Agilent 1100, Lichrocart C-

18 column (15 cm length), a Diode Array Detector Module 335 and an automatic injector. The mobile phase was a gradient solvent system of acetonitrile:methanol (9:1,v:v) (A) and ethyl acetate (B), from 0% to 100% of B using a linear gradient injected over 30 min, at a flow rate of 1 ml/min. The eluents were analyzed by Bruker Daltanic Model: Esquire 3000 to confirm mass of free lutein. MS was carried out in the positive ion measurement mode with a detection voltage of 1.6 kV, an APCI temperature of 400 °C, a curved desolvation line of 250 °C, and a block temperature of 200 °C. The flow rate of the nebulizer gas was 2.5 ml/min. Full scan spectra were obtained by scanning masses between m/z 200 and 800 (Kiyotaka et al., 2008).

3.2.7 Analysis of purified sample by Hydrogen Nuclear Magnetic Resonance Spectrometry (H-NMR)

Hydrogen Nuclear Magnetic Resonance Spectrometer (H-NMR) was acquired on a Varian INOVA model. All spectra were measured in CDCl_3 at 25°C with CP/MAS solid probe and Nano probe.

3.3. Results & discussion

3.3.1 Liquid chromatography purification

HPLC and LC-MS analyses were used to determine the components of the saponified samples. The HPLC analysis results indicated that the solution consisted of two major compounds whose retention times were about 10 and 11 min, respectively (Figure 3.1). The other impurities in saponified sample were detected at retention times of about 8 and 16 min. The identification of the compounds was then carried out by Liquid chromatography mass spectrometry (LC-MS), which indicated that the two compounds were corresponding to the mass of 568 and 551, respectively, free lutein and the anhydrolutein, a lutein compound whose molecule was absent of an OH group (Figure 3.2). This anhydrolutein might be a result of oxidization in the presence of oxygen by light or at moderate temperatures (Craft et al., 1992) during the extraction and saponification processes. LC-MS result of purified sample was compared to LC-MS result of lutein standard from Molnar's work (Molnar et al., 2004). From LC-MS results, purified sample contains free lutein, anhydrolutein and

small amount of other impurities but lutein standard contains only free lutein and anhydrolutein

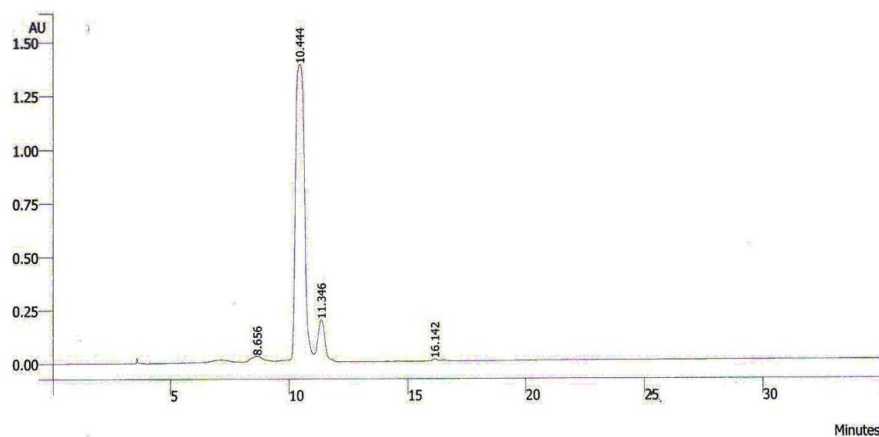


Figure 3.1 HPLC chromatogram of saponified lutein sample.

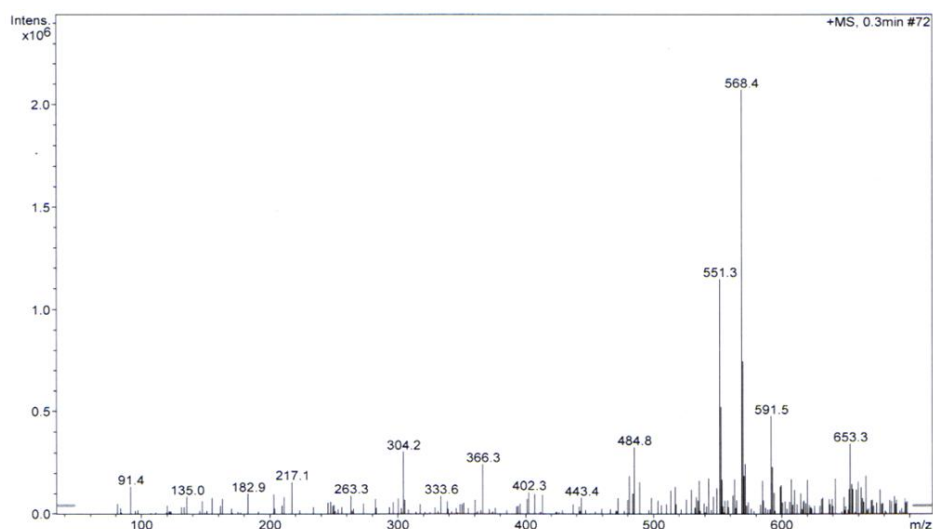


Figure 3.2 LC-MS chromatogram of saponified lutein sample.

3.3.1.1 Screening of mobile phase by thin layer chromatography (TLC)

The hexane:ethyl acetate mixtures of various compositions were tested. The results shown in Figure 3.3 indicated that the green spots of the samples were moved upwards from the base line when the mobile phase contains higher volume ratio of ethyl acetate. The most suitable ratio of the mobile phase was found to be 70:30 (hexane: ethyl acetate v/v), giving the clearest separation of the two major components.

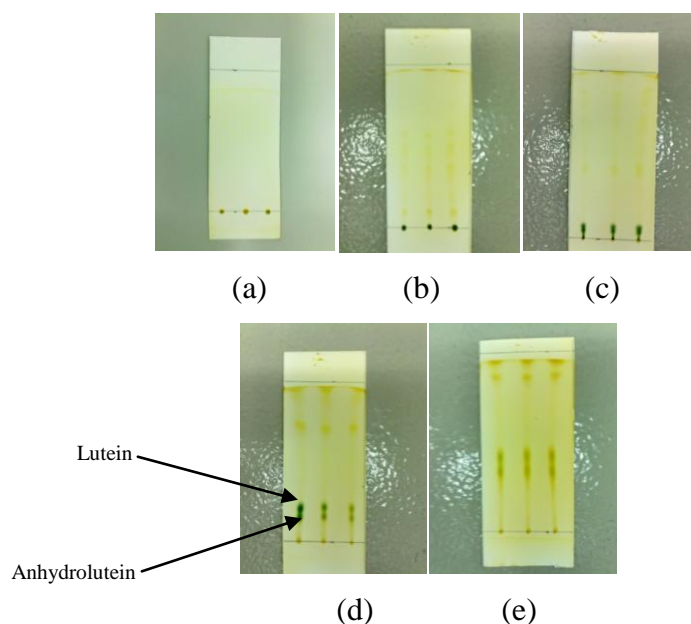


Figure 3.3 Separations on TLC by hexane: ethyl acetate mobile phases at various compositions: (a) hexane: ethyl acetate = 100:0 v/v, (b) hexane: ethyl acetate = 90:10 v/v, (c) hexane: ethyl acetate = 80:20 v/v, (d) hexane: ethyl acetate = 70:30 v/v, (e) hexane: ethyl acetate = 60:40 v/v.

3.3.1.2 Chromatographic purification on semi-preparative column

From the previous experiment, a mixture of hexane and ethyl acetate (70 : 30 v/v) shows the possibility to purify the free lutein from saponified solution. In this section, the 8 mm × 240 mm open column packed with silica and mixture of hexane and ethyl acetate (70 : 30 v/v) were used for preliminary study of free lutein purification. At this preliminary state, all the collected fractions were combined based on the color of the fractions that was observed visually on the semi-preparative columns as the samples were eluted, where two main color bands were observed: the yellow and the orange bands. The orange fractions eluted from the semi-preparative sample made up to relatively large amounts, which were expected to be mostly free lutein and its decomposed form mentioned above. Therefore the eluted fractions collected from this band were divided into 3 fractions and were analyzed by HPLC, the first and second combined fractions that were eluted from the semi-preparative column contain free lutein at rather high purity, whereas the last combined fractions of the same orange band contained the decomposed form of lutein, and thus has lower free lutein purity.

3.3.1.2 Chromatographic purification on preparative column

From the feasibility of semi-preparative column to purify free lutein, the larger scale of preparative chromatography of free lutein was studied for purifying free lutein from the saponified product. Originally, the scale up factor was calculated from the diameter of semi-preparative and preparative chromatography columns as 19.14 (Equation 3.1) which was then used to estimate the operational conditions such as mass of packing material, mobile phase flow rate and sample loading volume. For example, the scale up factor was multiplied by the previous conditions on semi-preparative open column (10 gram of packing material, 2.5 ml/min of flow rate and 0.5 ml sample loading). Consequently, the conditions estimated from this factor for the preparative chromatography column were 100 gram of packing material (silica gel), 70:30 v/v of hexane: ethyl acetate mixture mobile phase, the flow rate was at 50 ml/min and sample loading was 10 ml. However, due to the limit in the flow rate of the peristaltic pump currently employed in the study, the lower flow rate of 10 ml/min was used.

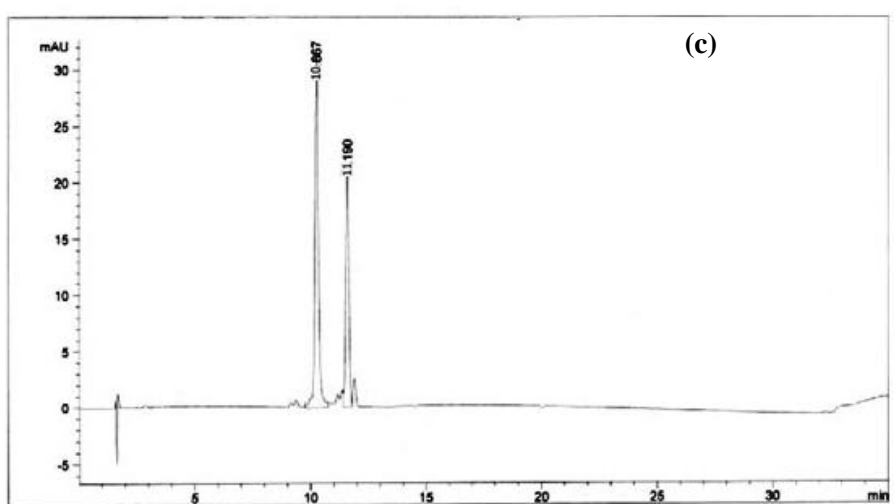
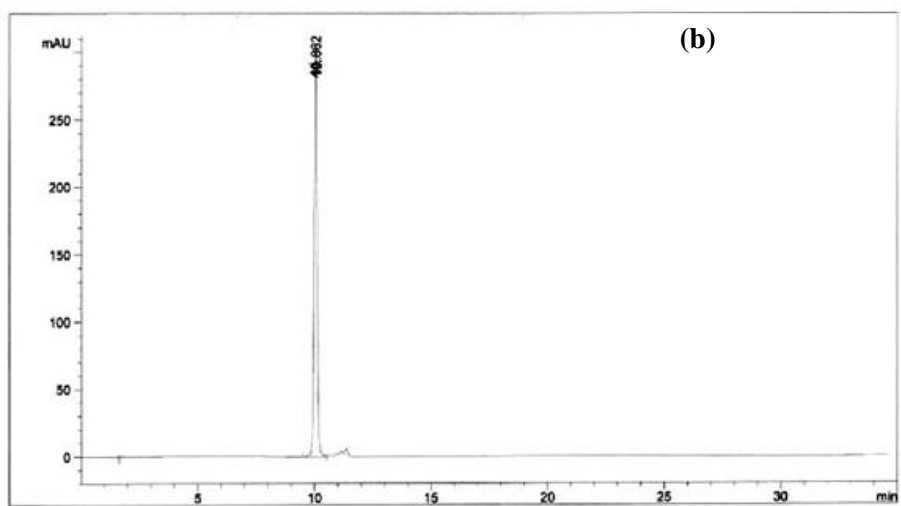
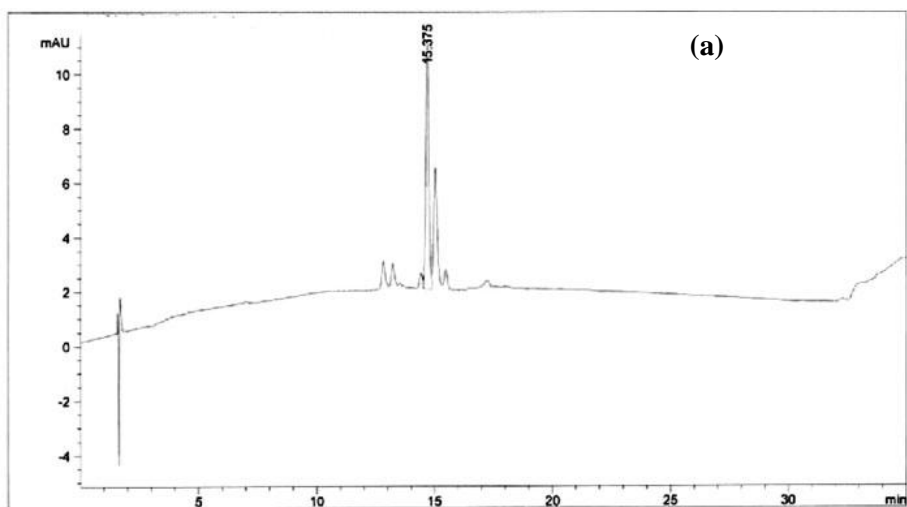
$$Scale\ up\ factor = \frac{\left(\frac{D_2}{2}\right)^2}{\left(\frac{D_1}{2}\right)^2} \quad (3.1)$$

Similar to semi-preparative purification, the two main color bands of yellow and the orange bands were observed. The purity, yield and amount of free lutein in each fractionated solutions is shown in Table 3.1. The first yellow bands were observed at fraction 2, 3 and 4 and the HPLC results show these fractions contain more impurities which were weakly adsorbed on silica gel, thus were eluted easily from the column (but eluted later from the HPLC reversed phase column) (Figure 3.4(a)). The colorless fractions were observed at fraction 5, 6 and 7 and no compound could be detected by HPLC from these fractions. The orange bands were observed in fraction 8 and 9 and the HPLC results show the higher purity of free lutein at 97.1% (based on the HPLC peak area ratios) (Figure 3.4(b)). Moreover, yield of free lutein which calculated base on the amount of free lutein in stock solution before chromatographic purification was about 61%. The mixed solution of free lutein and anhydrolutein was observed at fraction 10 to 17 (Figure 3.4(c)). The purity and yield of free lutein in these fractions were about 65% and 27% respectively. After the chromatographic separation, the

column was then washed by 100% ethyl acetate. This washed solution was also analyzed and was found to contain the impurities which were most strongly adsorbed on silica and also a small amount of free lutein (Figure 3.4(d)).

Table 3.1 Purity, yield and amount of free lutein in each fractionation solutions

Fraction number	Fraction color	Amount of free lutein detected by HPLC (mg)	% yield of free lutein (%)	Purity of free lutein (%)
1	Colorless	Not detected	0	0
2 - 4	Yellow	Not detected	0	0
5 - 7	Colorless	Not detected	0	0
8 - 9	Orange	6.43±0.38	61.78±3.63	97.1±1.85
10 - 17	Yellow	2.68±0.38	25.72±3.63	66.25±2.75
Washed solution	Light yellow	1.3±0.02	12.7±0.02	5±0.04



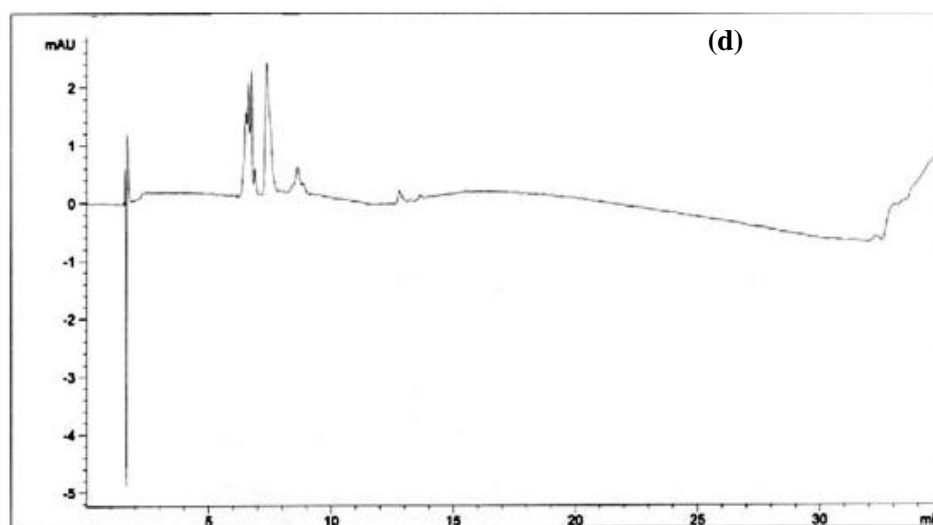


Figure 3.4 HPLC chromatograms of lutein sample after liquid chromatography purification ; (a) fraction 2-4, (b) fraction 8-9, (c) fraction 10-17, (d) washed solution.

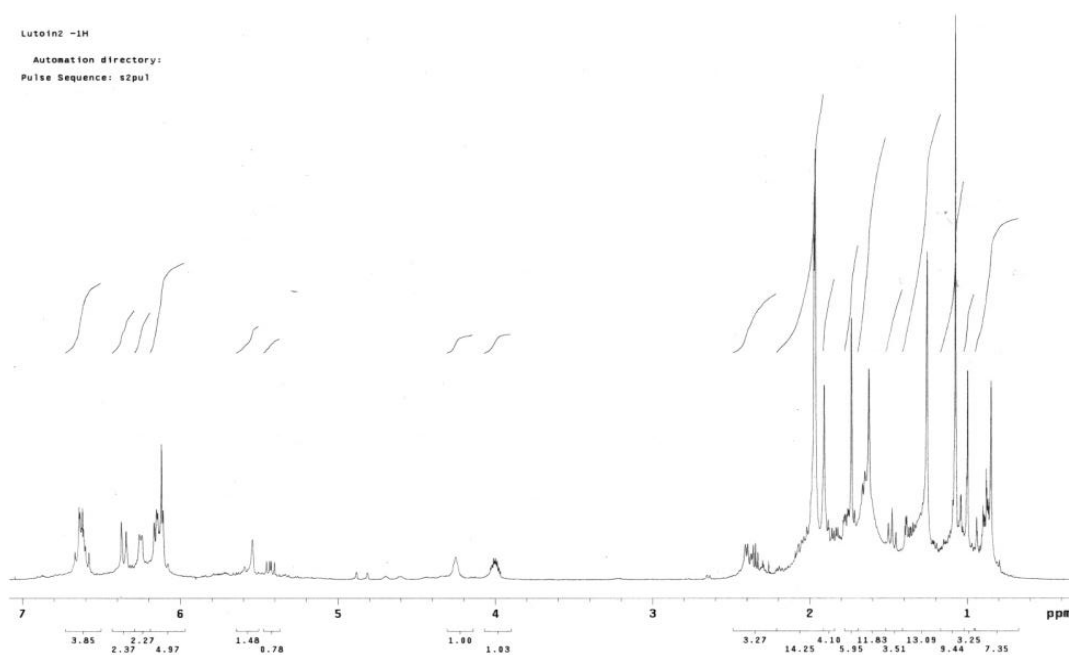


Figure 3.5 H-NMR chromatograms of lutein sample after chromatographic purification.

To confirm structure of free lutein after chromatographic purification, the purified free lutein sample was analyzed by H-NMR. The H-NMR result in Figure 3.5 showed the similar peak pattern to those of Aman's work (Aman et al., 2005) and

Khachik's work (Khachik et al., 1995). From the result, it can be concluded that the purified free lutein sample contained only free lutein, free lutein's stereoisomers and anhydrolutein. The H-NMR result thus verifies the HPLC analysis and the calculation of free lutein purify based on the HPLC peak area reported in Table 1.

3.4. Conclusions

Screening for suitability of mobile phase composition of different ratios of hexane:ethyl acetate mixture using thin layer chromatography, Hexane: ethyl acetate mixture at 70:30 volume ratio was found to be an appropriate mobile phase on the normal phase chromatography system. Semi-preparative column chromatography by using 70:30 volume ratio of hexane:ethyl acetate as mobile phase showed the feasibility for purifying free lutein from saponified solution. The scale up factor was then used to estimate the operational conditions for preparative column chromatography such as mass of packing material, mobile phase flow rate and sample loading volume. At the most suitable condition, preparative chromatography could produce high purity free lutein (>95%).

CHAPTER IV

SUPERCritical ANTI-SOLVENT MICRONIZATION OF MARIGOLD- DERIVED LUTEIN DISSOLVED IN DICHLOROMETHANE AND ETHANOL

4.1. Introduction

Lutein ($C_{40}H_{56}O_2$, MW = 568.87) whose molecular structure is shown in Figure 4.1, is an active pharmaceutical ingredient (API) that have received considerable interest as it possesses several beneficial properties such as preventing age-related macular degeneration and having high antioxidant activity (Burton et al., 1989, Granado et al., 2003). The compound has been shown to have an amorphous structure, and have the melting point of 177 °C and the heat of fusion of 27,500 kJ/mol (Miguel et al., 2008). Natural sources of lutein include various fruits and vegetables, many of which are taken as human diet. However, marigold flower is well perceived as the most important natural source of lutein currently produced commercially. Lutein is highly soluble in organic solvents such as tetrahydrofuran (THF) and chloroform (Reza et al., 2007) but almost insoluble in water. However, same as other drugs and APIs, lutein must be dissolved in water in order to exert their effects (Park et al., 2008).

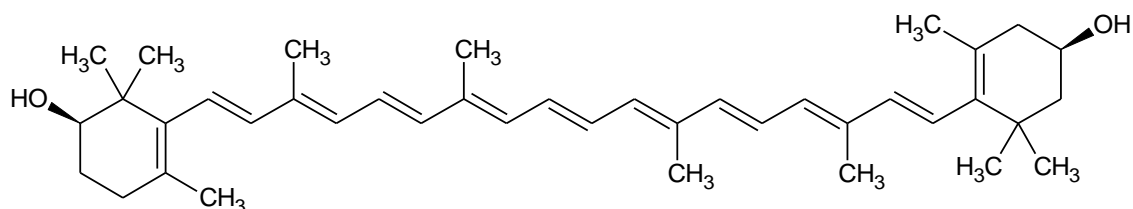


Figure 4.1 Chemical structure of lutein.

One approach to improve water solubility of drugs and APIs is by micronization of these compounds which leads to increased particle surface area (Perrut et al., 2005). Lutein made into nano-sized particles has been shown to have 76% solubility in water (Mitri et al., 2011). However, some problems arise when employing conventional micronization processes including the degradation of thermal labile compounds by frictional heat, such as in milling and grinding, and contamination with toxic solvents used in chemical method such as re-crystallization (Kwon et al., 2011).

Nowadays, techniques of particle micronization employing supercritical fluids are widely studied as they require mild operating temperatures, making the processes particularly suitable for heat-sensitive compounds. Of these techniques, supercritical anti-solvent (SAS) micronization is one of the simplest processes and is suitable for compounds that have rather low solubility in supercritical fluids. In a typical SAS process, a solution in an organic solvent is flown through a nozzle into a chamber simultaneously with a supercritical fluid, which acts as an anti-solvent. Mass transfer between the solution and the fluid thus occurs, leading to the supersaturation state, which then results in the formation of the solute particles. The particle morphology, size and size distribution are influenced by several factors such as experimental set up (nozzle type and nozzle inner diameter) and the nature of the organic solvent, as well as the operating conditions (pressure, temperature, and solution flow rate). Accurate prediction of the effects of the process variables to particle size and morphology is however difficult. This is due to the fact that SAS micronization involves several processes such as the solvent jet disintegration or solvent dispersion as it flows through the nozzle, mass transfer between the liquid jet and the supercritical anti-solvent, as well as particle nucleation and growth. Nevertheless, consideration of the mechanisms involved, together with the fluid phase equilibrium provides some basic guidelines of how particle size and morphology may be controlled (Yeo et al., 2003, Wang et al., 2006, Kim et al., 2007, Bahrami et al., 2007, Caputo et al., 2007, Reverchon et al., 2008, Byrappa et al., 2008, Badens et al., 2005).

In this study, the SAS technique using CO₂ as an anti-solvent was employed for micronization of marigold derived lutein particles, due to its near zero solubility in CO₂ at our operating conditions (Gomez-Prieto et al., 2007). Because their binary

phase equilibrium data with CO₂ are available in literature (Tsivintzelis et al., 2004), dichloromethane (DCM) and ethanol were chosen as solvents in which lutein was dissolved prior to the SAS experiments. The effects of micronization operating conditions including pressure and supercritical carbon dioxide (SC-CO₂) flow rate on the morphology, mean particle size (MPS) and particle size distribution (PSD) of the resulting particles were investigated.

4.2. Materials and Methods

4.2.1. Materials & chemicals

Dried powdered marigold flower sample was provided by PTT Global Chemical Public Company Limited (Rayong, Thailand). Hexane (purity >99.5%) used for sample preparation step was supplied by Sigma-Aldrich. Ethanol (95% purity) and potassium hydroxide (KOH, purity >99%) were purchased from Merck, USA. Diethyl ether (purity >99%), ethyl acetate (purity >99%) and sodium sulfate (Na₂SO₄, purity >99%) were supplied by Merck Ltd., Thailand. Liquid CO₂ was supplied by Uchimura Sanso Co. Ltd. (Osaka, Japan) with a purity of 99.97%. Hexane (purity >99.5%) and Ethyl acetate (purity >99%) used for SAS precipitation were supplied by Wako Pure Chemical Industries Inc. (Tokyo, Japan).

4.2.2. Preparation of lutein sample

Following the procedure described in Vechpanich et al., 2011, 100 g of dried marigold powder was extracted with 500 ml of hexane for 4 h at 40 °C in a stirred vessel whose temperature was controlled by a water bath. The system was then left to stand for 20 min at room temperature to allow the residue to settle and separate from the extract. Hexane in the extract was evaporated under vacuum at 40 °C, and the concentrated extract was further dried in a vacuum oven at 30 °C for 8 h. The dried marigold extract which is hereby called marigold oleoresin was further subjected to saponification to convert lutein in the esterified forms to the free lutein. 0.6 g KOH was dissolved in 10 ml of ethanol in a 125 ml Erlenmeyer flask, into which one gram of marigold oleoresin was then added. The flask was shaken at 150 rpm at 50 °C for 4 h. After the reaction was completed, 50 ml of ethanol was added into the saponified solution, and this solution was then transferred to a separation funnel, into which 100

ml of 5% Na₂SO₄ solution (in distilled water) and 80 ml of diethyl ether were added. All components were mixed thoroughly and the mixture was then allowed to be separated into two phases. The upper phase (the ether fraction) was collected and was then extracted with water to remove water-soluble impurities. After repeated extractions with water until the water phase became colorless, the ether upper phases were collected and combined to obtain the lutein stock solution (Shibata et al., 2004). This solution was then dried overnight in a vacuum oven. The SEM image of the resulting dried sample is shown in Figure 4.2 and the MPS was determined to be 202.3 μm. The dried sample was tightly wrapped and stored in a freezer for use in SAS micronization experiments.

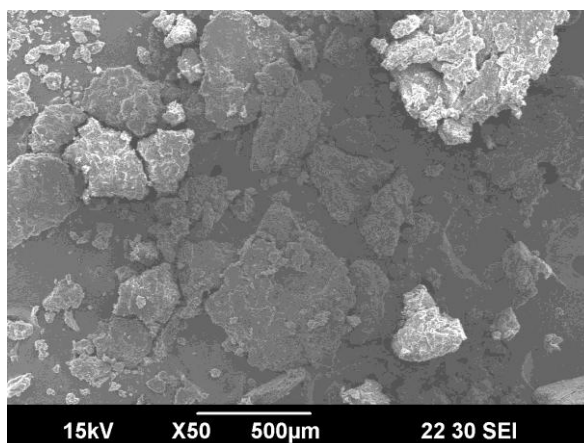


Figure 4.2 SEM image of un-processed lutein sample.

4.2.3. SAS Micronization of lutein

The apparatus for SAS micronization of lutein is shown in Figure 4.3, which consists of an LC-8A preparative liquid chromatography pump (Shimadzu, Japan), a PU-980 intelligent HPLC pump (Jasco, Japan), a cooler (Eyela Cool Ace CA 1100, Japan), a precipitation vessel (SUS316 cell, inner diameter: 3 cm, length: 17.0 cm, volume: 120.1 cm³, P-max: 30 MPa) and a double-tube nozzle (inner diameter: 1/16 and 1/8 inch) through which the CO₂ and lutein solution were delivered. The precipitation vessel was housed in a heating chamber whose temperature was controlled by air convection (AKICO, Japan T-max: 100 °C). The experiments begin with pumping liquid CO₂ through a cooler at 0 °C, to ensure the liquefaction of the gas to prevent cavitation, before being delivered to a precipitation vessel at a specified

flow rate through the annular cross-sectional surface of the concentric nozzle. The pressure of the precipitation vessel was set to a desired value by a backpressure regulator (AKICO, Japan). The temperature of the heating chamber was then set to a fixed value of 55 °C. The initial lutein solution in an organic solvent was prepared by dissolving lutein in DCM or ethanol with continuous stirring for 30 min. Although lutein solubility in DCM and ethanol at ambient temperature has been reported to be 0.8 and 0.3 mg/ml, respectively (Craft et al., 1992), at the same temperature as the SAS operating temperature (55 °C), lutein solution of higher concentration of 1 mg/ml could be prepared. The lutein solution was then pumped to the precipitation vessel by the HPLC pump, through the inner tube of the concentric nozzle. Precipitated lutein particles were trapped by a filter (SUS316, Swagelok) fixed at the bottom of the vessel. After the micronization process was completed, the flow of the lutein solution was stopped but that of pure SC-CO₂ was continued for an additional hour to ensure that all the residual solvent was removed from the lutein particles. No residual solvent could be detected by the gas chromatography (GC) analysis of the solution of micronized sample in chloroform. This was also confirmed by constantly weighing the micronized lutein sample that was placed in a rotary vacuum evaporator at 40 °C at every thirty minute interval for three hours. The SAS micronization experiments were conducted 2-3 times at some selected conditions to test the reproducibility of the results. The conditions employed for the SAS experiments with DCM and ethanol as solvents, respectively, are shown in Table 4.1 and Table 4.2, along with information on CO₂ density, Reynolds' numbers (*Re*) for solvent and CO₂ flows and the MPS of the resulted particles.

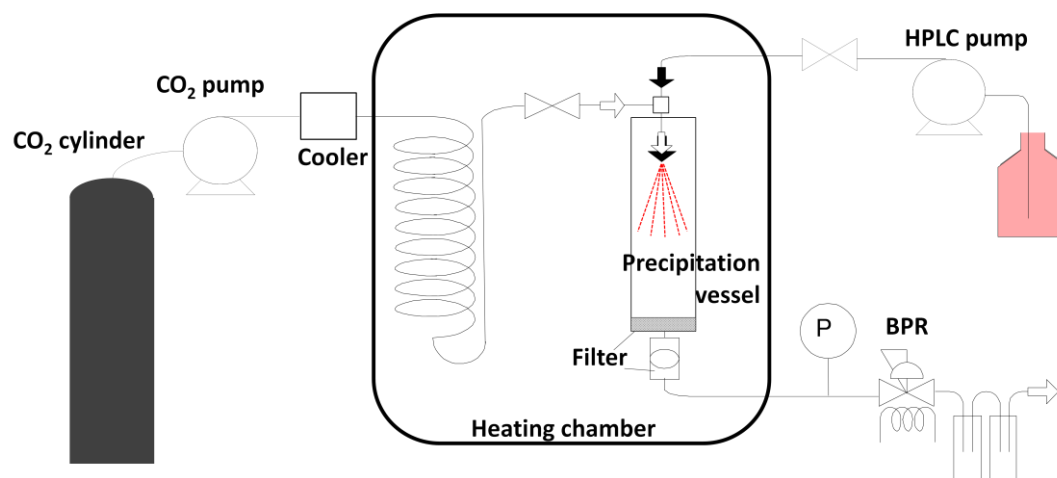


Figure 4.3 Schematic of supercritical anti solvent apparatus.

Table 4.1

Operating conditions for SAS micronization of lutein using DCM as solvent.

Sample number	P (MPa)	T (°C)	Solution flow (ml/min)	CO₂ flow (ml/min)	Density of CO₂ (kg/m³)	Re of CO₂	Re of DCM	CO₂ molar fraction*	Mean Particle size
1	8	55	0.25	20	205	8,261	489	0.935	-
2	10	55	0.25	20	303	9,543	482	0.935	2.05 μm
3	12	55	0.25	20	504	12,149	475	0.935	2.49 μm
4	8	55	0.25	25	205	10,326	489	0.947	-
5	10	55	0.25	25	303	11,929	482	0.947	1.58 μm
6	12	55	0.25	25	504	15,186	475	0.947	1.94 μm

* CO₂ molar fraction is based on the binary DCM-CO₂ system

Table 4.2

Operating conditions for SAS micronization of lutein using ethanol as solvent.

Sample number	P (MPa)	T (°C)	Solution flow (ml/min)	CO₂ flow (ml/min)	Density of CO₂ (kg/m³)	Re of CO₂	Re of ethanol	CO₂ molar fraction*	Mean Particle size
7	8	55	0.25	20	205	8,261	40.4	0.93	-
8	10	55	0.25	20	303	9,543	40.2	0.93	3.41 μm
9	12	55	0.25	20	504	12,149	40.0	0.93	1.58 μm
10	8	55	0.25	25	205	10,326	40.4	0.943	-
11	10	55	0.25	25	303	11,929	40.2	0.943	1.08 μm
12	12	55	0.25	25	504	15,186	40.0	0.943	902 nm

* CO₂ molar fraction is based on the binary ethanol-CO₂ system

4.2.4. Evaluation of particle morphology, MPS and PSD

A JEOL model JSM-6390LV scanning electron microscope (SEM) was used to examine the morphology and size of the particles. Conductive double-sided tape was used to fix the particles to the specimen holder. A thin layer of gold was sputtered onto the sample using an ion sputtering device (JEOL model JFC-1100E). In determining the MPS and PSD, 500 particles were measured using Image J analytical software.

4.3. Results and Discussion

4.3.1. SAS Micronization of lutein dissolved in DCM

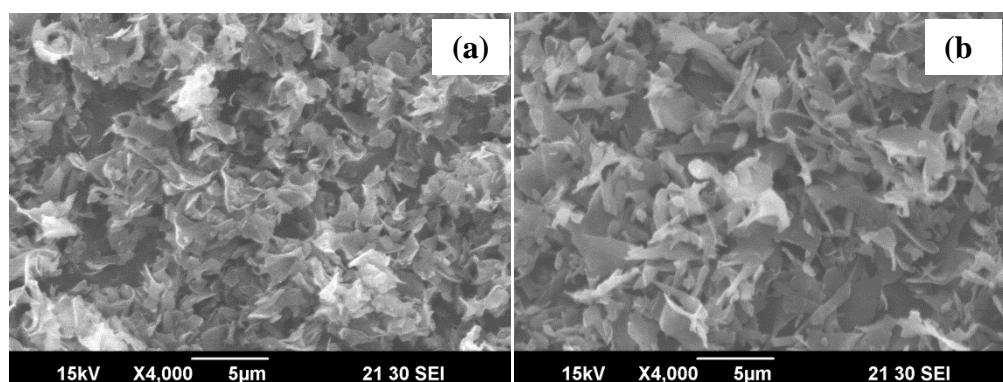
SAS micronization at various operating conditions of lutein dissolved in DCM resulted in particles of various MPS, PSDs, and morphologies. The effect of pressure (8, 10 and 12 MPa) on the morphology, MPS and PSD of lutein could be drawn from the sample numbers 1 to 3, whose operating conditions are listed in Table 4.1. At 8 MPa, no particles could be collected. This could be explained by considering the phase equilibrium data of all three components involved in the SAS process. Although the ternary data for lutein, DCM, and CO₂ are not available in literature, binary phase equilibrium data of CO₂ and DCM (Tsvintzelis et al. 2004) could be used initially to address the feasibility of the process. The fact that the operating condition at 8 MPa and 55 °C is located below the critical point of the binary mixture caused the liquid and vapor phases to coexist. Lutein then remained dissolved in the liquid organic solvent, which was then carried over by the flowing stream of carbon dioxide, through the filter, out of the micronization chamber, without forming any particles. On the other hand, the pressures of 10 MPa and 12 MPa were above the mixture critical point in which the single supercritical region is reached. At these conditions, SC-CO₂ became dissolved into the organic phase, causing the state of supersaturation, thus resulting in the production of fine particles (Figure 4.4(a) and 4.4(b)). In both cases, rather than being spherical, lutein particles have flake-like morphology, which can probably be explained by the competition of the diffusion rate of SC-CO₂ into organic solvent droplet as the solvent flowed out of the nozzle and the nucleation rate of the lutein particles. In this case, it was likely that the rate of SC-CO₂ diffusion was lower than that of particle nucleation, causing the nucleation to start as

soon as the diffusion front forms, and not far from the droplet surface. Thus, the flake-like particles whose morphology is similar to the droplet surface were formed (Dukhin et al., 2005). The results in Table 4.1 also indicated that the increase in pressure leads to the increase in lutein MPS. For the process operated at the SC-CO₂ flow rate of 20 ml/min, the increase in MPS from 2.05 to 2.49 μm was observed as the pressure increased from 10 MPa to 12 MPa, while for the SC-CO₂ flow rate of 25 ml/min, particle MPS increased from 1.58 to 1.94 μm with the same increased pressure. It should be noted that although the flake-like morphology might lead to overestimation of particle size when viewed under SEM, at all conditions, flake-like particles were obtained, thus general trend could still be drawn from the results of this present study. In addition to higher MPS, as shown in Figure 4.5, wider PSDs were observed at higher pressures. These results could largely be due to the effect of pressure on the characteristics of jet disintegration (Braeuer et al., 2011, Gokhale et al., 2007, Shekunov et al., 2001). Generally, depending on the flow rate and operating conditions such as temperature and pressure, three regimes of liquid phase dispersion are observed: (i) the dripping regime, in which the droplets are formed at the outlet of the nozzle; (ii) the laminar regime, in which the solvent flows smoothly and continuously before a break-up zone where uniform size droplets are formed; (iii) the turbulent regime, in which the jet surface becomes irregular and the resulting non-uniform droplets are formed as stretched or small broken droplets (Badens et al., 2005).

In general, the ratio of inertia force and viscous force of liquid flow, known as a Reynolds' number ($Re = \rho DU/\mu$; where ρ is density, D is nozzle diameter, U is liquid velocity and μ is liquid viscosity) can be used to estimate flow regime. The Re numbers of DCM at both pressures of 10 to 12 MPa were calculated to be about 400 (as shown in Table 1) which lie in the laminar flow regime. However Re alone could not describe such complicated system of SAS micronization. Indeed the jet hydrodynamics is determined by another important dimensionless number, namely a Ohnesorge number ($Oh = (\mu/(D\rho\sigma))^{1/2}$; where σ is interfacial tension), which relates the viscous force and the interfacial tension (Reverchon et al., 2011). However, since the data for the transient interfacial tension of our system at supercritical conditions is not available, it was not possible to estimate the Oh numbers for the systems in this

study. Despite the unavailability of Oh numbers, previous literature has shown that the interfacial tension of DCM-CO₂ and ethanol-CO₂ systems decreased with increasing pressure, and this in turn caused the transition in the modes of jet dispersion (Badens et al., 2005). At low pressure, and thus high system interfacial tension, the smooth and continuous solvent flow (laminar regime) is maintained, which results in the formation of symmetric jet and uniform drops of solvent. At higher pressure, solvent flow becomes irregular (turbulent) due to the low value of interfacial tension, thus non-uniform drops are formed. The increase in MPS and wide PSD as the pressure increased from 10 MPa to 12 MPa for this case suggested therefore that a transition from laminar to turbulent regime could have occurred.

The effects of SC-CO₂ flow rate on lutein particle morphology and MPS were observed for the SC-CO₂ flow rates of 20 and 25 ml/min at a fixed lutein solution flow rate of 0.25 ml/min. As shown in Figure 4.4(a) – 4.4(d), increasing SC-CO₂ flow rate shows no significant effect on particle morphology, that is, similar flake-like particles were observed at both SC-CO₂ flow conditions. However, the MPS of lutein decreased as the SC-CO₂ flow rate increased as shown in Table 4.1 (sample numbers 2, 3, 5 and 6). As SC-CO₂ flow rate increased, supersaturation was reached more readily as CO₂ diffuse into the droplet, resulting in precipitation of fine particles.



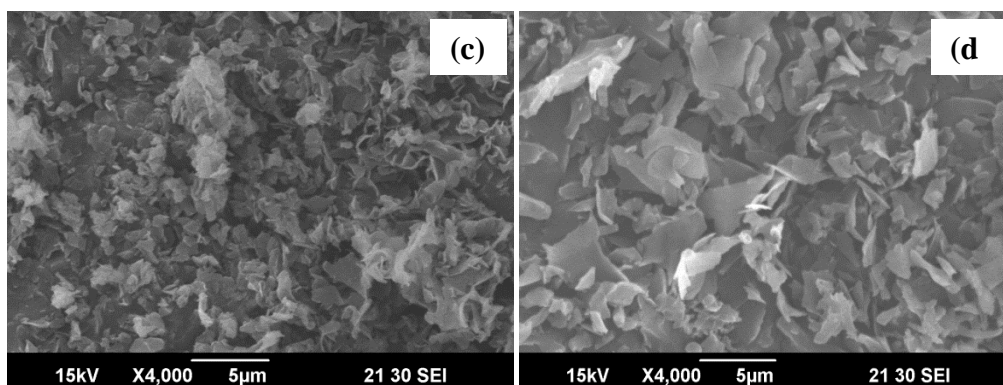
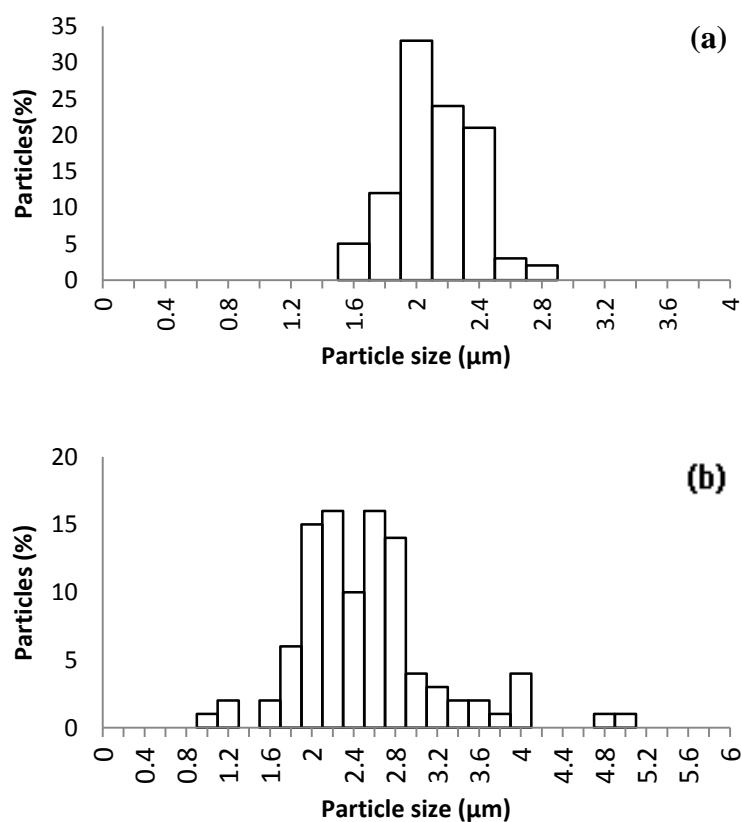


Figure 4.4 SEM images of SAS micronized lutein samples using DCM as solvent at 55 °C, 0.25 ml/min solution flow rate, and at pressure (a) 10 MPa (b) 12 MPa for 20 ml/min CO₂ flow rate, and (c) 10 MPa (d) 12 MPa for 25 ml/min CO₂ flow rate.



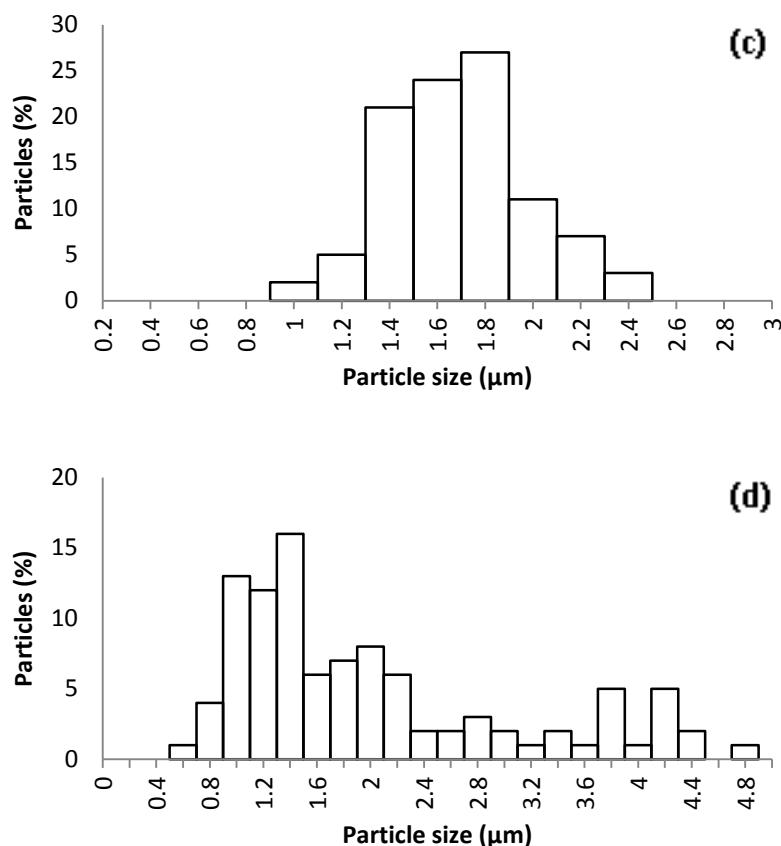


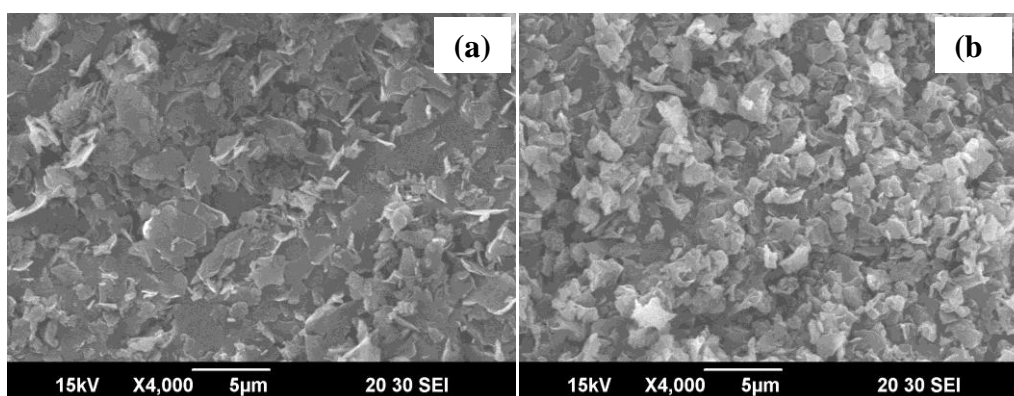
Figure 4.5 PSD of SAS micronized lutein samples using DCM as solvent at 55 °C, 0.25 ml/min solution flow rate, and at pressure (a) 10 MPa (b) 12 MPa for 20 ml/min CO₂ flow rate, and (c) 10 MPa (d) 12 MPa for 25 ml/min CO₂ flow rate.

4.3.2. SAS Micronization of lutein dissolved in ethanol

Similar to SAS micronization with DCM as a solvent, no particles could be formed by SAS micronization of lutein dissolved in ethanol at 8 MPa and 55 °C. Based on the binary phase equilibrium data reported by Tsivintzelis et al. 2004, this operating condition again was below the critical point of ethanol and CO₂ mixture and thus lie within the two phases region. Operated at higher pressures, SAS micronization at 10 MPa and 12 MPa resulted in flake-like lutein particles (Figure 4.6(a) and 4.6(b)). On the contrary to the previous results with DCM as a solvent, when ethanol was used as a solvent, the increase in pressure leads to the decrease in lutein MPS. The decrease of MPS from 3.41 to 1.58 μm and from 1.08 μm to 902 nm was observed for the SC-CO₂ flow rates of 20 ml/min and 25 ml/min, respectively.

Moreover, narrower PSDs were observed at higher pressures (as shown in Figure 4.7). The Re numbers for ethanol flow at both 10 and 12 MPa were about 40 (as shown in Table 4.2), which was similar to the system with DCM, which lie in the laminar flow regime. The decrease in MPS at higher pressure of 12 MPa however suggested that the jet dispersion characteristics of this system might be different. As the interfacial tension of ethanol- CO_2 system was reported to be lower than that of DCM- CO_2 at ambient condition (about 22 versus 28 mN/m) (Badens et al., 2005), it might be drawn from this data that at higher pressure of 12 MPa, the ethanol- CO_2 interfacial tension would also be lower and would possibly approach zero. When this is the case, jet dispersion behavior did not follow any of the three flow regimes described earlier, instead no distinct droplets are formed and the particle formation on the other hand occurred in favor of gas-phase nucleation and growth within the dispersed gas plume, resulting in very fine nano-sized particles (Reverchon et al., 2011). The decrease in lutein MPS and narrower range of PSDs observed at higher pressures in these experiments was possibly the results of this shift from droplet formation to gas mixing.

The effect of SC- CO_2 flow rate on morphology and MPS of lutein was carried out at 20 and 25 ml/min. Similar to the previous results with DCM, an increase in SC- CO_2 flow rate showed no significant effect on particle morphology: flake-like lutein particles were observed as shown in Figure 4.6(a) – 4.6(d). The decrease in MPS of lutein particles could be obtained when the SC- CO_2 flow rate is increased as shown in Table 4.2 (sample numbers 8, 9, 11 and 12).



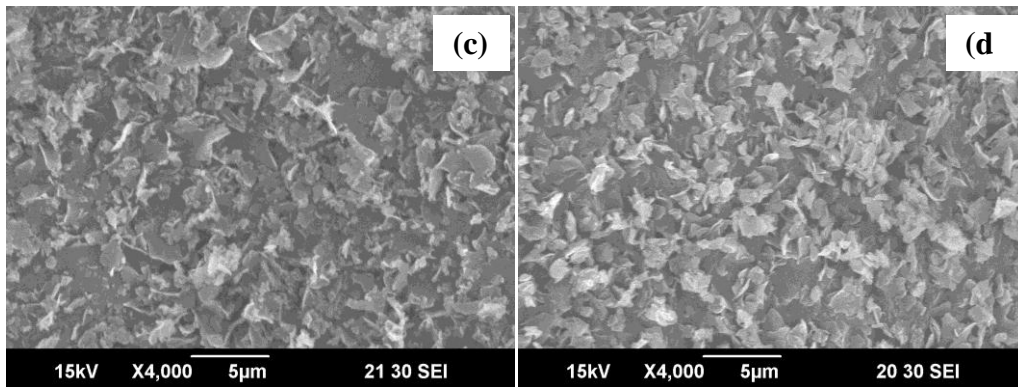
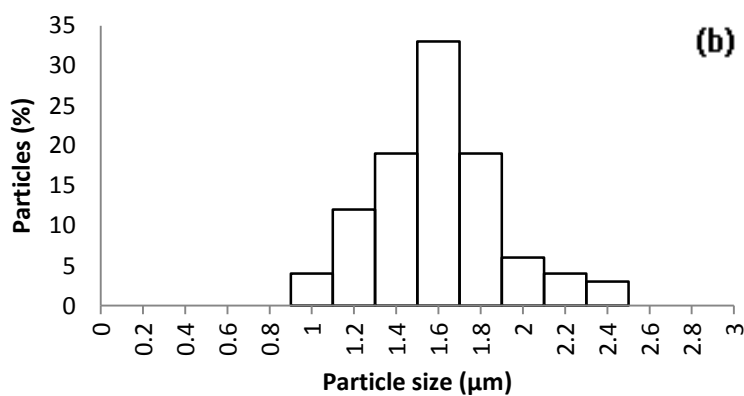
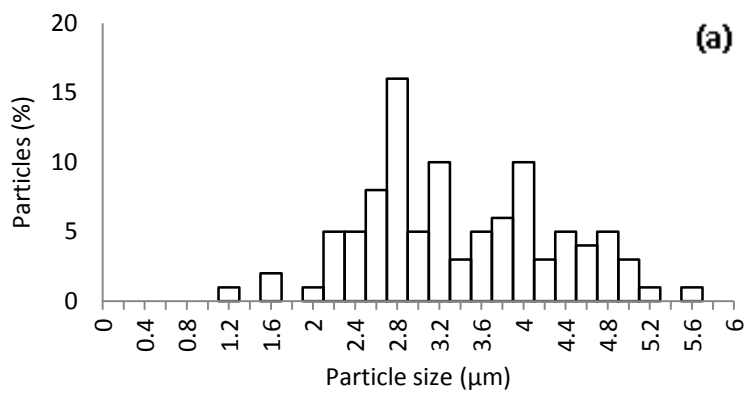


Figure 4.6 SEM images of SAS micronized lutein samples using ethanol as solvent at 55 °C, 0.25 ml/min solution flow rate and pressure (a) 10 MPa (b) 12 MPa for 20 ml/min CO₂ flow rate and (c) 10 MPa (d) 12 MPa for 25 ml/min CO₂ flow rate.



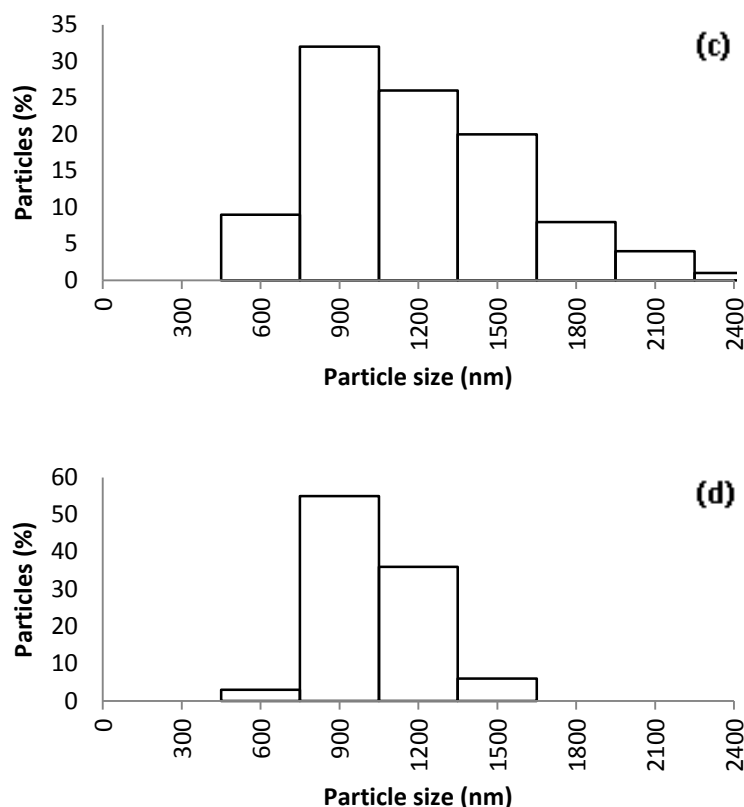


Figure 4.7 PSD of SAS micronized lutein samples using ethanol as solvent at 55 °C, 0.25 ml/min solution flow rate, and (a) 10 MPa (b) 12 MPa for 20 ml/min CO₂ flow rate, and (c) 10 MPa (d) 12 MPa for 25 ml/min CO₂ flow rate.

4.4. Conclusions

Supercritical anti-solvent (SAS) micronization using DCM and ethanol was shown to effectively produce fine particles of lutein derived from marigold flowers. In both solvent systems, the increase in pressure and SC-CO₂ flow rate did not have significant effects on lutein particle morphology. However, significant effects of increasing pressure on MPS and PSDs of lutein particles were observed. The increase in SC-CO₂ flow rate from 20 to 25 ml/min shows the reduction of MPS in both DCM and ethanol system. It is noted some loss of product was observed in this study and this was attributed to the relatively large filter pore diameter (1 μ m). Thus, filter with small pore size should be used in future study. In addition, in order to further gain better insights into the entire process, the investigations on interfacial tension and

other hydrodynamic parameters such as jet breakup lengths and diffusion lengths should be carried out.

CHAPTER V

SUPERCRITICAL ANTI-SOLVENT MICRONIZATION OF CHROMATOGRAPHY PURIFIED MARIGOLD LUTEIN USING HEXANE AND ETHYL ACETATE SOLVENT MIXTURE

5.1. Introduction

Lutein ($C_{40}H_{56}O_2$, MW = 568.87) whose molecular structure is shown in Figure 5.1, is one of the most important active pharmaceutical ingredients (APIs), which is now widely used as natural colorants. In addition, due to its high antioxidant activity, the compound exhibits other positive effects such as reducing the failure of the eyesight due to age-related macular degeneration, as well as fighting against coronary heart disease and cancers (Burton et al., 1989, Granado et al., 2003). Although lutein can be found in various fruits and vegetables, one of the richest natural sources of lutein is known to be marigold flowers (Ausich et al. 1997). Therefore, a number of studies have been conducted on extraction and purification of lutein from this source (Khachik et al., 1995, 2001, Vechpanich et al., 2011). Recently, we successfully employed preparative chromatography technique to purify marigold derived lutein to the purity up to 97%. In this process, silica gel was used as a stationary phase and a mixture of hexane:ethyl acetate (70:30 v/v) was used as a mobile phase (Boonnoun et al., 2012).

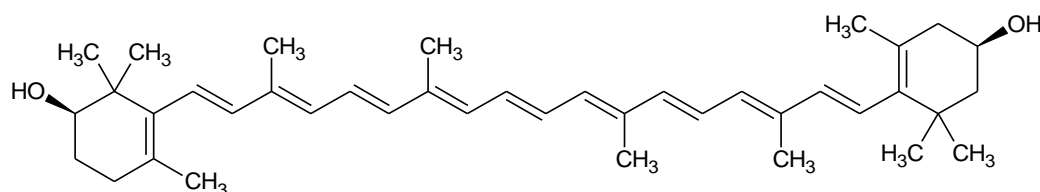


Figure 5.1 Chemical structure of lutein ($C_{40}H_{56}O_2$, M.W. = 568.87).

Despite having high medicinal activities, many APIs and lutein alike, are of low bioavailability due largely to their low solubility in water (Varughese et al., 2010). An improvement in aqueous solubility of an API can generally be achieved by micronizing it to smaller particles. As a result, the surface area increases, and thus the dissolution rate increases (Turk et al., 2006, Zhao et al., 2011). This not only helps lower the dosage requirement, it can also reduce any possible side effects associated with up-taking the compound (Su et al., 2009). However, there are some concerns over the conventional particle micronization such as grinding, milling, chemical precipitation and spray drying. APIs undergoing mechanical processes could be degraded by friction heat; and those undergoing chemical processes may contain toxic organic solvent residues.

Alternatively, supercritical fluids, especially carbon dioxide (CO₂), have recently played an important role in the processing of natural compounds, polymers, drugs and APIs. Micronization of particles with supercritical carbon dioxide (SC-CO₂) requires mild operating temperature; and is therefore suitable for thermally labile compounds. In addition, SC-CO₂ can easily be separated from the particles as it returns to gas phase at ambient temperature and pressure, leaving a solvent-free product (Can et al., 2009). Among several particle micronization techniques using supercritical fluids, supercritical anti-solvent (SAS) micronization has been widely studied due to the effectiveness of the method in making fine particles from various sources of compounds (Cho et al., 2011, Reverchon et al., 2006, Wang et al., 2006, Reverchon et al., 2004 De Marco et al., 2008). In a typical SAS process with SC-CO₂ used as an anti-solvent, the interested solute is first dissolved in an organic solvent, which is then flown simultaneously with SC-CO₂ through a nozzle. The solution becomes supersaturated, and the solute is thus forced to precipitate into fine particles. Previous research has demonstrated that beside the process conditions such as temperature, pressure, as well as solution and SC-CO₂ flow rates, the type of organic solvents in which the solute is initially dissolved also plays a key role in the formation of the particles by the SAS process (Kim et al., 2007, Gokhale et al., 2007, Obrzut et al., 2007). Common organic solvents used include ethanol and dichloromethane and their equilibrium data with CO₂ have been determined (Tsivintzelis et al., 2004). We have indeed demonstrated that SAS micronization of lutein was possible using

ethanol and dichloromethane at some specified process conditions (Boonnoun et al., 2013).

In this work, the feasibility of employing SAS technique was determined for micronization of marigold derived purified lutein that was dissolved in the mixture of hexane and ethyl acetate (70:30 v/v), the solvent used as the mobile phase for the prior chromatographic purification step (Boonnoun et al., 2012). This solvent system was hardly used in previous SAS micronization study, and to our knowledge, the phase equilibrium data with CO₂ are not available. Here, the effects of SAS micronization conditions including pressure, the initial concentration of lutein in the solvent and the supercritical carbon dioxide (SC-CO₂) flow rate were determined on particle morphology, mean particle size (MPS) and particle size distribution (PSD). In addition, the crystallinity of the micronized particles was examined from the X-ray diffraction (XRD) patterns and any chemical structural changes of the micronized lutein particles compared to un-processed lutein were examined by the analysis of Fourier transform infrared (FTIR) spectrum. Furthermore, the solubility in aqueous solution of micronized lutein and un-processed lutein were also investigated. The success of SAS micronization using the same solvent system as the mobile phase of the chromatography process will imply that a step of solvent evaporation from the eluted samples and re-dissolving the dried sample into another organic solvent can be omitted. By this, not only the process cost can be reduced, the degradation of lutein during complicated processing steps can also be minimized.

5.2. Materials and Methods

5.2.1 Materials & chemicals

Dried powdered marigold flower sample was provided by PTT Global Chemical Public Company Limited (Rayong, Thailand). Hexane (purity >99.5%) used for sample preparation step was supplied by Sigma-Aldrich. Ethanol (95% purity) and potassium hydroxide (KOH, purity >99%) were purchased from Merck, USA. Diethyl ether (purity >99%), ethyl acetate (purity >99%) and sodium sulfate (Na₂SO₄, purity >99%) were supplied by Merck Ltd., Thailand. Liquid CO₂ was supplied by Uchimura Sanso Co. Ltd. (Osaka, Japan) with a purity of 99.97%. Hexane (purity >99.5%) and Ethyl acetate (purity >99%) used for SAS precipitation were

supplied by Wako Pure Chemical Industries Inc. (Tokyo, Japan). Lutein standards (purity >90%) were purchased from Sigma-Aldrich, Germany.

5.2.2 Sample preparation

Following the procedure described in Vechpanich et al., 2011, 100 g of dried marigold powder was extracted with 500 ml of hexane for 4 h at 40 °C in a stirred vessel whose temperature was controlled by a water bath. The system was left to stand for 20 min at room temperature to allow the residue to settle and separate from the extract. Hexane in the extract was evaporated under vacuum at 40 °C, and the concentrated extract was further dried in a vacuum oven at 30 °C for 8 h. The dried marigold extract which is hereby called marigold oleoresin was further subjected to saponification to convert lutein in the esterified forms to the free lutein. 0.6 g KOH was dissolved in 10 ml of ethanol in a 125 ml Erlenmeyer flask, into which one gram of marigold oleoresin was then added. The flask was shaken at 150 rpm at 50 °C for 4 h. After the reaction was completed, 50 ml of ethanol was added into the saponified solution, and this solution was then transferred to a separation funnel, into which 100 ml of 5% Na₂SO₄ solution (in distilled water) and 80 ml of diethyl ether were added. All components were mixed thoroughly and the mixture was then allowed to be separated into two phases. The upper phase (the ether fraction) was collected and was then extracted with water to remove water-soluble impurities. After repeated extractions with water until the water phase became colorless, the ether upper phases were collected and combined to obtain the lutein stock solution (Shibata et al., 2004). This solution was then dried overnight in a vacuum oven. The dried sample was tightly wrapped and stored in a freezer for use in SAS micronization experiments. This sample if further purified by chromatography according to Boonnoun et al., 2012 lutein of up to 97% purity would be obtained. In this micronization study however, we employed the extracted and saponified lutein prepared as described earlier. The analysis of the sample by HPLC following the method given in Boonnoun et al., 2012 indicated that the purity of the sample used in this study was about 89%.

5.2.3 SAS Micronization of lutein

The apparatus for SAS micronization of lutein is shown in Figure 5.2, which consists of an LC-8A preparative liquid chromatography pump (Shimadzu, Japan), a PU-980 intelligent HPLC pump (Jasco, Japan), a cooler (Eyela Cool Ace CA 1100, Japan), a precipitation vessel (SUS316 cell, inner diameter: 3 cm, length: 17.0 cm, volume: 120.1 cm³, P-max: 30 MPa) and a double-tube nozzle (inner diameter: 1/16 and 1/8 in.) through which the CO₂ and lutein solution were delivered. The precipitation vessel was housed in a heating chamber whose temperature was controlled by air convection (AKICO, Japan T-max: 100 °C). The experiments begin with pumping liquid CO₂ through a cooler at 0 °C, to ensure the liquefaction of the gas to prevent cavitation, before being delivered to a precipitation vessel at a specified flow rate through the annular cross-sectional surface of the concentric nozzle. The pressure of the precipitation vessel was set to a desired value by a backpressure regulator (AKICO, Japan). The temperature of the heating chamber was then set to a fixed value of 50 °C, after which the lutein solution in mixture of hexane and ethyl acetate (70:30 v/v) was then pumped to the precipitation vessel by the HPLC pump, through the inner tube of the concentric nozzle. Precipitated lutein particles were trapped by a filter (SUS316, Swagelok) whose nominal pore diameter was 1 μm fixed at the bottom of the vessel. After the micronization process was completed, the flow of the lutein solution was stopped but that of SC-CO₂ was continued for an additional hour to ensure that all the residual solvent was removed from the lutein particles. At some selected conditions, SAS micronization of lutein was conducted 2-3 times to test the repeatability of the results. The purity of micronized samples was determined to be the same as before SAS micronization (89% purity). The conditions employed for the SAS experiments are shown in Table 5.1, along with the MPS and yields of the resulted particles. The yields of lutein from SAS micronization was calculated based on the equation 5.1.

$$\text{Yield of lutein} = \frac{\text{weight of free lutein final product (collected at filter)}}{\text{dry weight of free lutein before SAS precipitation}} \times 100\% \quad (5.1)$$

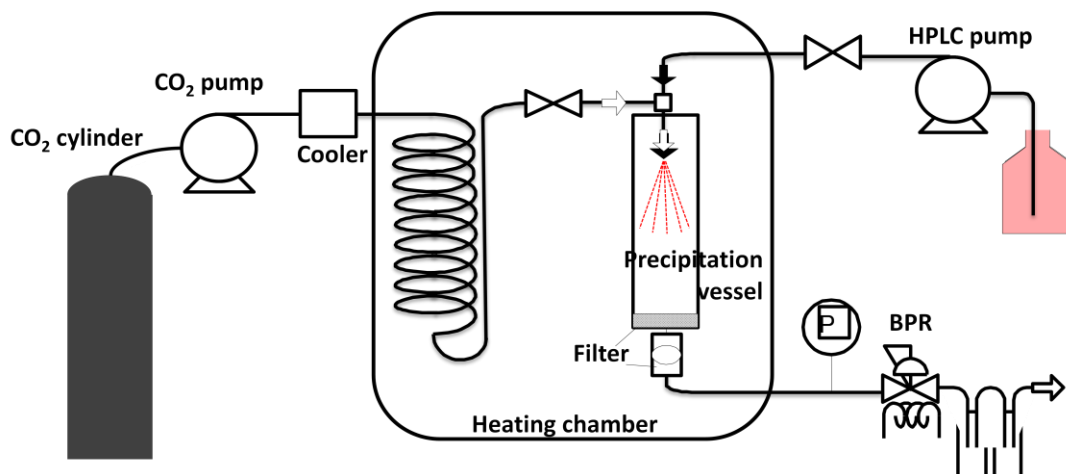


Figure 5.2 Schematic diagram of SAS micronization apparatus.

Table 5.1

Operating conditions for SAS micronization of free lutein and resulting mean particle size (MPS) and yield

Sample number	P (MPa)	T (°C)	C ₀ (mg/ml)	Lutein solution* flow rate (ml/min)	CO ₂ flow rate (ml/min)	CO ₂ molar fraction**	Mean Particle size (µm)	Yield (%)
1	6.5	50	2.5	0.5	20	0.931	-	0.0
2	8	50	2.5	0.5	20	0.931	2.1	58
3	12	50	2.5	0.5	20	0.931	Agg	30
4	10	50	1.5	0.5	20	0.931	Agg	21
5	10	50	2.5	0.5	20	0.931	Agg	23
6	10	50	3.2	0.5	20	0.931	Agg	27
7	8	50	2.5	0.25	15	0.953	2.2	67
8	8	50	2.5	0.25	20	0.964	2.0	31
9	8	50	2.5	0.25	25	0.971	0.8	27

* Lutein dissolved in the mixture of hexane and ethyl acetate (70:30 v/v)

** CO₂ molar fraction is based on the tertiary Hexane-Ethyl acetate-CO₂ system

Agg = Agglomerated particles

5.2.4. Evaluation of particle morphology, MPS, and PSD of micronized lutein samples

A JEOL model JSM-6390LV scanning electron microscope (SEM) was used to examine the morphology particles. Conductive double-sided tape was used to fix the particles to the specimen holder. A thin layer of gold was sputtered onto the sample using an ion sputtering device (JEOL model JFC-1100E). The sizes of lutein particles were analyzed. To determine the mean particle size (MPS) and particle size distribution (PSD), lutein samples were suspended into DI water and 1000 particles were measured three times by HORIBA Laser Scattering Particle Size Distribution Analyzer model LA-950.

5.2.5 Particle characterization

5.2.5.1 X-ray powder diffraction (XRD)

X-ray scattering measurements were performed on a Rigaku RAD-1B Discover diffractometer. The dried sample powders were prepared in a 0.5 mm thick specimen holder. Background (air scattering) was measured for the same sampling time, typically 30 min, and was subtracted from each measurement.

5.2.5.2 Fourier Transform Infrared Spectrometer (FT-IR)

Micronized lutein FTIR spectra was recorded between 4000 and 400 cm^{-1} in transmission/absorbance mode on FTIR Spectrum One spectrometer (Perkin-Elmer, Norwalk, USA).

5.2.5.3 Dissolution test

The dissolution test was performed for processed and un-processed lutein by SAS micronization using a USP II rotating paddle apparatus Pharmatest PTW SIII (Pharma Test, Germany) at 37 °C at rotating speed of 100 rpm in 500 ml of a buffer prepared by mixing 50 ml of 0.2 M KCl with 85 ml of 0.2 M HCl at pH 1.2. 15 mg of lutein samples were then placed in the basket which was connected to rotating paddle apparatus. Then 5 ml of liquid samples were withdrawn at selected time intervals of 5, 15, 30, 45 and 60 min. Aliquots were filtered through 0.22 μm filters and assayed by a UV spectrophotometer at 450 nm (Mitri et al., 2011).

5.3. Results and Discussion

5.3.1 Micronization of lutein by supercritical anti solvent (SAS)

5.3.1.1 Effect of pressure

The effect of pressure on the morphology of micronized lutein could be drawn from the sample numbers 1, 2, 3 and 5, listed in Table 5.1, which were obtained at 6.5, 8, 12 and 10 MPa, respectively. At 6.5 MPa however, no particles could be collected. It was possible that the condition at 6.5 MPa and 50 °C was below the mixture critical condition, thus CO₂ did not act as an anti-solvent. Thus the two phases coexisted in the system at this condition, in which the lutein remained dissolved in the organic liquid phase, which was then carried over out of system by the flowing stream of CO₂. As the pressure of the system increases to 8 MPa, the single supercritical region may have been reached, the solubility of lutein in organic solvent decreased, due to an increase of SC-CO₂ concentration in the organic liquid phase (Miguel et al., 2008). As a result, the lutein solution immediately reached the supersaturation state, resulting in the production of fine particles at 8 MPa or higher pressures. However, the resulted lutein particles have different appearances. As shown in Figure 5.3(a) and 5.3(b), fine powder with the MPS of 2.1 μm was obtained at 8 MPa, while particles obtained at 10 and 12 MPa tended to be agglomerated. Due to the agglomeration of the particles, it was difficult to measure the MPS at these conditions. Therefore, the effect of pressure on MPS and PSDs of micronized lutein could not be drawn. In addition, the agglomerated particles are likely to adhere to the wall of the precipitation vessel, resulting in much smaller yield (30%), compared with the non-agglomerated particles obtained at 8 MPa (58%), whose loss was mainly attributed to the loss of particles of smaller size than the filter pores (1 μm). At 8 MPa, the resulted particles possess the ellipsoid to spheroid morphology as shown in Figure 5.4(a). At 10 and 12 MPa on the other hand, the flake-like and the twisted leaf-like particles were obtained, respectively (Figure 5.4(b) and 5.4(c)).

The different morphologies could largely be due to the effect of pressure on the characteristics of jet disintegration (Braeuer et al., 2011, Shekunov et al., 2001). This jet disintegration occurs at the early stage in the process as organic solvent flows out of the nozzle. The jet flow behavior is connected to the presence of two distinct

fluid phases because there is no mass transfer between the organic solvent and anti-solvent at this stage. Therefore, it could be classified by principal regime of liquid phase dispersion observed for liquid–liquid and liquid–gas systems (Badens et al., 2005). Although phase equilibrium behavior, on the other hand, comes in to play at a later stage, it determines the success of the SAS process, and the micronization conditions must lie above the mixture critical point as previously described. Generally, depending on the flow rate and operating conditions such as temperature and pressure, three regimes of liquid phase dispersion are observed: (i) the dripping regime, in which the droplets are formed at the outlet of the nozzle; (ii) the laminar regime, in which the solvent was flowed smoothly and continuously before a break-up zone where uniform size droplets are formed; (iii) the turbulent regime, in which the jet surface becomes irregular (Badens et al., 2005) and the resulting non-uniform droplets are formed as stretched and small broken droplets. The ellipsoid-spheroid morphologies observed at 8 MPa suggested that the jet disintegration occurred at the laminar regime. As the pressure increased to 10 and 12 MPa, the organic solvent and CO₂ interfacial surface tension decreased, the jet disintegration entered the turbulent regime (Badens et al., 2005), resulting in irregular jet surface. As a result, non-uniform flake-like and twisted leaf-like particles were formed.

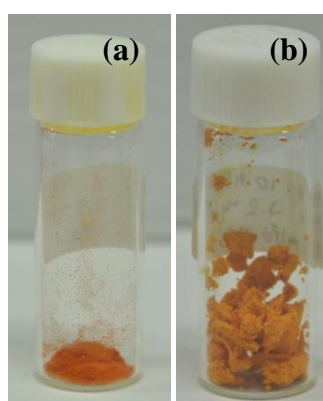


Figure 5.3 SAS micronized lutein samples: (a) fine powder obtained at 8 MPa, (b) agglomerated particles obtained at 10 and 12 MPa.

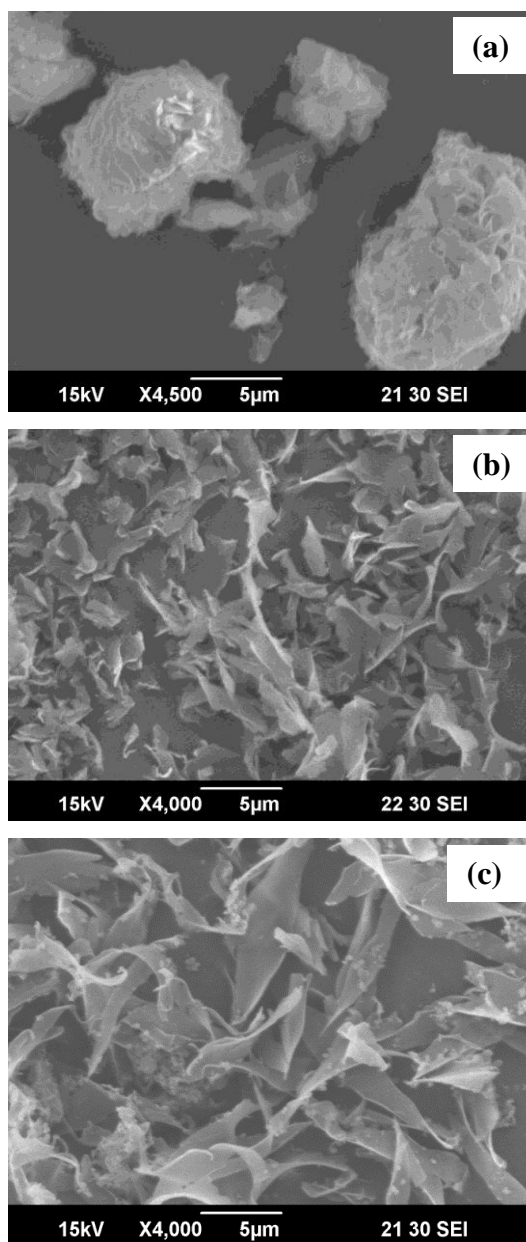


Figure 5.4 SEM images of SAS micronized lutein samples obtained at 50 °C, 0.5 ml/min solution flow rate, 20 ml/min CO₂ flow rate, 2.5 mg/ml lutein concentration, and at various pressures (a) 8 MPa, (b) 10 MPa, (c) 12 MPa (sample number 2, 5, and 3).

5.3.1.2 Effect of lutein initial concentration

The effect of lutein initial concentration (1.5, 2.5 and 3.2 mg/ml) on the particle morphology could be observed from sample numbers 4, 5 and 6 for the fixed pressure of 10 MPa and the fixed SC-CO₂ flow rate of 20 ml/min. The SEM images

of the resulted particles are shown in Figure 5.5(a), 5.5(b) and 5.5(c). There seemed to be no differences in the morphologies of the particles obtained with different lutein initial concentrations. In all cases, the flake-like particles of lutein were obtained. However, as mentioned above, the particles formed at 10 MPa tended to be agglomerated. As a result, large lumps of particles were seen for the samples formed from the lutein solution as the initial concentration increased.

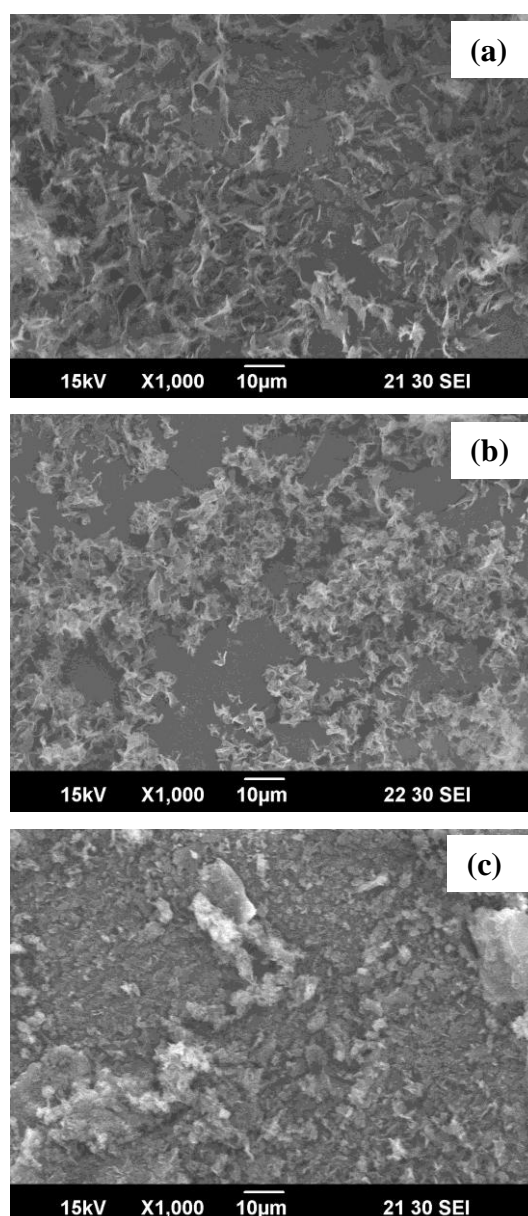
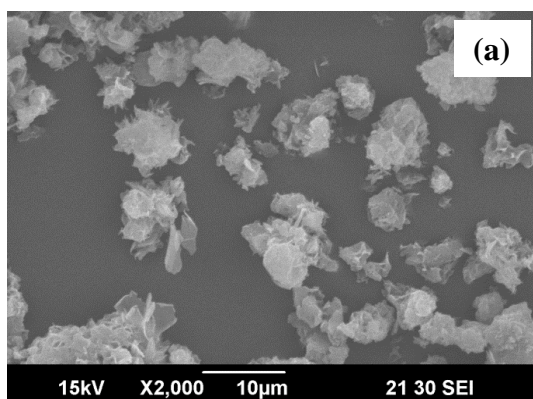


Figure 5.5 SEM images of SAS micronized lutein samples obtained at 50 °C, 10 MPa, 0.5 ml/min solution flow rate, 20 ml/min CO₂ flow rate, and various lutein concentrations (a) 1.5 mg/ml, (b) 2.5 mg/ml, (c) 3.2 mg/ml (sample number 4, 5, and 6).

5.3.1.3 Effect of SC-CO₂ flow rate

The effect of SC-CO₂ flow rate on morphology, MPS and PSD of micronized lutein could be observed from sample numbers 7, 8 and 9 for the fixed pressure of 8 MPa and the fixed lutein initial concentration of 2.5 mg/ml. As shown in Figure 5.6, at 8 MPa, similar ellipsoid-spheroid shape morphology of micronized lutein particles were observed for all SC-CO₂ flow rates (15, 20 and 25 ml/min). However, as SC-CO₂ flow rate increased, MPS decreased from 2.2 to 0.8 μm . At higher SC-CO₂ flow rates, supersaturation was reached more readily as CO₂ quickly diffuse into the droplet, resulting in precipitation of very fine particles.

Moreover, the size distributions of the particles obtained at various SC-CO₂ flow rates are shown in Figure 5.7. It can be inferred from Figure 5.7 that some particles whose size was smaller than the filter pores were lost as it passed through the filter. Considerable loss was observed particularly at the SC-CO₂ flow rate of 25 ml/min, in which particles of the smallest MPS were formed giving the yield of only 27%. Despite this, it could still be drawn from Figure 5.7 that slightly wider lutein PSD was observed when the SC-CO₂ flow rate increased from 15 to 20 ml/min, while increasing SC-CO₂ from 20 to 25 ml/min, on the other hand, resulted in narrower PSD. The larger PSD as the SC-CO₂ flow rate increased initially from 15 to 20 ml/min could be due to the interference by the increased aerodynamic force resulted from the increasing of SC-CO₂ flow rate, thus the liquid phase dispersion became irregular and the uniform size of droplet cannot be formed. When the SC-CO₂ flow rate increased to 25 ml/min however, much smaller particles were formed, thus the PSD became narrower.



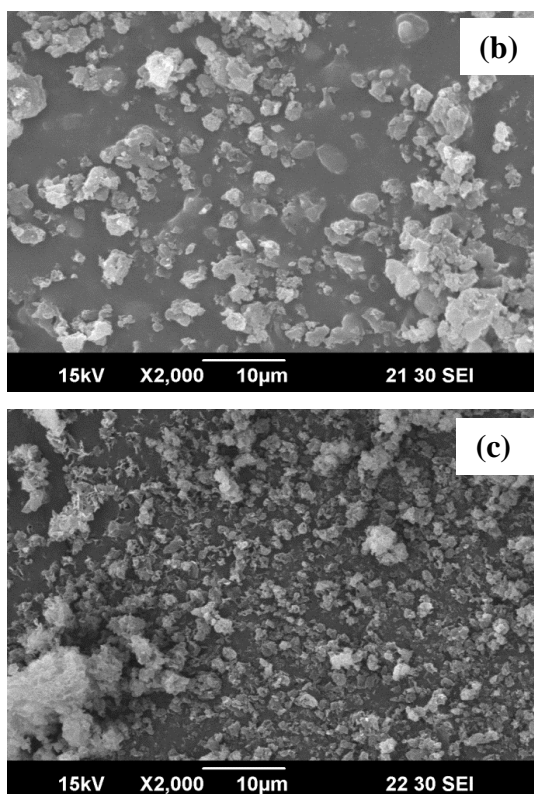
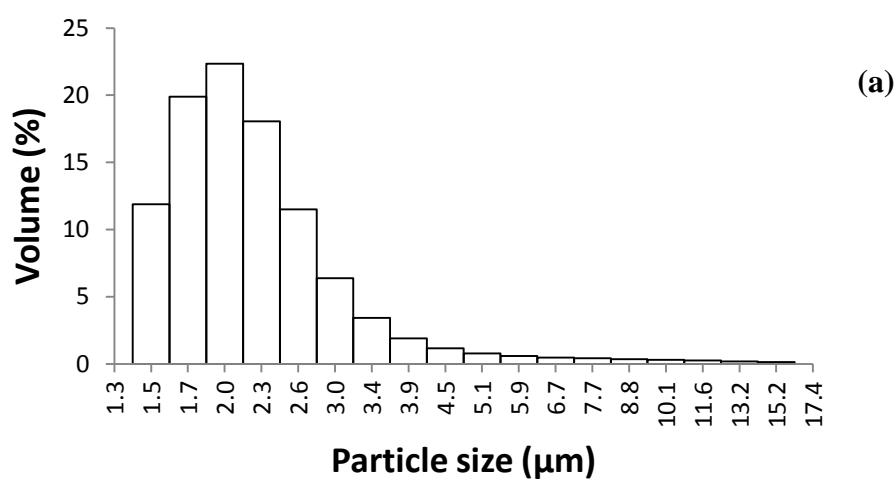


Figure 5.6 SEM images of SAS micronized lutein samples obtained at 50 °C, 8 MPa, 0.25 ml/min solution flow rate, 2.5 mg/ml lutein concentration, and various CO₂ flow rates (a) 15 ml/min, (b) 20 ml/min, (c) 25 ml/min (sample number 7, 8, and 9).



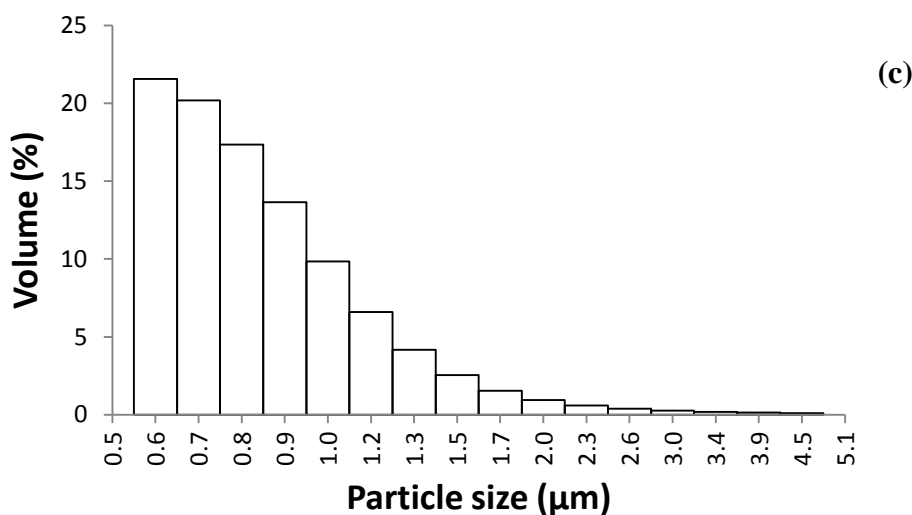
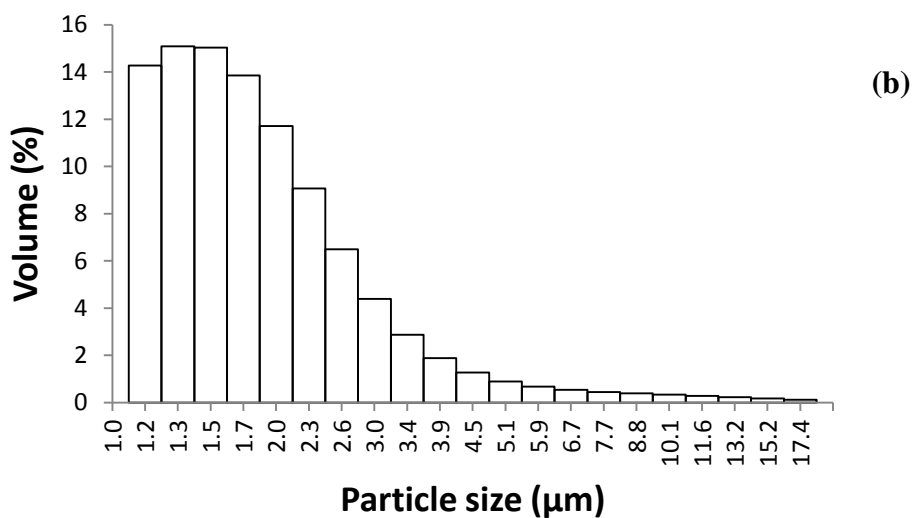


Figure 5.7 PSD of SAS micronized lutein samples obtained at 50 °C, 8 MPa, 0.25 ml/min solution flow rate, 2.5 mg/ml lutein concentration, and various CO₂ flow rates (a) 15 ml/min, (b) 20 ml/min, (c) 25 ml/min (sample number 7, 8, and 9).

5.3.2 Characterization of micronized lutein

Because the highest yield of non agglomerated micronized lutein particles were obtained for the sample number 7 (operated at pressure 8 MPa, 15 ml/min of SC-CO₂ flow rate and 2.5 mg/ml of lutein initial concentration), the particles were subjected to characterization study to examine the particle crystallinity and the changes in the chemical structures using XRD and FTIR analyses, respectively.

The XRD patterns of un-processed lutein and micronized lutein powder shown in Figure 5.8 imply that lutein was completely amorphous in nature. The amorphous structure could be attributed to the fact that the supersaturation state was reached suddenly as a result in of the solubility decrease by the diffusion of SC-CO₂ into the solvent. Moreover, the FTIR spectroscopy results of the processed and un-processed lutein particles are shown in Figure 5.9. The corresponding OH stretching vibration band between 3200 and 3600 cm⁻¹ is a rather broad peak. The bands corresponding to stretching vibrations in the CH₂ groups are at 2852 cm⁻¹ and 2922 cm⁻¹. The band assigned to the stretching vibrations of the C=C groups is at 1630 cm⁻¹. The bands corresponding to bending vibrations in the CH₃ groups are at 1447 cm⁻¹ and 1376 cm⁻¹. The out of plane deformation of =C-H group (oop bend) is present at 966 cm⁻¹. From the FTIR results, no chemical structural change in the micronized lutein particles occurred as a result of the SAS process.

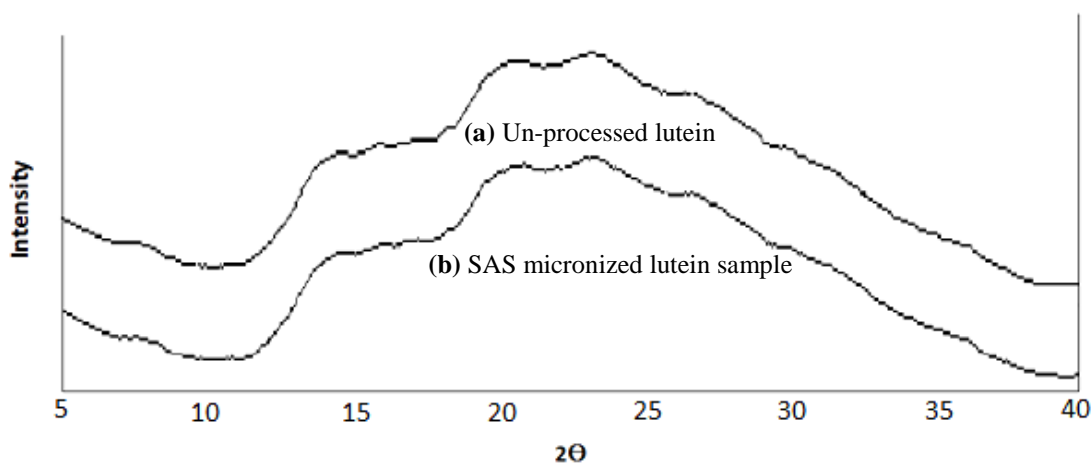


Figure 5.8 XRD pattern of SAS micronized lutein samples; (a) un-processed lutein (b) SAS micronized lutein sample obtained at 50 °C, 8 MPa, 0.25 ml/min solution flow rate, 2.5 mg/ml lutein concentration, and 15 ml/min CO₂ flow rates.

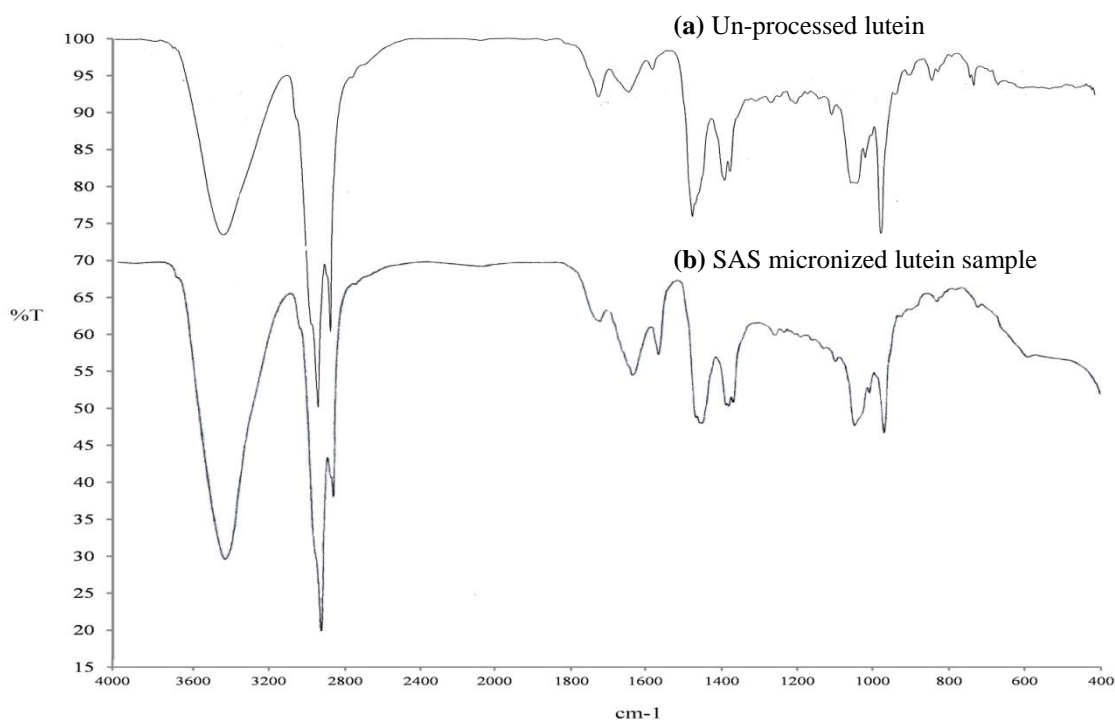


Figure 5.9 FTIR Transmission of lutein samples; (a) un-processed lutein (b) SAS micronized lutein sample obtained at 50 °C, 8 MPa, 0.25 ml/min solution flow rate, 2.5 mg/ml lutein concentration, and 15 ml/min CO₂ flow rates.

5.3.3 Dissolution of micronized lutein particles

Dissolution study was conducted on the micronized lutein powder obtained for the sample number 7 (operated at pressure 8 MPa, 15 ml/min of SC-CO₂ flow rate and 2.5 mg/ml of lutein initial concentration) and the un-processed lutein. As shown in Figure 5.10, the un-processed lutein was found to be hardly soluble in the aqueous solution, while the % dissolution of the micronized lutein particles sharply increased to about 17% within 5 min, then slowly increased, and reached 20% in 60 min. The improvement in % dissolution of the micronized lutein particles could be explained by the increased surface area as the MPS reduced from 202.3 μm to 2.2 μm (Table 5.1).

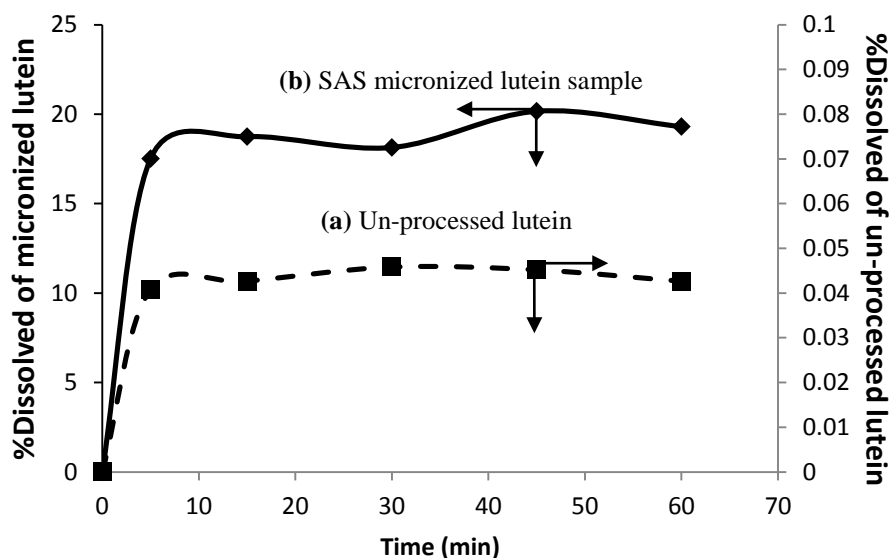


Figure 5.10 Dissolution profile of (a) un-processed lutein and (b) SAS micronized lutein sample obtained at 50 °C, 8 MPa, 0.25 ml/min solution flow rate, 2.5 mg/ml lutein concentration, 15 ml/min CO₂ flow rates (dissolution conditions at 37 °C, rotating speed of 100 rpm, 15 mg of samples in 500 ml of medium solution (pH=1.2)).

5.4. Conclusions

The supercritical anti-solvent (SAS) process could be employed for the micronization marigold lutein particles, using a mixture of hexane and ethyl acetate, the mobile phase in the earlier step of chromatography purification. Pressure was found to have significant effect on the particle morphology. The increase in lutein initial concentration from 1.5 to 3.2 mg/ml and the increase in SC-CO₂ flow rate from 15 to 25 ml/min show no significant effect on the morphology of the micronized lutein particles. However, the reduction of lutein particle size from about 2 to 0.8 μm by increasing SC-CO₂ flow rate was observed. The suitable conditions for lutein micronization in this work were found to be at 8 MPa, 2.5 mg/ml initial concentration and 25 ml/min SC-CO₂ flow rate, giving non-agglomerated fine particles of 0.8 μm MPS. The micronized lutein particles were found to be amorphous and no significant changes in the chemical structure of lutein were observed after the SAS micronization process. Moreover, significant improvement in the dissolution micronized lutein

particles was found compared to the un-processed lutein. In addition, in order to further gain better insights into the entire process, further investigations on phase equilibrium of the system and regime of liquid phase dispersion should be carried out.

CHAPTER VI

CONCLUSIONS & RECOMMENDATIONS

6.1 Conclusions

6.1.1 Purification of free lutein from marigold flowers by liquid chromatography

- Thin layer chromatography was initially employed for screening for the suitable mobile phase composition of hexane:ethyl acetate mixture used as a mobile phase. Hexane: ethyl acetate mixture at volume ratio of 70:30 was found to be an appropriate mobile phase for purification of free lutein on a normal phase chromatography system.
- With the suitable volume ratio of 70:30 of hexane:ethyl acetate used as a mobile phase, semi-preparative column chromatography of saponified marigold extract was shown to give purified free lutein product.
- Based on geometric similarity of the chromatography column, a scale up factor was used to roughly estimate the process conditions for a larger scale preparative column chromatography such as mass of packing material, mobile phase flow rate and sample loading volume. At the most suitable condition, a preliminary study employing the preparative chromatography was found to give high purity free lutein (> 95% purity) whose yield was approximately 60%.

6.1.2 Supercritical anti solvent (SAS) micronization of marigold-derived lutein dissolved in dichloromethane and ethanol

- Supercritical anti solvent (SAS) micronization using either dichloromethane or ethanol as a solvent was shown to effectively produce fine particles of lutein derived from marigold flowers.
- In both solvent systems, the increase in pressure and supercritical carbon dioxide (SC-CO₂) flow rate did not have significant effects on lutein particle morphology.
- Pressure was found to have significant effect on mean particle size and particle size distribution of lutein particles.
- The increase in SC-CO₂ flow rate from 20 to 25 ml/min resulted in the reduction of mean particle size in both dichloromethane and ethanol systems.

- Compared dichloromethane, ethanol was found to be more suitable solvent for SAS micronization of lutein as particles of smaller mean particle size were obtained.

6.1.3 Supercritical anti solvent (SAS) micronization of chromatography purified marigold lutein using hexane and ethyl acetate solvent mixture

- A mixture of hexane and ethyl acetate, the mobile phase in the earlier step of chromatography purification, could be used as a solvent in the micronization SAS process to produce fine lutein particles.
- Pressure was found to have significant effect on the particle morphology.
- The increase in lutein initial concentration from 1.5 to 3.2 mg/ml showed no significant effect on the morphology of the micronized lutein particles.
- The increase in supercritical carbon dioxide (SC-CO₂) flow rate from 15 to 25 ml/min showed no significant effect on the morphology of the micronized lutein particles.
- The reduction of lutein particle size from about 2 to 0.8 µm by increasing supercritical carbon dioxide (SC-CO₂) flow rate from 15 to 25 ml/min was observed.
- The suitable conditions for lutein micronization in this system were found to be at 8 MPa, 2.5 mg/ml initial concentration and 25 ml/min supercritical carbon dioxide (SC-CO₂) flow rate, giving non-agglomerated fine particles of 0.8 µm MPS.
- The micronized lutein particles were found to be amorphous and no significant changes in the chemical structure of lutein were observed after the SAS micronization process. Moreover, water dissolution of micronized lutein particles was found to be significantly improved over the un-processed lutein.

6.2 Research contributions

- Based on the information regarding the suitable composition of the mobile phase determined by thin layer chromatography experiment, the preliminary results on semi-preparative and preparative chromatography, a protocol could be developed for a large-scale recovering and purifying of this high value compound (whose price is as high as 570-790 USD per kilogram) from a local plant. Furthermore, the process may also be applied for separation and purification of lutein from other sources such as from microalga *Chlorella* sp., as well as for separation and purification of similar compounds (i.e., other carotenoids) from various fruits and vegetables.

- SAS process shows the possibility for micronizing of lutein derived from marigold flower. Since lutein particle size reduced into micron and sub-micron range, the significant improvement in the dissolution rate of SAS micronized lutein particles compared to the un-processed lutein was observed. This subsequently improves its bioavailability and leads to lower the dosage requirement and also reduces any possible side effects associated with up-taking. Moreover, due to mild operating temperature requirement and no friction heat generating, SAS technique is considered to be suitable process for micronization of lutein and other thermally labile compounds. In addition, the success of SAS micronization using the same solvent system as the mobile phase (hexane:ethyl acetate (70:30 v/v)) of the chromatography process will imply that a step of solvent evaporation from the eluted samples and re-dissolving the dried sample into another organic solvent can be omitted. By this, not only the process cost can be reduced, the degradation of lutein during complicated processing steps can also be minimized.

6.3 Recommendations

6.3.1 Purification of free lutein from marigold flowers by liquid chromatography

- The other important factors such as mobile phase flow rate, maximum sample loading, sample to packing material mass ratio affected to the performance of chromatographic purification should be further optimized to provide higher yield and purity of free lutein.

- Since the scale up factor used in this study was based only on a simple geometric similarity criterion, the behavior of the larger scale process may not be exactly the same as that in the smaller scale. More accurate prediction of the process requires understandings of fundamental transport phenomena and mass transfer processes involved, and this should be the subject of future investigation.

6.3.2 Supercritical anti solvent (SAS) micronization

- Because the particle morphology, size and size distribution are also influenced by experimental set up such as nozzle type and nozzle inner diameter, thus the suitable experimental set up should be further optimized.

- Due to the fact that SAS micronization involves several processes such as the solvent jet disintegration or solvent dispersion as it flows through the nozzle, mass

transfer between the liquid jet and the supercritical anti-solvent, as well as particle nucleation and growth. The further investigations on regime of liquid phase dispersion, interfacial tension of the system and other hydrodynamic parameters such as jet breakup lengths and diffusion lengths should be carried out in order to further gain better insights into the entire SAS process.

- The lower yields of SAS micronized lutein samples observed in this work was attributed to the relatively large filter pore diameter (1 μm). Therefore, the better sample collection method such as using nano-sized pore membrane should be future developed.

REFERENCES

- Alisa, P., Helen, R., Elizabeth, J. J. Xanthophyll (lutein, zeaxanthin) content in fruits, vegetables and corn and egg products. Journal of Food Composition and Analysis 22 (2009): 9–15
- Aman, R., Biehl, J., Carle, R., Conrad, J., Beifuss, U., Schieber A. Application of HPLC coupled with DAD, APcI-MS and NMR to the analysis of lutein and zeaxanthin stereoisomers in thermally processed vegetables. Food Chemistry 92 (2005): 753–763
- Asplund, K. Antioxidant vitamins in the prevention of cardiovascular disease: a systematic review. J. Intern. Med. 251 (2002): 372–392
- Ausich, R.L., Sanders, D.J. Process for the formation, isolation and purification of comestible xanthophylls crystals from plants. US Patent (1997) 5648564
- Badens, E., Boutin, O., Charbit, G. Laminar jet dispersion and jet atomization in pressurized carbon dioxide. J. Supercritical Fluids 36 (2005): 81-90
- Bahrami, M., Ranjbarian, S. Production of micro- and nano-composite particles by supercritical carbon dioxide. J. Supercritical Fluids 40 (2007): 263-283
- Bartlett, H.E., Eperjesi, F. Carotenoids and ocular disease: a review. Agro Food Ind. Hi - Tech. 15 (2004): 19–21
- Boonnoun, P., Opaskonkun, T., Prasitchoke, P., Shotipruk, A. Purification of Free Lutein from Marigold Flowers by Liquid Chromatography. Engineering Journal 16 (2012): 145-156
- Boonnoun, P., Nerome, H., Machmudah, S., Goto, M., Shotipruk, A., Supercritical anti-solvent micronization of marigold-derived lutein dissolved in dichloromethane and ethanol, J. Supercritical Fluids 77 (2013): 103-109
- Braeuer, A., Adami, R., Dowy, S., Rossmann, M., Leipertz, A. Observation of liquid solution volume expansion during particle precipitation in the supercritical CO₂ antisolvent process. J. Supercritical Fluids 56 (2011): 121-124
- Brunner, G., Budich, M. Chapter 4.2 - Separation of organic compounds from aqueous solutions by means of supercritical carbon dioxide. Supercritical Fluids as Solvents and Reaction Media. (2004): 489-522

- Burton, G.W. Antioxidant action of carotenoids. J. Nutrition 119 (1989): 109-111
- Byrappa, K., Ohara, S., Adschiri, T. Nanoparticles synthesis using supercritical fluid technology – towards biomedical applications. Advanced Drug Delivery Reviews 60 (2008): 299-327
- Can, Q., Carlfors, J., Turner, C. Carotenoids Particle Formation by Supercritical Fluid Technologies. Chinese J. Chemical Engineering 17 (2009): 344-349
- Caputo, G., Reverchon, E. Use of Urea as Habit Modifier in the Supercritical Antisolvent Micronization of Sulfathiazole. Industrial & Engineering Chemistry Research 46 (12) (2007): 4265-4272
- Chang, S.C., Lee, M.J., Lin, H.M. The influence of phase behavior on the morphology of protein α -chymotrypsin prepared via a supercritical anti-solvent process. J. of Supercritical Fluids 44 (2008): 219–229
- Chang, S.C., Hsu, T.H., Chu, Y.H., Lin H.M., Lee, M.J. Micronization of aztreonam with supercritical anti-solvent process. Journal of the Taiwan Institute of Chemical Engineers 43 (2012): 790–797
- Cho, Y.C., Cheng, J.H., Hsu, S.L., Hong, S.E., Lee, T.M., Chang, C.M.J. Supercritical carbon dioxide anti-solvent precipitation of anti-oxidative zeaxanthin highly recovered by elution chromatography from *Nannochloropsis oculata*. Separation and Purification Technology 78 (2011): 274-280
- Craft E. Relative Solubility, Stability, and Absorptivity of Lutein and β -Carotene in Organic Solvents. J. Agricultural and Food Chemistry 40 (1992): 431-434
- Curt, E., Lane, C. S., Steven J. S. Capability of a polymeric C30 stationary phase to resolve cis-trans carotenoid isomers in reversed-phase liquid chromatography. Journal of Chromatography A. 707 (2) (1995): 205-216
- De Marco, I., Reverchon, E. Supercritical antisolvent micronization of cyclodextrins. Powder Technology 183 (2008): 239-246
- Dias, G., Filomena G.F.C. Luisa, O. Carotenoids in traditional Portuguese fruits and vegetables. Food Chemistry. 113 (2009): 808–815
- Dohrn, R., Brunner, C. High-Pressure Fluids-Phase Equilibria: Experimental Methods and System Investigated (1988-1993). Fluid Phase Equilibria 106 (1995): 213-282

- Dukhin, S.S., Shen, Y., Dave, R., Pfeffer, R. Droplet mass transfer, intradroplet nucleation and submicron particle production in two-phase flow of solvent-supercritical anti solvent emulsion. Colloids and Surfaces A: Physicochem. Eng. Aspects 261 (2005): 163–176
- Facundo, M., Ángel, M., María J. C. Carotenoid processing with supercritical fluids. Journal of Food Engineering, 93 (3) (2009): 255-265
- Fonseca, M.S., Dohrn R., Peper, S. High-pressure fluid-phase equilibria: Experimental methods and systems investigated (2005–2008). Fluid Phase Equilibria 300 (2011): 1–69
- Franceschi, E., Kunita, M.H., Tres, M.S., Rubira, A.F., Muniz, E.C., Corazza, M.L., Dariva, C., Ferreira, S.R.S., Oliveira, J.V. Phase behavior and process parameters effects on the characteristics of precipitated theophylline using carbon dioxide as antisolvent. J. of Supercritical Fluids. 44 (2008): 8–20
- Gokhale, A., Khusid, B., Dave, R. N., Pfeffer, R. Effect of solvent strength and operating pressure on the formation of submicrometer polymer particles in supercritical microjets. J. Supercritical Fluids 43 (2007): 341-356
- Gomez-Prieto, M. S., Ruiz del Castillo, M. L., Flores, G., Santa-Maria, G., Blanch, G. P. Application of Chrastil's model to the extraction in SC-CO₂ of β -carotene and lutein in *Mentha spicata* L. J. Supercritical Fluids 43 (2007): 32-36
- Gosselin, P.M., Thibert, R., Preda, M., McMullen, J.N. Polymorphic properties of micronized carbamazepine produced by RESS. Int J Pharm. 252 (2003): 225–233.
- Granado, F., Olmedilla, B., Blanco, I. Nutritional and clinical relevance of lutein in human health. British J. Nutrition 90 (2003): 487-502
- Hak, A.E., Ma, J., Powell, C.B., Campos, H., Gaziano, J.M., Willett, W.C., Stampfer, M.J. Prospective study of plasma carotenoids and tocopherols in relation to risk of ischemic stroke. Stroke 35 (2004): 1584–1588
- Hakuta, Y., Hayashi, H., Arai, K. Fine particle formation using supercritical fluids. Current Opinion in Solid State and Materials Science. 7 (2003): 341–351
- Hong, L., Guo, J., Gao, Y., Yuan, W.K. Precipitation of microparticulate organic pigment powders by a supercritical antisolvent process. Ind. Eng. Chem. Res. 39 (2000): 4882

- Hu, G., Chen, H., Cai, J., Deng, X. Solubility and micronization of griseofulvin in supercritical CO₂ with cosolvent acetone. In: Proc 6th Int Symp Supercrit Fluid. 3 (2003): 1725–1734
- Imsanguan, P., Pongamphai, S., Douglas, S., Teppaitoon, W., Douglas, P.L. Supercritical antisolvent precipitation of andrographolide from *Andrographis paniculata* extracts: Effect of pressure, temperature and CO₂ flow rate. Powder Technology 200 (2010): 246–253
- Jiang, S.Y., Chen, M., Zhao, Y.P. A study on micronization of phytosterol by the RESS technique with supercritical CO₂. Proc 6th Int Symp Supercrit Fluid. 3 (2003): 1653–1658
- Jiang, X.Y., Chen, L.S., Zhou, C.S. Lutein and lutein ester in marigold flowers by high performance chromatography. J. cent. South Univ. Technol. 12 (2005): 1005 – 9784
- Kayrak, D., Akman, U., Hortacsu, O. Micronization of ibuprofen by RESS. J Supercrit Fluid. 26 (2003): 17–31
- Khachik, F., Beltsville, M. Process for isolation, purification, and recrystallization of lutein from saponified marigold oleoresin and uses thereof. United States Patent, 5382714 (1995)
- Khachik, F., Englert, G., Beecher, G.R., Smith Jr J.C. Isolation, structural elucidation, and partial synthesis of lutein dehydration products in extracts from human plasma. J. of Chromatography B 670 (1995): 219-233
- Khachik, F., Beltsville, M. Process for extraction, purification of lutein, zeaxanthin and rare carotenoids from marigold flowers and plants. United States Patent, 6262284 (2001)
- Kim, M.S., Lee, S., Park J.S., Woo J.S., Hwang S.J. Micronization of cilostazol using supercritical antisolvent (SAS) process: effect of process parameters. Powder Technology 177 (2007): 64-70.
- Kiyotaka, N., Takehiro, K., Kejiro, H., Akira, A., Fumiko, K., Phumon, S., Tsuyoshi, T., Hiroyuki, A., Teruo, M. Development of a high-performance liquid chromatography-based assay for carotenoids in human red blood cells: Application to clinical studies. Analytical Biochemistry 381 (2008): 129–134

- Kwon, K.T., Uddin, M.S., Jung, G.W., Chun, B.S. Preparation of micro particles of functional pigments by gas-saturated solution process using supercritical carbon dioxide and polyethylene glycol. Korean J. Chemical Engineering 28(10) (2011): 2044-2049
- Landrum, J.T., Bone, R.A. Lutein, zeaxanthin, and the macular pigment. Arch. Biochem. Biophys. 385 (2001): 28–40
- Lee, E.H., Faulhaber, D., Hanson, K.M., Ding, W., Peters, S., Kodali, S., Granstein, R.D. Dietary lutein reduces ultraviolet radiation-induced inflammation and immunosuppression. J. Invest. Dermatol. 122 (2004): 510–517
- Lindenberg, C., Mazzotti, M. Effect of temperature on the nucleation kinetics of α L-glutamic acid. Journal of Crystal Growth 311 (2009): 1178–1184
- Martín, L., González-Coloma, A., Adami, R., Scognamiglio, M., Reverchon, E., DellaPorta, G., Urieta, J.S., Mainar, A.M. Supercritical anti solvent fractionation of ryanodol from *Persea indica*. J. of Supercritical Fluids 60 (2011): 16–20
- Miguel, F., Martín, A., Mattea, F., Cocero, M.J. Precipitation of lutein and co-precipitation of lutein and poly-lactic acid with the supercritical anti-solvent process. Chemical Engineering and Processing 47 (2008): 1594-1602
- Mingchen, W., Rong, T., Shanfeng, Z., Ziming, D., Raymond, Y., Jianhua, G., Yingxin, P. Antioxidant activity, mutagenicity/anti-mutagenicity, and clastogenicity/anti-clastogenicity of lutein from marigold flowers. Food and Chemical Toxicology. 44 (9) (2006): 1522-1529
- Mitri, K., Shegokar, R., Gohla, S., Anselmi, C., Muller, R.H. Lutein nanocrystals as antioxidant formulation for oral and dermal delivery. International J. Pharmaceutics 420 (2011): 141-146
- Moeller, S.M., Volland, R., Tinker, L., Blodi, B.A., Klein, M.L., Gehrs, K.M., Johnson, E.J., Snodderly, D.M., Wallace, R.B., Chappell, R.J., Parekh, N., Ritenbaugh, C., Mares, J.A. Associations between age-related nuclear cataract and lutein and zeaxanthin in the diet and serum in the carotenoids in the age-related eye disease study, an ancillary study of the women's health initiative. Arch. Ophthalmol. 126 (2008): 354–364

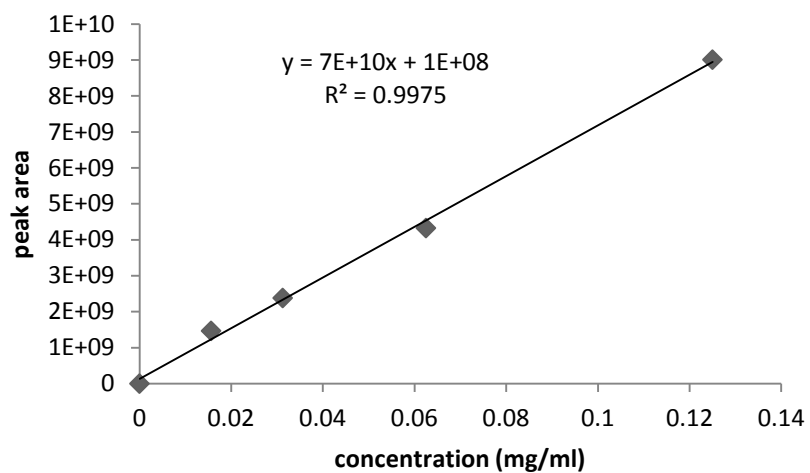
- Molnar, P., Szabo, Z., Osz, E., Olah, P., Toth, G., Deli, J. Separation and Identification of Lutein Derivatives in Processed Foods. Chromatographia 60 (2004): S101-S105
- Obrzut, D.L., Bell, P.W., Roberts, C.B., Duke, S.R. Effect of process conditions on the spray characteristics of a PLA plus methylene chloride solution in the supercritical antisolvent precipitation process. J. Supercritical Fluids 42 (2007): 299-309.
- Olmedilla, B., Granado, F., Blanco, I., Vaquero, M. Lutein, but not alpha-tocopherol, supplementation improves visual function in patients with age-related cataracts: a 2-year double-blind, placebo-controlled pilot study. Nutrition 19(2003): 21–24.
- Palombo, P., Fabrizi, G., Ruocco, V., Ruocco, E., Fluhr, J., Roberts, R., Morganti, P. Beneficial long-term effects of combined oral/topical antioxidant treatment with the carotenoids lutein and zeaxanthin on human skin: a double-blind, placebo-controlled study. Skin Pharmacol. Physiol. 20 (2007): 199–210
- Palumpitag, W., Prasitchoke, P., Goto, M., Shotipruk, A. Supercritical Carbon Dioxide Extraction of Marigold Lutein Fatty Acid Esters: Effects of Cosolvents and Saponification Conditions. Separation Science and Technology, 46 (4) (2011): 605-610.
- Park, C.I., Shin, M. S., Kim, H. Micronization of arbutine using supercritical antisolvent. Korean J. Chemical Engineering 25(3) (2008): 581-584
- Perrut, M., Jung, J., Leboeuf, F. Enhancement of dissolution rate of poorly soluble active ingredients by supercritical fluid processes Part II: Preparation of composite particles. International J. Pharmaceutics 288 (2005): 11-16
- Piccaglia, R., Marotti, M., Grandi, S. Lutein and lutein ester content in different types of *Tagetes patula* and *T. erecta*. Industrial Crops and Products. 8 (1998): 45–51.
- Reverchon, E., De Marco, I. Supercritical antisolvent micronization of cefonicid: thermodynamic interpretation of results. J. Supercritical Fluids 31 (2004): 207-215.
- Reverchon, E., De Marco, I. Supercritical antisolvent precipitation of Cephalosporins. Powder Technology 164 (2006): 139-146

- Reverchon, E., Adami, R., Caputo, G., DeMarco, I. Spherical microparticles production by supercritical antisolvent precipitation: Interpretation of results. J. Supercritical Fluids 47 (2008): 70-84
- Reverchon, E., De Marco, I. Mechanisms controlling supercritical antisolvent precipitate morphology. Chemical Engineering Journal 169 (2011): 358-370
- Reverchon, E., Torino, E., Dowy, S., Braeuer, A., Leipertz, A. Interactions of phase equilibria, jet fluid dynamics and mass transfer during supercritical antisolvent micronization. Chemical Engineering Journal 156 (2010): 446-458
- Reza, M., Schafer, L., Lambert, C., Breithaupt, D.E., Biesalski, H.K., Frank, J. Solubility, uptake and biocompatibility of lutein and zeaxanthin delivered to cultured human retinal pigment epithelial cells in tween40 micelles. European J. Nutrition 46 (2007): 79-86
- Sarkari, M., Darrat, I., Knutson, B.L. Generation of microparticles using CO₂ and CO₂-philic antisolvents, AIChE J. 46 (2000): 1850.
- Shekunov, B.Y., Baldyga, J. Particle formation by mixing with supercritical antisolvent at high Reynolds numbers, P. York. Chemical Engineering Science 56 (2001): 2421-2433
- Shibata, S., Ishihara, C., Matsumoto, C. Improved Separation Method for Highly Purified Lutein from Chlorella Powder Using Jet Mill and Flash Column Chromatography on Silica Gel J. Agric. Food Chem. 52 (2004): 6283-6286
- Shimasaki, S., Taniguchi, S. Formation of Uniformly-sized Droplets from Capillary Jet by Electromagnetic Force. Seventh International Conference on CFD in the Minerals and Process Industries CSIRO, Melbourne, Australia 9-11 December 2009
- Sowbhagya, H.B., Sampathu, S.R., Krishnamurthy N. Natural Colorant from Marigold-Chemistry and Technology. Food Reviews International 20 (2004): 33-50.
- Snyder, L.R. Changing reversed-phase high performance liquid chromatography selectivity Which variables should be tried first?. Journal of Chromatography B: Biomedical Sciences and Applications. 689 (1) (1997): 105-115.

- Su, C.S., Tang, M., Chen, Y.P. Recrystallization of pharmaceuticals using the batch supercritical anti-solvent process. Chemical Engineering and Processing 48 (2009): 92-100
- Tsvintzelis, I., Missopolinou, D., Kalogiannis, K., Panayiotou, C. Phase compositions and saturated densities for the binary systems of carbon dioxide with ethanol and dichloromethane. Fluid Phase Equilibria 224 (2004): 89-96
- Turk, M., Upper, G., Hils, P. Formation of composite drug-polymer particles by coprecipitation during the rapid expansion of supercritical fluids. J. of Supercritical Fluids. 39 (2006): 253-263.
- Varughese, P., Li, J., Wang, W., Winstead, D. Supercritical antisolvent processing of γ -Indomethacin: Effects of solvent, concentration, pressure and temperature on SAS processed Indomethacin. Powder Technology 201 (2010): 64-69
- Vechpanich, J., Shotipruk, A. Recovery of free lutein from *Tagetes erecta*: Determination of Suitable Saponification and Crystallization Conditions, Separation Science and Technology 46 (2011): 265-271.
- Verghese, J. Focus on xanthophylls from *Tagetes Erecta* L the giant natural complex-I. Indian Spices. 33(4) (1998): 8-13.
- Wang, M., Tsao, R., Zhang, S., Dong, Z., Yang, R., Gong, J., Pei, Y. Antioxidant activity, mutagenicity/anti-mutagenicity, and clastogenicity/anti clastogenicity of lutein from marigold flowers. Food and Chemical Toxicology 44 (2006): 1522-1529
- Wang, Y., Wang, Y., Yang, J., Pfeffer, R., Dave R., Michniak B. The application of a supercritical antisolvent process for sustained drug delivery. Powder Technology 164 (2006): 94-102
- Werling, J.O., Debenedetti, P. G. Numerical modeling of mass transfer in the supercritical anti solvent process. Journal of Supercritical Fluids 16 (1999): 167-181
- Wolcott, R.G., Dolan, J.W., Snyder, L.R., Bakalyar, S.R., Arnold, M.A., Nichols, J.A. Control of column temperature in reversed-phase liquid chromatography. Journal of Chromatography A. 869 (2000): 211-230

- Wu, H.T., Lee, M.J., Lin, H.M. Nano-particles formation for pigment red 177 via a continuous supercritical anti-solvent process. J. of Supercritical Fluids. 33 (2005): 173–182
- Yeo, S.D., Kim, M.S., Lee, J.C. Recrystallization of sulfathiazole and chlorpropamide using the supercritical fluid antisolvent process. J. Supercritical Fluids 25 (2003): 143-154
- Zhao, C., Wang, L., Zu, Y., Li, C., Liu, S., Yang, L., Zhao, X., Zu, B. Micronization of Ginkgo biloba extract using supercritical antisolvent process. Powder Technology 209 (2011): 73-80

APPENDIX

Calibration curve of standard lutein by HPLC analysis**Lutein Calibration Curve**

Concentration (mg/ml)	Peak area
0.125	9011448126
0.0625	4326849909
0.03125	2382018714
0.015625	1466382330

NMR results

Index	PPM
1	0.847
2	0.878
3	0.996
4	1.071
5	1.252
6	1.623
7	1.734
8	1.907
9	1.964
10	1.970
11	2.261
12	2.299
13	2.330
14	2.345
15	2.411
16	4.000
17	4.012
18	4.251
19	6.118
20	6.152
21	6.619
22	6.640

Properties of CO₂ at 55°C and various pressures

Pressure (MPa)	Density (kg/m³)	Viscosity (Pa.s)
8	205.7	0.00002218
10	303.2	0.0000283
12	504.5	0.00003699

Properties of DCM at 55°C and various pressures

Pressure (MPa)	Density (kg/m³)	Viscosity (Pa.s)
8	1151	0.00007859
10	1154	0.00007994
12	1158	0.00008127

Properties of ethanol at 55°C and various pressures

Pressure (MPa)	Density (kg/m³)	Viscosity (Pa.s)
8	777.6	0.0006424
10	780	0.000648
12	782.4	0.0006534

Phase equilibrium data of binary system of DCM-CO₂

Pressure (MPa)	Molar fraction in liquid phase (x)	Molar fraction in vapor phase (y)
2.05	0.1391	0.8691
3.1	0.2245	0.9084
3.7	0.2793	0.921
4.58	0.3588	0.928
5.31	0.4332	0.9308
5.76	0.4874	0.9318
6.54	0.5804	0.9339
7	0.6355	0.9363
7.63	0.7088	0.9342
7.95	0.7481	0.9323
8.55	0.8223	0.9302
8.85	0.8556	0.9259

Phase equilibrium data of binary system of ethanol-CO₂

Pressure (MPa)	Molar fraction in liquid phase (x)	Molar fraction in vapor phase (y)
1.65	0.0778	0.9726
2.1	0.095	0.9769
2.78	0.1245	0.9805
3.5	0.1623	0.9821
4.37	0.2075	0.9822
5.02	0.2384	0.9821
5.82	0.2825	0.9803
6.8	0.3453	0.9797
8.26	0.4742	0.97
8.91	0.541	0.9662
9.24	0.5922	0.9624
9.42	0.6351	0.9549

Dissolution data of un-processed lutein and SAS micronized lutein sample obtained at 50 °C, 8 MPa, 0.25 ml/min solution flow rate, 2.5 mg/ml lutein concentration, 15 ml/min CO₂ flow rates (dissolution conditions at 37 °C, rotating speed of 100 rpm, 15 mg of samples in 500 ml of medium solution (pH=1.2)).

Time (min)	%dissolved micronized lutein	%dissolved un-processed lutein
0	0	0
5	17.52	0.04
15	18.75	0.04
30	18.14	0.05
45	20.17	0.05
60	19.31	0.04

VITA

Mr. Panatpong Boonnoun was born in Uttaradit, on October 5, 1984. He finished high school from Phitsanulok pittayakom School, Phitsanulok in 2002. He received his Bachelor's Degree in Chemical Engineering from Thammasat University in 2006. He continued studying Master's Degree in Chemical Engineering Chulalongkorn University in 2007 and graduated in 2008. During studying Master's Degree, he received grant fund from Ptt chemical Public Company Limited (Thailand). He subsequently continued studying Doctoral degree of Chemical Engineering, Chulalongkorn University since October 2009 and received grant fund from Thailand Research Fund (TRF) through the Royal Golden Jubilee Ph.D. Program (RGJ-TRF), His publications are as follows:

1. Panatpong Boonnoun, Thanawich Opaskonkun, Phattanon Prasitchoke, Motonobu Goto, Artiwan Shotipruk. Purification of Free Lutein from Marigold Flowers by Liquid Chromatography. *Engineering Journal*, 16 (2012) 145-156
2. Panatpong Boonnoun, Hazuki Nerome, Siti Machmudah, Motonobu Goto, Artiwan Shotipruk. Supercritical Anti-solvent Micronization of Marigold-derived Lutein Dissolved in Dichloromethane and Ethanol. *J. Supercritical Fluids* 77 (2013) 103-109
3. Panatpong Boonnoun, Hazuki Nerome, Siti Machmudah, Motonobu Goto, Artiwan Shotipruk. Supercritical Anti-solvent Micronization of Chromatography Purified Marigold Lutein Using Hexane and Ethyl Acetate Solvent Mixture. *J. Supercritical Fluids* (2013), in press.